Anatomy and phylogenetic relationships of *Tazoudasaurus naimi* (Dinosauria, Sauropoda) from the late Early Jurassic of Morocco

Ronan ALLAIN
Muséum national d'Histoire naturelle, Département Histoire de la Terre,
UMR-CNRS 5143 "Paléobiodiversité",
case postale 38, 57 rue Cuvier, F-75231 Paris cedex 05 (France)
and Université Cadi Ayyad, Faculté des Sciences Semlalia,
équipe Évolution des Vertébrés et Paléoenvironnements,
BP 2390, 40000 Marrakech (Morocco)
rallain@mnhn.fr

Najat AQUESBI
Université Mohamed V, Faculté des Sciences,
Rabat (Morocco)

Allain R. & Aquesbi N. 2008. — Anatomy and phylogenetic relationships of *Tazoudasaurus naimi* (Dinosauria, Sauropoda) from the late Early Jurassic of Morocco. *Geodiversitas* 30 (2) : 345-424.

ABSTRACT
The complete osteology of the basal sauropod *Tazoudasaurus naimi* from the late Early Jurassic Toundoute continental series of Ouarzazate Province, Morocco, is presented. The described material belongs to juvenile to adult individuals. The skeleton of *Tazoudasaurus* is virtually complete except for the skull and presents a combination of plesiomorphic and apomorphic sauropodomorph characters. Phylogenetic analysis indicates that *Tazoudasaurus* shares with *Vulcanodon* several derived features that include strongly transversely flattened tibial shaft and the marked dorsoventral flattening of the unguals of pedal digits II and III. Both taxa are placed within the Vulcanodontidae, at the base of a new clade named Gravisauria n. nom. Our analysis underscores the major morphological changes that occur among Gravisauria between the Vulcanodontidae and the Eusauropoda. The numerous remains of *Tazoudasaurus* were recovered from a bone-bed associated with a few remains of the basal abelisauroid *Berberosaurus*. A minimum of six individuals was buried at the site. Taphonomical data suggest

that *Tazoudasaurus* had a gregarious behaviour. The different interpretations of the evolution of the configuration and posture of the manus in basal sauropods can be tested thanks to the discovery of a complete articulated manus of *Tazoudasaurus*. The latter is clearly digitigrade with a spreading configuration of the metacarpus. Early sauropod evolution is analyzed in a broad extinction/radiation perspective. Prosauropoda and Coelophysoidea extinction around the Pliensbachian-Toarcian boundary, followed by the late Early Jurassic to Middle Jurassic radiation of Gravisauria, Neoceratosauria, Tetanurae and Euornithopoda are linked to the Pliensbachian-Toarcian mass extinction event.

KEY WORDS
Dinosauria,
Sauropoda,
Vulcanodontidae,
Early Jurassic,
Africa,
Morocco,
High Atlas,
anatomy,
phylogeny.

RÉSUMÉ
Anatomie et relations phylogénétiques de Tazoudasaurus naimi *(Dinosauria, Sauropoda) de la fin du Jurassique inférieur du Maroc.*
L'ostéologie complète du sauropode basal *Tazoudasaurus naimi* de la fin du Jurassique inférieur de la série continentale de Toundoute, de la Province de Ouarzazate au Maroc est présentée. Le matériel décrit appartient à des individus jeunes à adultes. Le squelette de *Tazoudasaurus* est virtuellement complet à l'exception de son crâne et possède une combinaison de caractères de sauropodomorphes plesiomorphes et apomorphes. Les résultats de notre analyse phylogénétique indiquent que *Tazoudasaurus* partage avec *Vulcanodon* plusieurs caractères dérivés parmi lesquels : une diaphyse du tibia fortement comprimée transversalement et un aplatissement dorsoventral marqué des ongles des doigts II et III du pied. Les deux taxons sont placés au sein des Vulcanodontidae, à la base d'un nouveau clade appelé Gravisauria n. nom. Notre analyse souligne les changements morphologiques majeurs qui interviennent au sein des Gravisauria, entre les Vulcanodontidae et les Eusauropoda. Les nombreux restes de *Tazoudasaurus* ont été retrouvés dans un bone-bed, associés avec quelques restes d'un abelisauroïde basal. Un minimum de six individus s'est fossilisé sur le site. Les données taphonomiques suggèrent que *Tazoudasaurus* avait un comportement grégaire. Les différentes interprétations de l'évolution de la configuration et de la position de la main chez les sauropodes ont pu être testées grâce à la découverte d'une main complète et articulée de *Tazoudasaurus*. Cette dernière est clairement digitigrade et possède des métacarpiens étalés. L'évolution des premiers sauropodes est analysée dans une perspective d'extinction/radiation. Un lien est établi entre l'extinction des Prosauropoda et des Coelophysoidea vers la limite Pliensbachien-Toarcien, suivie de la radiation à la fin du Jurassique inférieur et au Jurassique moyen des Gravisauria, des Neoceratosauria, des Tetanurae et des Euornithopoda, et l'extinction de masse enregistrée à la transition Pliensbachien-Toarcien.

MOTS CLÉS
Dinosauria,
Sauropoda,
Vulcanodontidae,
Jurassique inférieur,
Afrique,
Maroc,
Haut Atlas,
anatomie,
phylogénie.

INTRODUCTION

The increasing number of paleontological fieldworks in Africa during the past decade has greatly improved our knowledge on the diversity of African dinosaurs. However, the fieldworks were mostly focused on the end of the Mesozoic era, and most of the newly described taxa were unearthed from Lower to Upper Cretaceous strata, in Niger (Sereno *et al.* 1994, 1998, 1999, 2004; Taquet & Russell 1998, 1999),

Madagascar (Sampson *et al.* 1996, 1998, 2001; Dodson *et al.* 1998; Forster *et al.* 1998; Krause *et al.* 1999; Curry Rogers & Forster 2001; Rogers *et al.* 2003), and to a lesser extent in Malawi (Jacobs *et al.* 1993, 1996; Gomani 1999), Sudan (Rauhut & Werner 1995), Egypt (Churcher 1999; Smith *et al.* 2001), Tunisia (Buffetaut & Ouaja 2002) and Morocco (Kellner & Mader 1997; Russell 1996; Sereno *et al.* 1996; Mahler 2005).

Following the exhibition called "Maroc, Mémoire de la Terre" at the Muséum national d'Histoire naturelle, Paris in 1999, the Dinoatlas Project was conceived in order to carry out new fieldwork in the Jurassic strata from the High Atlas Mountains in Morocco. Except for the re-examination or study of previously collected dinosaur material from the Jurassic of Africa (Monbaron *et al.* 1999; Knoll & Battail 2001; Knoll 2002; Rauhut 2005), the results of these five years' work are the only ones that make up for the lack of new data on the African Jurassic dinosaur faunas. Thus, two new Early Jurassic taxa from the Toundoute series in High Atlas have been described so far: the basal abelisauroid theropod *Berberosaurus liassicus* Allain, Tykoski, Aquesbi, Jalil, Monbaron, Russell & Taquet, 2007 (Allain *et al.* 2007), and the vulcanodontid sauropod *Tazoudasaurus naimi* Allain, Aquesbi, Dejax, Meyer, Monbaron, Montenat, Richir, Rochdy, Russell & Taquet, 2004 (Allain *et al.* 2004), the detailed osteology of which is described here.

Geological and paleontological overview of the Jurassic in the High Atlas Mountains

Except for the Bathonian localities of El Mers (Termier *et al.* 1940; Lapparent 1955) and Boulahfa (Charroud & Fedan 1992) located in the Middle Atlas Mountains, most of the places that have yielded dinosaur remains from the Jurassic in Morocco are located in the High Atlas and refer to the geological maps of Beni Mellal (Monbaron 1985), Azilal (Jenny 1985), and Demnat (Le Marrec 1985) (Fig. 1).

The detrital continental deposits in which the dinosaur remains from the High Atlas have been collected have been termed "Red beds" (*s.l.*). Indeed, there are four different red detrital episodes in the High Atlas Mountains which have yielded vertebrates remains ("Red beds" [*s.l.*]). They are related to the Permo-Triassic, the Toarcian-Aalenian, the Middle Jurassic to Early Cretaceous, and the Albian-Cenomanian (Jenny *et al.* 1981a). For convenience and for the purpose of clarity, the term Red beds (*s.s*) is now restricted to the complex dated from the Middle Jurassic to the Early Cretaceous (Jenny *et al.* 1980, 1981a; Monbaron *et al.* 1990; Haddoumi *et al.* 1998; Charrière *et al.* 2005). This terminology is followed here (Fig. 2). Although the Albian-Cenomanian red deposits have yielded carcharodontosaurid remains in the vicinity of Ouaouizaght (pers. obs.), only Jurassic deposits are considered in the present overview (Figs 1; 2).

In the central Atlasic area, the Red beds complex is underlain by the Middle Jurassic (Aalenian-Bajocian) limestones of the Bin el Ouidane Formation and overlain by Aptian marls and limestones (Jenny *et al.* 1981a). It is constituted by three successive lithologic formations, the ages of which have long been debated: the Djebel Sidal, the Iouaridene and the Guettioua formations (Fig. 2). Neither tracks nor dinosaur remains have been found in the Djebel Sidal Formation. This formation has been assigned to various stratigraphic positions from Middle Jurassic to the Lower Cretaceous (see Jenny *et al.* 1981a). The recent discovery of Lower Cretaceous ostracods in the upper member of the Iouaridene Formation suggests that the Djebel Sidal Formation can be attributed to the Barremian (Charrière *et al.* 2005; Fig. 2). The Iouaridene Formation is famous for the numerous dinosaur trackways that it has yielded, especially near Demnat (Plateau *et al.* 1937; Lapparent 1945; Dutuit & Ouazzou 1980; Jenny *et al.* 1981b). This formation has long been considered Bathonian-Callovian in age, but it has been shown recently that ostracod and charophyte assemblages have an age stretching from the end of the Bathonian to the beginning of the Barremian. The tracks of Demnat must be connected with the Upper Jurassic (Oxfordian?-Kimmeridgian) (Charrière *et al.* 2005; Fig. 2). The Bathonian Guettioua Formation has yielded the skeleton of the sauropod *Atlasaurus imelakei* Monbaron, Russell & Taquet, 1999 (Monbaron & Taquet 1981; Monbaron *et al.* 1999), and its lateral equivalent in the Middle Atlas, the El Mers Formation, the remains of "*Cetiosaurus*" *mogrebiensis* Lapparent, 1955 (Termier *et al.* 1940; Lapparent 1955). The osteology and the phylogenetic relationships of *Atlasaurus* and "*Cetiosaurus*" *mogrebiensis* are

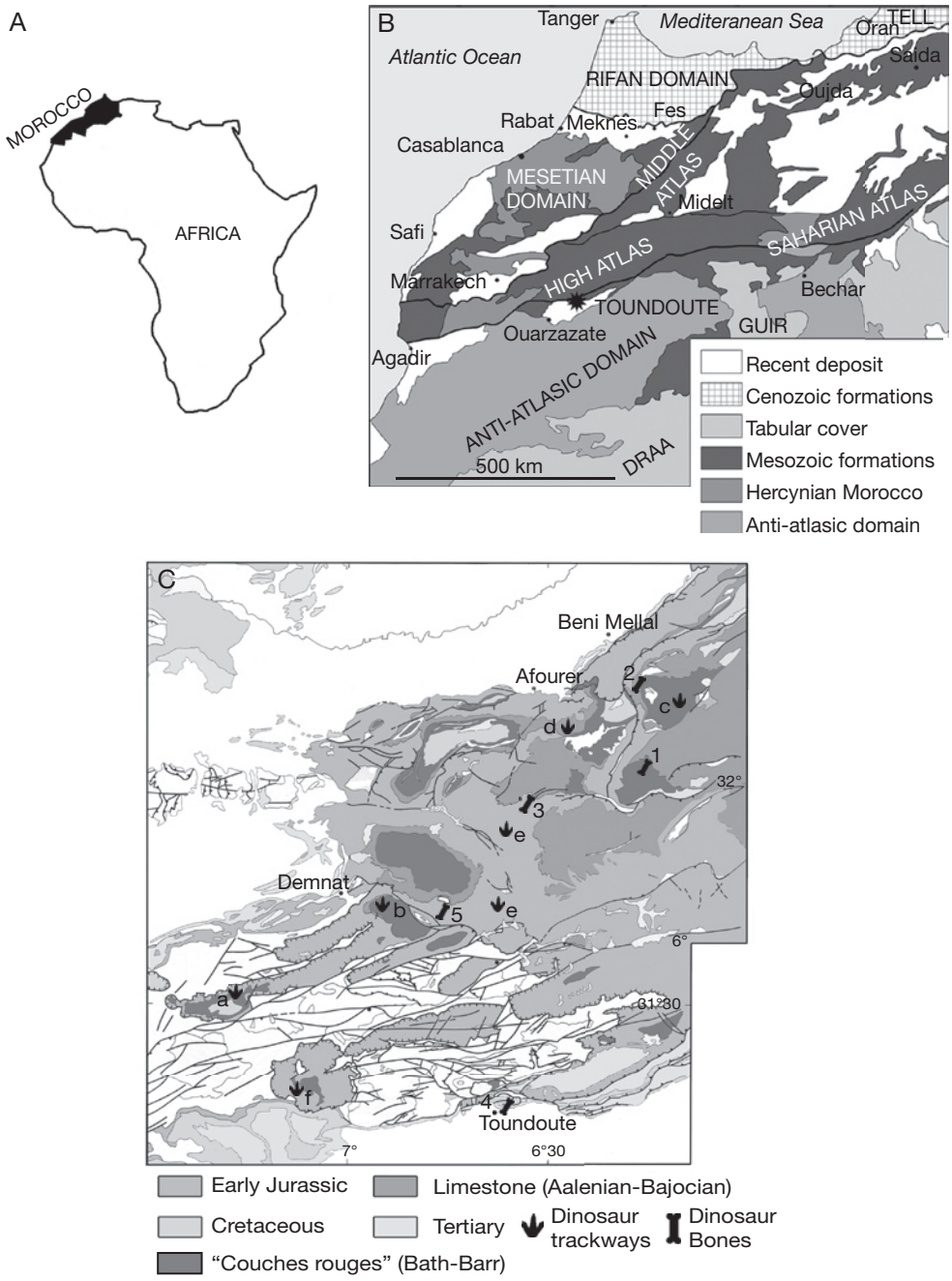

FIG. 1. — Location maps of the site of Toundoute where the remains of *Tazoudasaurus naimi* were found. **A**, **B**, geographic location; **C**, simplified geological map of the High Atlas Mountains (Morocco) showing the main fossil dinosaur tracks localities and taxa involved in the DinoAtlas Project. Abbreviations: **a**, Tamadout; **b**, Demnat; **c**, syncline of Taguelft; **d**, Bin el Ouidane; **e**, Aganane Formation; **f**, Aglagal; **1**, *Atlasaurus imelakei*; **2**, Sauropoda indet.; **3**, Sauropoda undescribed species; **4**, *Tazoudasaurus naimi*; **5**, Theropoda from Wazzant.

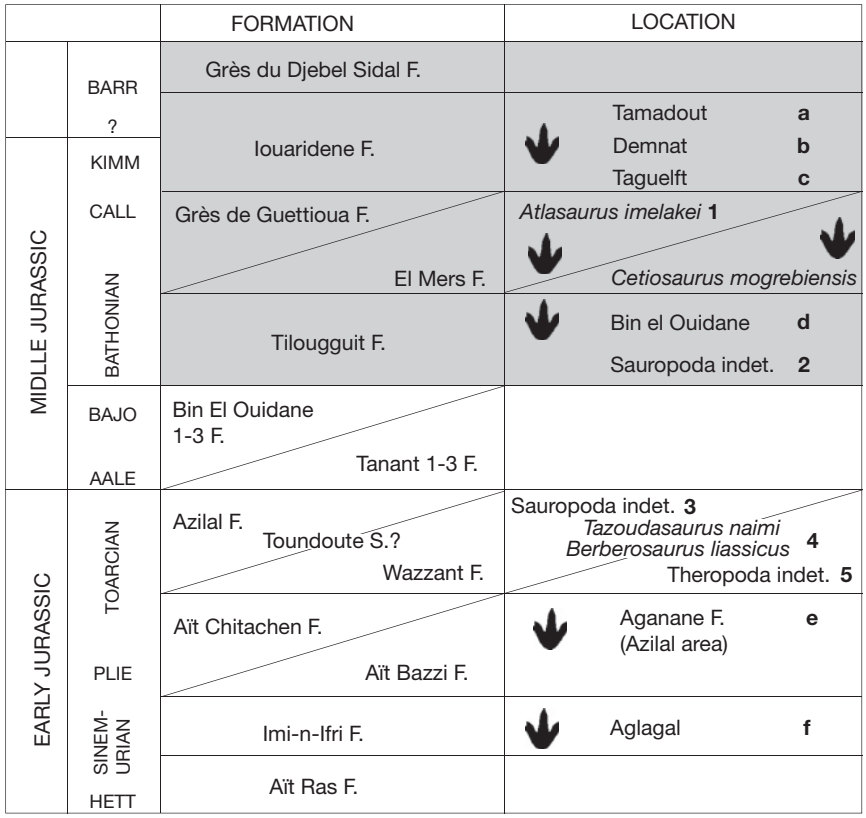

FIG. 2. — Stratigraphic distribution of the main fossil dinosaur tracks localities and taxa discovered in the High and Middle Atlas Mountains (Morocco): in grey, "couches rouges". Abbreviations: **a**, Tamadout; **b**, Demnat; **c**, syncline of Taguelft; **d**, Bin El Ouidane; **e**, Aganane Formation; **f**, Aglagal; **1**, *Atlasaurus imelakei*; **2**, Sauropoda indet.; **3**, Sauropoda undescribed species.; **4**, *Tazoudasaurus naimi*; **5**, Theropoda from Wazzant.

beyond the scope of this paper, but both specimens are currently in revision and their detailed description should be published shortly.

The continental Red beds complex is generally situated at the top of the Tillougguit Formation (Fig. 2), the alternating continental and marine facies of which is transitional to the Aaleno-Bajocian platform limestones of the Bin el Ouidane and Tanant formations (Jenny *et al.* 1981a). The Tillouguit Formation has yielded some sauropod remains, as well as dinosaurs tracks (Jenny *et al.* 1981b).

The Azilal Formation and its lateral equivalent the Wazzant Formation are the only continental units known from the Early Jurassic in the central High Atlas (Fig. 2). They are considered to be of Toarcian to Early Aalenian age (Jenny *et al.* 1980; Jenny 1985). The Azilal Formation has yielded sauropod remains (Termier 1942; Jenny *et al.* 1980), while small theropod skeletons, under preparation in the Muséum national d'Histoire naturelle, Paris, were found in Wazzant Formation (Jenny *et al.* 1980; Taquet 1984). It is very likely that the Toundoute continental series that has yielded *Tazoudasaurus* is a lateral equivalent of the Toarcian Azilal and Wazzant formations (Montenat *et al.* 2005). The Early Jurassic carbonated substratum of these continental formations have yielded numerous dinosaur trackways in the Pliensbachian Aganane Formation (Jenny & Jossens 1982; Ishigaki 1988), and in the Imi-n-Ifri Formation (Monbaron *et al.* 1985) (Figs 1; 2). Thus, the dinosaur fossil record for the Jurassic in the High Atlas is well sampled between the Sinemurian and the Kimmerdgian.

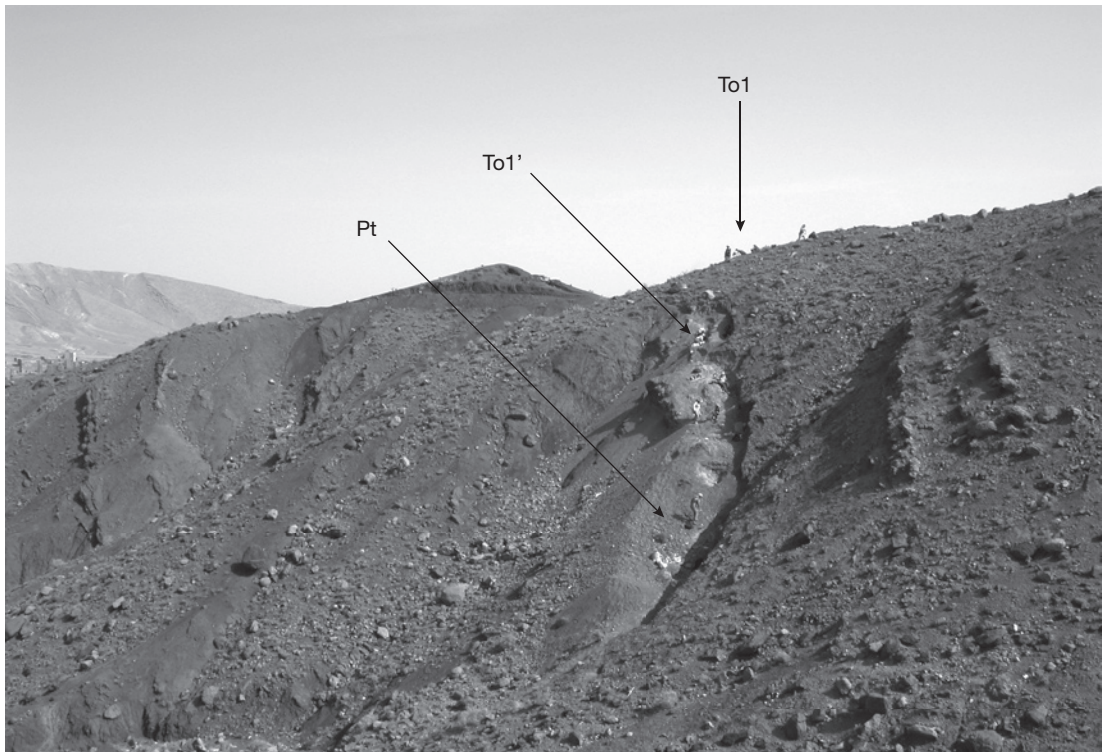

FIG. 3. — Upper bone-bed of the continental series of Toundoute. Picture of the upper bone-bed showing the different localities (To1; To1'; Pt) which have yielded dinosaur remains.

ABBREVIATIONS

MHNM	Muséum d'Histoire naturelle, Marrakech;
CPSGM	collections paléontologiques du Service géologique du Maroc, direction de la Géologie, ministère de l'Énergie et des Mines, Rabat.
acdl	anterior centrodiapophyseal lamina;
acpl	anterior centroparapophyseal lamina;
cpol	centropostzygapophyseal lamina;
cprl	centroprezygapophyseal lamina;
l.spol	lateral spinopostzygapophyseal lamina;
m.spol	medial spinopostzygapophyseal lamina;
pcdl	posterior centrodiapophyseal lamina;
pcpl	posterior centroparapophyseal lamina;
podl	postzygodiapophyseal lamina;
posl	postspinal lamina;
ppdl	parapodiapophyseal lamina;
prdl	prezygodiapophyseal lamina;
prpl	prezygoparapophyseal lamina;
prsl	prespinal lamina;
spdl	spinodiapophyseal lamina;
spol	spinopostzygapohyseal lamina;
sprl	spinoprezygapophyseal lamina;
tpol	intrapostzygapophyseal lamina;
tprl	intraprezygapophyseal lamina.

SYSTEMATICS

DINOSAURIA Owen, 1842
SAUROPODOMORPHA Huene, 1932
SAUROPODA Marsh, 1878
VULCANODONTIDAE Cooper, 1984
Genre *Tazoudasaurus*
Allain, Aquesbi, Dejax, Meyer, Monbaron, Montenat, Richir, Rochdy, Russell & Taquet, 2004

Tazoudasaurus naimi
Allain, Aquesbi, Dejax, Meyer, Monbaron, Montenat, Richir, Rochdy, Russell & Taquet, 2004
(Figs 4-44)

FIG. 4. — Femur and tibiae of *Tazoudasaurus naimi* found in close association in the locality To1'. **To1'-380**, right tibia; **To1'-381**, right femur; **To1'-382**, left tibia. Abbreviations: **4tr**, fourth trochanter; **lt**, lesser trochanter.

HOLOTYPE. — Material figured in the original publication (Allain *et al.* 2004) and belonging to a single individual: left mandible (CPSGM To1-275); left postorbital (CPSGM To1); right quadrate (CPSGM To1); tooth (CPSGM To1-20); three dorsal vertebrae in connection (CPSGM To1-38); distal chevron (CPSGM To1-129); right pubis (CPSGM To1-103); right astragalus (CPSGM To1-31); ungual phalanx of pedal digit II (CPSGM To1-114); left metatarsal II (CPSGM To1-265).

REFERRED MATERIAL. — The material described in this paper belongs to the holotypic specimen or to different adult or juvenile specimens.

HORIZON AND LOCALITY. — Douar of Tazouda, near the village of Toundoute in the Province of Ouarzazate, High Atlas of Morocco. Lower and upper bone-beds ("Fossil locality A (or To2) and B (or To1/Pt)" of Allain *et al.* 2004; Fig. 3) of the Toundoute continental series, middle to late Early Jurassic (Pliensbachian-Toarcian; Montenat *et al.* 2005).

REVISED DIAGNOSIS. — A primitive sauropod displaying the following autapomorphies: thin bony plate extending from the posterodorsal margin of the postorbital; vertically oriented elliptical foramen magnum; absence of cpol on the presacral vertebrae; distal chevrons bridged proximally and forked distally with unfused anterior and posterior processes; phalangeal formula of the manus is 2-3-2-2-2; developed medial bump on the anterior surface of the proximal end of the metatarsal IV.

DESCRIPTION

SKULL

For the moment, the skull of *Tazoudasaurus* is far from being complete but further works in the Toundoute Series raises the possibility of new finds of skull material in this area. Nevertheless, some disarticulated elements of the skull roof and of the braincase have been tentatively identified and are described here.

Fronto-parietal

The frontal and the parietal are incomplete, the former being broken anteriorly and the latter posteriorly. Most of the contact areas with the adjacent bones are damaged and the relations between the fronto-parietal and the postorbital, the squamosal, the prefrontal and the supraoccipital are not clear. The left frontal and parietal are firmly fused together, so that the oblique (posteromedial-anterolateral in ventral view) suture between the two bones is nearly indiscernible in dorsal view (Fig. 5D, E). The midline contact between both fronto-parietals, in contrast, is nearly smooth and lacks the fine interdigitations seen in most saurischians. The fronto-parietals form the widest part of the skull roof over the orbit and the supratemporal fenestra. The articulated frontals were probably longer anteroposteriorly than wide transversely. The dorsal surface of the frontal is flat posteriorly where it fuses with the parietal. The frontal participates posterolaterally in the anterior margin of the supratemporal fossa (Fig. 5D).

The parietal is nearly completely preserved, except for its posterior margin and for the distal end of the squamosal process (Fig. 5D, F). Unlike most sauropods but as in prosauropods, the parietal lacks an anterolateral process that contacts the postorbital, and thus is considerably wider posteriorly than anteriorly, and allows the frontal to contribute to the supratemporal fossa. Posteriorly, the flat dorsal surface of the parietal slopes slightly ventrally. The supratemporal fenestra was probably elliptical, with its long axis perpendicular to that of the skull. Although it is eroded, the posteromedial corner of the parietal is very thickened ventrally where it contacts the supraoccipittal (Fig. 5E).

Postorbital

The left postorbital was already figured in the original publication naming *Tazoudasaurus* (Allain *et al.* 2004: fig. 2k). The distal tip of both the ventral and anterior processes are missing (Fig. 5A, B), but the ventral process was longer than the dorsal. The ventral process is narrower transversely than anteroposteriorly, whereas the anterior process is wider dorsomedially than deep dorsoventrally. The ventral process narrows anterposteriorly towards its distal end. Although it is broken in its distal part, the anterior process curves inwards to contact the frontal. In dorsal view, a shallow supratemporal fossa is present on the medial side of the anterior process of the postorbital. The postorbital contacts the squamosal posteriorly through a thin and dorsoventrally expanded bony plate, which probably overlapped laterally the anterior process of the squamosal. This condition differs from the transversal and planar postorbital-squamosal articulation of *Nemegtosaurus* Nowinski, 1971, but also from the typical tongue-and-groove articulation of other sauropods (Wilson 2005c). There is no orbital ornamentation on the three processes of the postorbital (Fig. 5A).

Squamosal

The dorsal margin of the recovered right squamosal is eroded and the distal end of its ventral and anterior processes are broken (Fig. 5H, I). Thus, only the stout part of the squamosal surrounding the quadrate fossa and the posterodorsal corner of the lateral temporal fenestra is preserved. In lateral view, the squamosal consists of an anterior, a posterior, and a ventral processes. The anterior process is thin, probably plate-like, and would have contacted anteriorly the postorbital to form the temporal bar. The hook-shaped posterior process defines a deep socket that receives the head of the quadrate (Fig. 5I). Medially to the quadrate socket, the posterior part of the squamosal is also expanded to form a small bulge which likely contacted the distal end of the paroccipital process (Fig. 5H). The ventral process, which tapers towards its distal end, forms the posterior margin of the lateral temporal fenestra and a shallow lateral temporal fossa is preserved on its anterodorsal aspect (Fig. 5I).

Quadrate

The right quadrate was also already figured in the original publication of *Tazoudasaurus* (Allain *et al.* 2004: fig. 2c, d). The head of the quadrate, which contacts the squamosal as well as the anterior part of the pterygoid flange, is broken (Fig. 5F, G). In posterior view, the dorsal two thirds of the quadrate shaft is bent slightly laterally as in *Plateosaurus* Meyer, 1837. The posterior surface of the quadrate is flat to nearly convex transversely and lacks the quadrate fossa seen in other sauropods (Fig. 5G). The preserved basal portion of the pterygoid flange is very thin transversely, especially in its dorsal part (Fig. 5F). It seems the pterygoid flange was directed

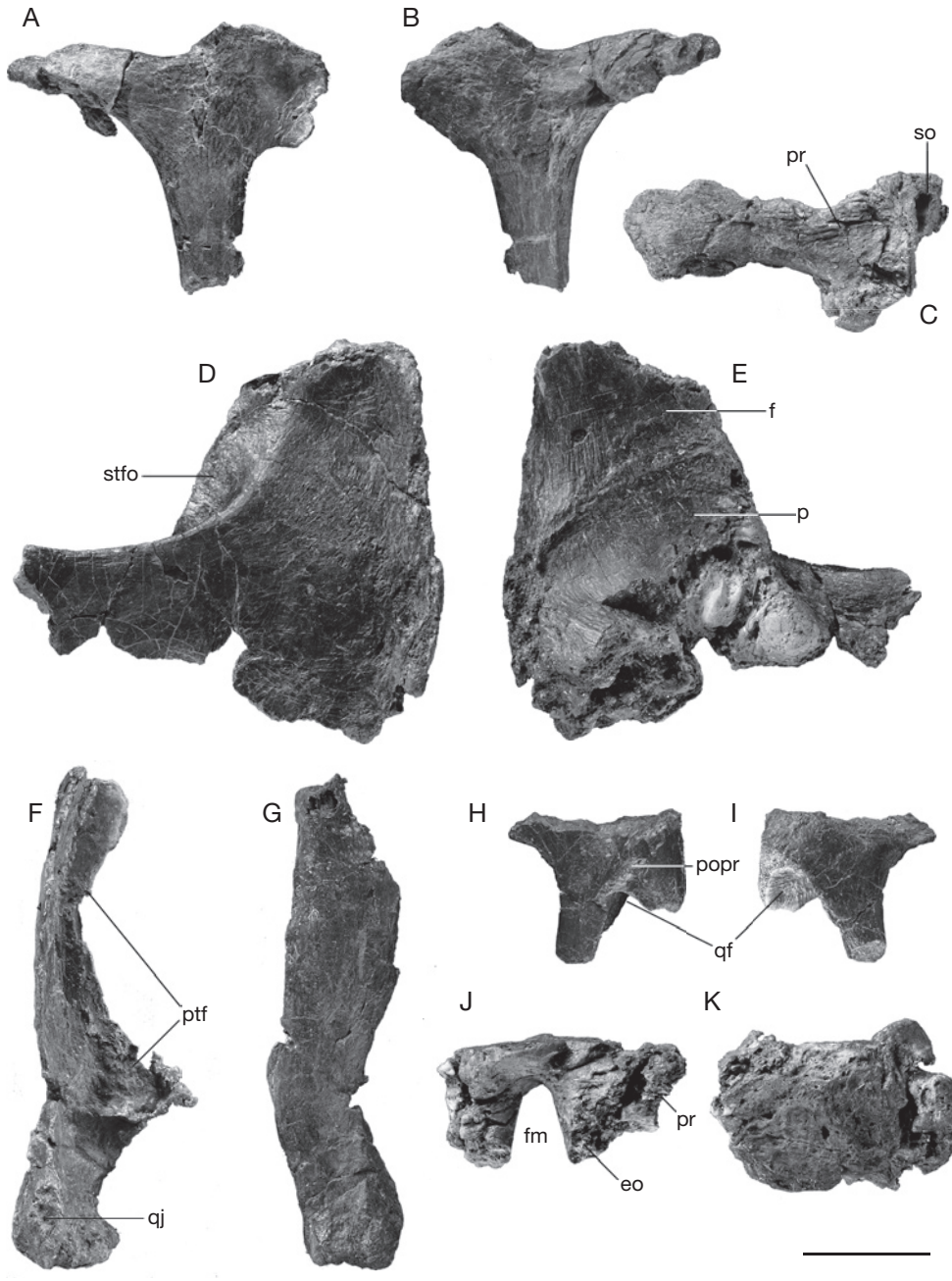

FIG. 5. — *Tazoudasaurus naimi*, skull elements: left postorbital in lateral (**A**) and medial (**B**) views; right exoccipital-opisthotic in anterior view (**C**); left frontoparietal in dorsal (**D**) and ventral (**E**) views; right quadrate in lateral (**F**) and posterior (**G**) views; right squamosal in medial (**H**) and lateral (**I**) views; supraoccipital in posteroventral (**J**) and posterodorsal (**K**) views. Abbreviations: **eo**, exoccipital; **f**, frontal; **fm**, foramen magnum; **p**, parietal; **popr**, paroccipital process; **pr**, prootic; **ptf**, pterygoid flange; **qf**, quadrate fossa; **qj**, quadratojujal facet; **so**, supraoccipital; **stfo**, supratemporal fossa. Scale bar: 3 cm.

mainly anteriorly and very slightly medially. A rugose, V-shaped scar for the quadratojugal is present on the distolateral surface of the quadrate (Fig. 5F). It extends proximally one third of the preserved length of the quadrate body. The articular condyle of the quadrate is slightly eroded distally. It is wider transversely than long anteroposteriorly and has convex posterior margin and slightly concave anterior margin.

Supraoccipital

The supraoccipital is a median element that forms the entire dorsal margin of the foramen magnum (Fig. 5J, K). It contacts the the skull roof via the parietal anterodorsally but the suture between the two bones is too eroded to be described. The lateral "wings" of the supraoccipital are broken distally. Two strong processes project anterolaterally from the skull roof of the supraoccipital and bear two thick, rugose intersected sutural surfaces for the exoccipital lateroventrally and for the prootic anterolaterally (Fig. 5J). The posterodorsal surface of the supraoccipital is nearly flat and strongly compressed. Although it is eroded, it bears a median triangular ridge, the anterodorsal extension of which can not be determined (Fig. 5K). In posteroventral view, the supraoccipital part of the foramen magnum is semi-elleptical with a vertically directed great axis (Fig. 5J).

Exoccipital-opisthotic

The right exoccipital-opisthotic is completely preserved, even if it is somewhat eroded in its medial portion where it contacts the supraoccipital and the basioccipital, precluding the recognition of the exits of cranial nerves (Fig. 5C). The exoccipital and opisthotic are firmly fused to each other, with no trace of a suture, and extend laterally as the paroccipital process. The exoccipital forms the entire lateral border of the foramen magnum. It also has a small contribution to the occipital condyle, forming its dorsolateral margin. It contacts dorsomedially the supraoccipital and ventromedially the basioccipital through rugose interdigitating sutural surfaces. The prootic extended against the furrowed anterior surface of the opisthotic, over the proximal half of the length of the paraoccipital process (Fig. 5C). The paroccipital process was mainly directed laterally. The paroccipital process is wider anteroposteriorly than deep dorso-ventrally at its base, and expands dorsoventrally at its distal end to articulate with the squamosal. It is slightly constricted along its dorsal margin prior to this distal expansion, where it presumably formed the ventral margin of the posttemporal foramen.

LOWER JAW

The lower jaws of *Tazoudasaurus* are known by a complete left mandible (CPSGM To1-275; Fig. 6), by the median part of a right dentary, and by the anterior end of a left dentary of another individual (MHNM To1-223; Fig. 7G). The left mandible is crushed at the level of the last three dentary alveoli. Thus, the posterior part of the dentary and most of the splenial are damaged, and the posterior portion of the mandible including the angular, the prearticular and the surangular is rotated about 45° dorsally relative to the tooth row, but is not distorted and the different mandibular bones are still in connection. Therefore, the jaw articulation should be below the mandibular tooth row, as in other sauropods. The coronoid and the articular have not been preserved. The complete disarticulation of the dentary symphysis suggests a weak connection between the left and right lower jaws. Given the restricted inward anterior curvature of the dentary, the articulated mandibles was to form more a V-shaped structure in dorsal view, rather than the U-shaped outline seen in later sauropods (e.g., *Shunosaurus* Dong, Zhou & Zhang, 1983, *Omeisaurus* Young, 1939), although the anterior end of the conjoined mandibles was more rounded than in prosauropods. Proportionally, the lower jaw is extremely slender and deepest in the external mandibular fenestra region. Although it is damaged anteriorly, this latter was clearly present in *Tazoudasaurus* ahead of the surangular, and was probably bounded anteriorly and ventrally by the dentary and the angular respectively (Fig. 6).

Dentary

The left dentary To1-275 is about 240 mm long and is more than half the length of the jaw. It is 55 mm deep at the symphysis. The minimum depth of the dentary ramus is 44 mm at the level of the 8th alveolus. Thus, the maximum depth of the dentary at the symphysis is 125% of the minimum depth of the ramus, which means more than in prosauropods,

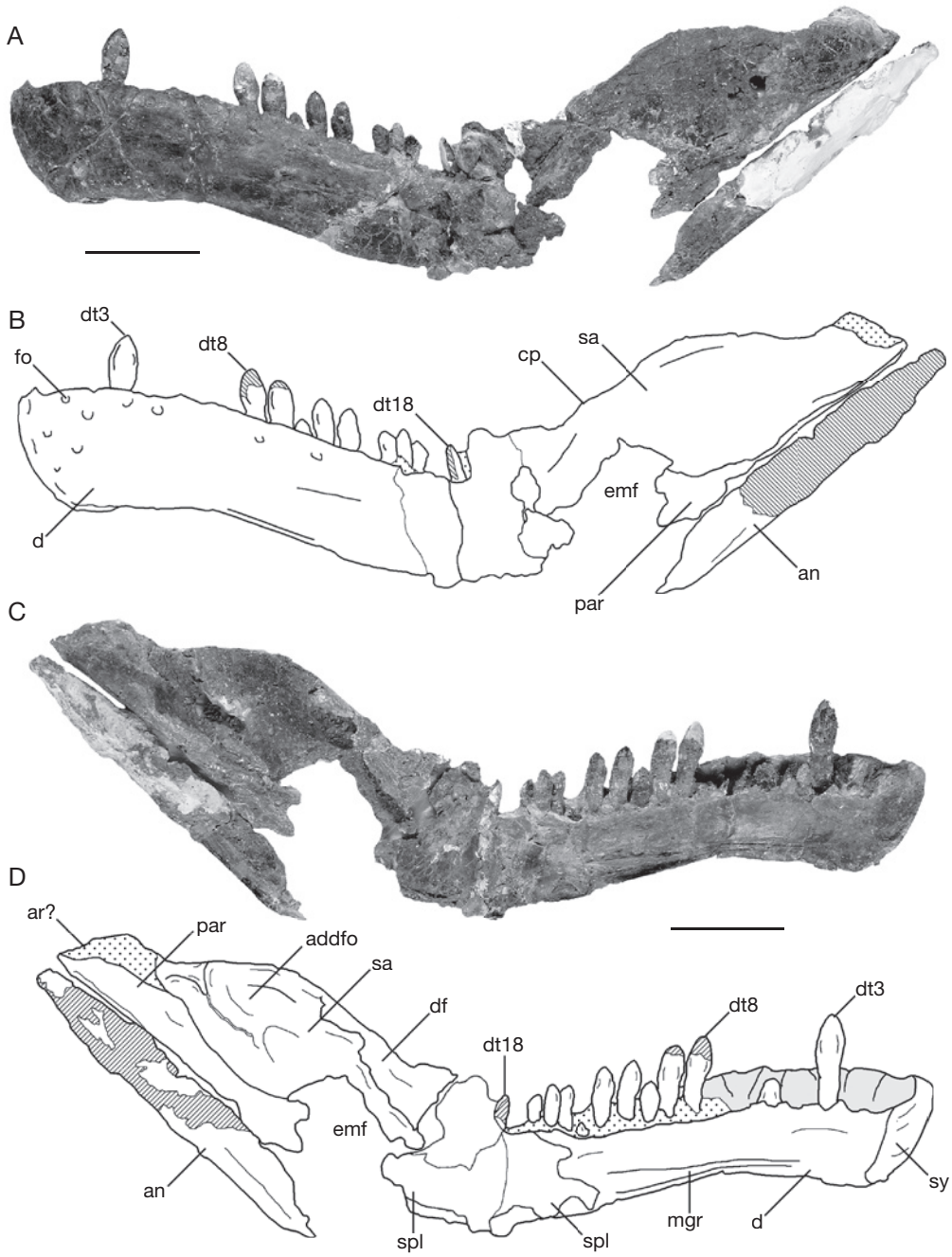

FIG. 6. — *Tazoudasaurus naimi*, left mandible (To1-275): **A**, **B**, lateral view; **C**, **D**, medial view. Abbreviations: **addfo**, adductor fossa; **an**, angular; **ar**, articular; **cp**, coronoid process; **d**, dentary; **df**, surangular facet for articulation with dentary; **dt**, dentary tooth; **emf**, external mandibular fenestra; **fo**, foramen; **mgr**, Meckel's groove; **par**, prearticular; **sa**, surangular; **spl**, splenial; **sy**, symphysis. Arabic numerals indicate dental tooth position. Scale bars: 5 cm.

but less than in more advanced dinosaurs such as Shunosaurus or Omeisaurus (Wilson & Sereno 1998). The slight curvature of the dentary toward the midline begins at the level of the 5th alveolus.

In lateral view, the dorsal margin of the dentary is convex, but the ventral margin is concave. Several nutrient foramina are found anteriorly and dorsally below alveoli, on the lateral surface of the dentary (Fig. 6A, B). The dentary is slightly dorsoventrally expanded posteriorly. It contacts the surangular posterodorsally, and probably the angular posteroventrally, but due to the damage of this area, it is not clear if the posterior portion of the dentary is divided into well distinct dorsal and ventral rami.

In medial view, the dorsoventral axis of the symphyseal surface angles anteriorly to the long axis of the dentary. It is triangular with a narrow ventral apex and broad dorsal base. On the medial surface of the dentary, there is a well-defined longitudinal Meckelian groove which extends forward almost to the fifth alveolus (Fig. 6C, D). This groove deepens posteriorly and was likely overlapped by the splenial medially.

The dentary is dentigerous over almost all its length, possessing 18 alveoli (not 20 as it has been previously stated, Allain *et al.* 2004). The tooth row begins just posterior to the symphysis. The alveoli in the dentary decrease in size posteriorly. The medial interdental plates are not fused and are consistently lower than the lateral plate (Fig. 6C, D). Replacement foramina are visible on the medial margin of the tooth row between the interdental plates. Functional teeth are visible in the alveoli 3, 8, 9, 11, 12, 14-16 and 18. Only tooth tips can be observed in the alveoli of teeth 5, 10, and 13. Replacing teeth appear on the lingual surface of the functional tooth in the left dentary To1-223 at tooth positions 1, 3, 4, and 8.

Splenial

The splenial (Fig. 6C, D) is badly crushed and its overall morphology is difficult to assess. In medial view, it contacts the surangular posterodorsally and the dentary anteroventrally. The splenial likely continued anteriorly nearly to fifth alveolus, as indicated by the well-defined Meckelian groove on the dentary, but its posterior extension is not determinable, even if it would have also contact the angular posteroventrally.

Surangular

The left surangular is nearly complete, except for its thin central portion (Fig. 6). It is an elongate and deep plate that covers the posterodorsal region of the lower jaw in lateral view (Fig. 6A, B). The surangular forms the outer wall of the adductor fossa and is convex dorsoventrally and anteroposteriorly in lateral view. The ventral margin is slightly damaged but was straight or gently convex, and its posterior portion was overlapped laterally by the angular. The dorsal margin of the surangular is only very slightly convex, except its concave posterior half that slopes towards the articular. Thus, the coronoid process is not very prominent as in prosauropod. A sharply rised coronoid process is found in macronarians, rebacchisaurids but also in *Omeisaurus* (He *et al.* 1988). Neither the anterior nor the posterior surangular foramen has been identified on the lateral surface of the surangular. The dorsal margin of the surangular is thickened medially. The medial surface of the coronoid region of the surangular bears a facet for the distal end of the posterodorsal ramus of the dentary (Fig. 6C, D). This facet stretches ventrally and borders dorsally and medially the coronoid fossa. The adductor fossa is bordered posteroventrally by a thin and prominent ridge.

Angular

The angular is broken posteriorly and anteriorly, but a fossil impression of its medial surface was preserved and casted (Fig. 6 C, D). The angular is a long and thin plate that forms the base of the posterior half of the lower jaw. It is very shallow dorsoventrally and tapers posteriorly towards the jaw joint and anteriorly towards its articulation with the dentary. The ventral margin of the angular is nearly straight. It is thick and rounded, but thins to a narrow dorsal margin.

Prearticular

The prearticular is broken anteriorly. The prearticular is visible in medial view, where it forms the medial wall of the adductor fossa, and slightly in lateral view because the ventral margin of the surangular is broken (Fig. 6A, B). As the angular, the prearticular has the form of an elongate, horizontal thin plate. Its ventral margin is nearly straight. It has been slightly rotated laterally and is pressed against

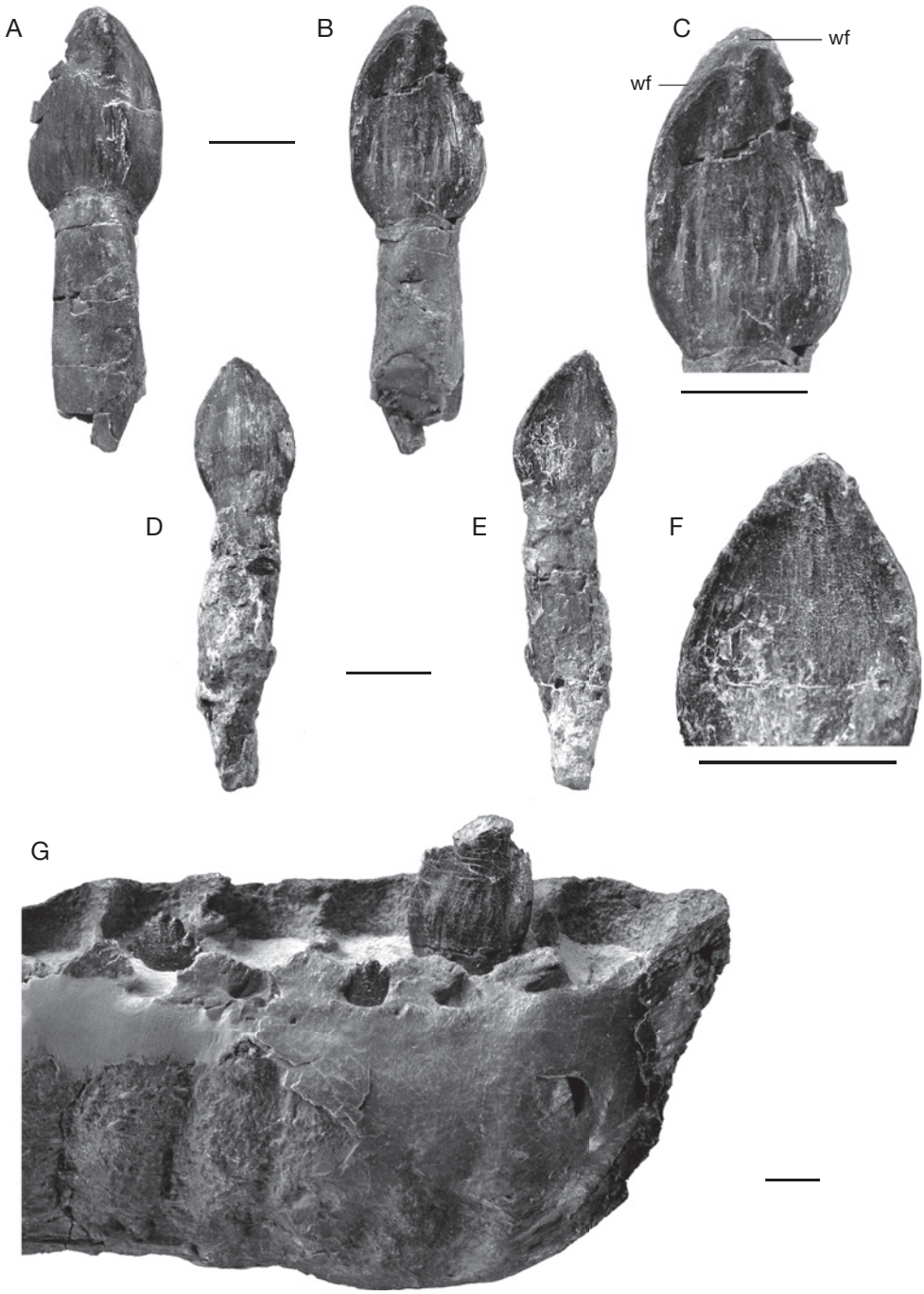

FIG. 7. — *Tazoudasaurus naimi*, teeth (To2-43; To1-20): **A**, **D**, labial view; **B**, **E**, lingual view; **C**, **F**, detailed view of the lingual side; **G**, detailed medial view of the left dentary (To1-223). Abbreviation: **wf**, wear facet. Scale bars: 1 cm.

the medial surface of the surangular. Thus, the narrow and elongate lateral surface, which articulates with the angular, is in ventral position.

Teeth

Nearly complete crowns are preserved in the tooth row of the dentaries To1-223 and To1-275, and numerous additional isolated teeth have been found in Toundoute. As discussed above, there are 18 teeth in the lower jaws. The teeth are angled slightly anteriorly relative to the long axis of the dentary and adjacent crowns overlap (Fig. 6). All the teeth found in Toundoute are D-shaped in cross section at mid-crown. They are also asymmetrical in lingual and labial views, the mesial margin of the crown being less vertical and more convex than the distal margin. The labial side of the crown is strongly convex both mesiodistally and vertically (Fig. 7A, D), whereas the lingual side is only very slightly concave (Fig. 7B, E). The crowns are broad and expand from their roots before they taper near their apex. As in all sauropods, the enamel is wrinkled throughout the crown and coarse vertical ridges are visible on the ventral part of the lingual side of the crown (Fig. 7B, C). As in prosauropods and some basal sauropods, conical denticles are present on the mesial and distal margins of the crown of *Tazoudasaurus* (Fig. 7G). The long axis of each denticle is angled toward the apex of the crown. In most posterior teeth, the number of denticles is greater on the distal margin. In some fully erupted or isolated teeth, the marginal denticles are no more visible and V-shaped wear facets develop along the mesial and distal margins of the crown (Fig. 7B, C), suggesting a precise occlusion in which the upper and lower tooth crowns interdigitated during jaw closure.

CERVICAL VERTEBRAE

Axis

Neither the axial intercentrum, which was not fused with the pleurocentrum, nor the odontoid have been preserved, and only the axial pleurocentrum (MHNM To1-239) is described here (Fig. 8). The centrum is elongate, with its length more than twice its height, and is slightly taller than broad anteriorly, but broader than tall posteriorly (Table 1). The posterior face is deeply concave to receive the convex anterior face of the third cervical centrum (Fig. 8C, D). The neural canal is broad and circular throughout its length (Fig. 8C, D). The centrum is pinched laterally but has no pneumatic fossae (Fig. 8A, B). Neither the axial pleurocentrum nor neural arch of *Tazoudasaurus* exhibits the marked external pneumatic structures seen in more advanced sauropods (Wilson & Mohabey 2006). The parapophysis seems to be positioned on the anteroventral corner of the centrum, although this region is slightly crushed (Fig. 8A, B). The ventral surface of the centrum is concave anteroposteriorly and bears a prominent midline keel. The neural arch extends the full length of the centrum, and there is no trace of the neurocentral suture. The neural arch is 1.49 times the height of the centrum (Table 1). Only the left elements of the neural arch are preserved and described here. With only five laminae (Wilson 1999), the neural arch lamination of the axis of *Tazoudasaurus* is more rudimentary than in other cervical vertebrae (see below). The diapophysis is broken distally but should have a reduced size (Fig. 8E, F). The centrodiapophyseal laminae are not readily distinguishable on the axis of *Tazoudasaurus*. In contrast with *Patagosaurus* Bonaparte, 1979 and *Omeisaurus*, it seems that the acdl is absent (Table 2), whereas the pcdl is developed as a faint but broad ridge extending posteroventrally from the diapophysis (Fig. 8A, B). The prezygapophysis is weakly developed and does not project from the neural arch. It forms the roof of the neural canal and is directed dorsolaterally. The left prezygapophysis is at the same height as the diapophysis, and the prdl is thus horizontal. The postzygapophysis is more developed than the prezygapophysis and extends posteriorly and laterally beyond the centrum (Fig. 8). As a consequence, a relatively large postspinous fossa is present posteriorly (Fig. 8C, D). The podl is well developed on the lateral side of the neural arch (Fig. 8A, B), and tpol laminae are also present posteriorly. Unlike other sauropods (Table 2), the cpol laminae are lacking except if they are autapomorphically merged with the lateral margin of the neural canal and the tpol. The postzygapophyseal articular facet is not visible in lateral view. The neural spine is convex in lateral view and differs from the Chinese sauropods such as *Omeisaurus* (He *et al.* 1988), *Shunosaurus* (Zhang 1988), and *Mamenchisaurus* Young, 1954 (Young & Zhao 1972), and the Rutland *Cetiosaurus* Owen, 1841

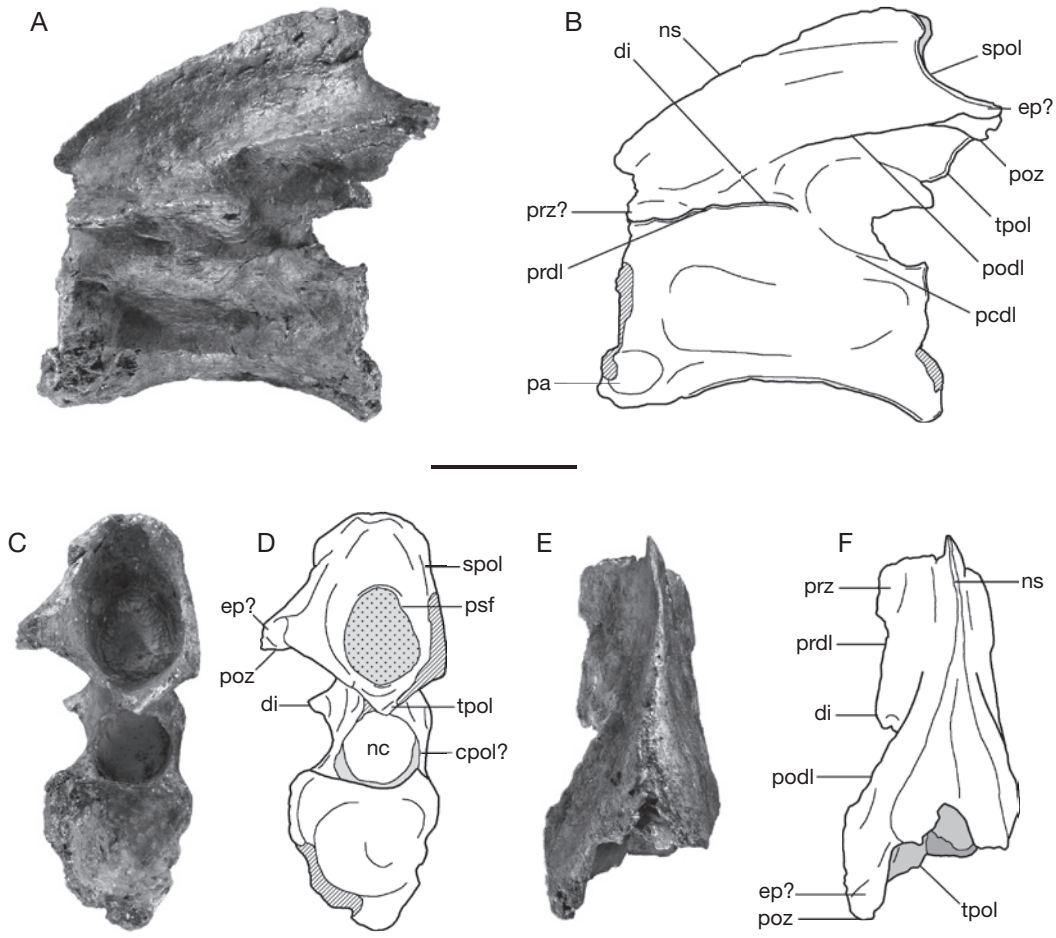

FIG. 8. — *Tazoudasaurus naimi*, axis (To1-239): **A**, **B**, left lateral view; **C**, **D**, posterior view; **E**, **F**, dorsal view. Abbreviations: **cpol**, centropostzygapophyseal lamina; **di**, diapophysis; **ep**, epipophysis; **nc**, neural canal; **ns**, neural spine; **pa**, parapophysis; **pcdl**, posterior centrodiapophyseal lamina; **podl**, postzygodiapophyseal lamina; **poz**, postzygapophysis; **prdl**, prezygodiapophyseal lamina; **prz**, prezygapophysis; **psf**, postspinal fossa; **spol**, spinopostzygapophyseal lamina; **tpol**, intrapostzygapophyseal lamina. Scale bar: 5 cm.

(Upchurch & Martin 2002). The neural spine is flattened laterally, except in its most posterior part (Fig. 8E, F) and reaches maximum height near the posterior margin of the centrum. The spol are clearly visible in both lateral and dorsal views.

Middle cervical vertebrae

For the moment, only two cervical vertebrae of *Tazoudasaurus* (MHNM To1-354; MHNM To1-64) have been prepared, but according to field observations, at least another five cervical vertebrae have been recovered in Toundoute. According to the length of the centra (Table 1), the position and orientation of their parapophyses and the orientation of the pcdl, To1-354 (Fig. 9) is a more anterior cervical vertebra than To1-64 (Fig. 10), probably a middle cervical vertebra. Only the centrum and a small part of the neural arch of To1-64 are preserved, whereas To1-354 is nearly complete except for the prezygapophyses and the neural spine. The length/height ratios for both cervicals are around 2.5, substantially less than in *Omeisaurus*, *Mamenchisaurus*, *Euhelopus* Romer, 1956, *Rapetosaurus* Curry Rogers & Forster, 2001 or diplodocids. The anterior and posterior articular

TABLE 1. — Measurements (in mm) of some vertebrae of *Tazoudasaurus naimi*. Abbreviations: **e**, estimated; **Lc**, length of centrum; **Antw**, width of centrum on its anterior surface; **Medw**, width of centrum on its median part; **Posw**, width of centrum on its posterior surface; **Anth**, height of centrum on its anterior surface; **Posh**, height of centrum on its posterior surface; **H**, total height; **Nah**, height of neural arch; **Nsh**, height of neural spine; **Przw**, width across prezygapophyses; **Nsl**, length of neural spine; **Nsw**, width of neural spine; *****, slightly bent specimen.

Specimen	Lc	Antw	Medw	Posw	Anth	Posh	H	Nah	Nsh	Przw	Nsl	Nsw
Cervical												
To1-239 (axis)	121e	40e	16	50	44	49	145	73	49	–	108	6e
To1-354	250	66	48	90e	82	97	290e	150e	–	–	35	–
To1-64*	260	68	48	85	100	110	–	–	–	–	–	–
Dorsal												
To1-69	85	95	70	165	130	145	500	350	155	150e	25	127
To1-38a	122	110			127		400					
To1-38b	120	110			127		390					
To1-38c	120	110			127		?					
To1-156	101	140	87	137e	136	140	465	330	180	100	55	70
Caudal												
To1-100	78	148	82	165	170	182	–	–	–	??	70	16
To1-288	88	117	83	121	146	147	–	–	–	–	65e	–
To1-88	141	105	55	93	142	152	265	120	108	47	62	18
To1-303a*	115	–	–	–	117	–	330	220	123	45	66	13,3
To1-303b*	107	–	–	–	115	–	330	205	124	–	72	10
To1-303c*	110	–	–	–	–	–	320	200	123	–	65	11

surfaces of the centra are higher than broad (Table 1). The centra are strongly opisthocoelous. The ventral margin of the concave posterior articular surface projects more posteriorly than the dorsal margin (Fig. 10A, B). The ventral surface is anteroposteriorly concave (Figs 9A, B; 10A, B). Transversely, this surface is deeply concave between the parapophyses and becomes flat to nearly convex towards the posterior end. Two deep fossae invade the anterior part of the ventral surface of the centrum between the parapophyses. They are bordered anteriorly by prominent lateral ridges and separated by a high longitudinal midline keel (Figs 9E, F; 10C, D) that extends posteriorly and decreases in height. The parapophyses are situated at the anteroventral corner of the lateral surface of each centrum. The articular surfaces of the parapophyses are circular (Figs 9E, F; 10A, B). There is a depression on the lateral sides of the centrum that is very shallow and restricted to the anterior centrum in To1-354 (Fig. 9A, B), and it is deeper and more posteriorly extended in To1-64 (Fig. 10A, B). In the latter, a second depression (pleurocoel?) seems to hollow out the median area of the right lateral surface of the centrum. Such a depression is not well-defined on the left lateral surface, but the septum between left and right depressions (pleurocoels?) is very thin.

Nothing of the neural arch of To1-64 is preserved but the pcdl and acdl which meet at right angle (Fig. 10A, B). The distribution of the vertebral laminae as defined by Wilson (1999) and discussed below is given in Table 2. The neural arch lamination of To1-354 is well developed as in other primitive sauropods. The distal end of the right prezygapophysis is broken but was projected forwards beyond the anterior end of the articular surface of the centrum (Fig. 9A, B). The prezygapophysis is supported from below by a large, undivided, anterodorsally directed cprl (Fig. 9G, H). It is joined to the neural spine by a prominent, anterolaterally directed sprl (Fig. 9C, D). A third lamina joins medially the prezygapophysis to the top of the neural canal (Fig. 9C, D, G, H). This lamina is arched dorsomedially and contacts the median dorsal margin of the neural canal. This lamina is clearly homologous to the tprl described by Wilson (1999). In *Apatosaurus* Marsh, 1877 (Wilson 1999) or *Cetiosaurus* (Upchurch & Martin 2002), the tprl's meet above the neural canal and connect the latter

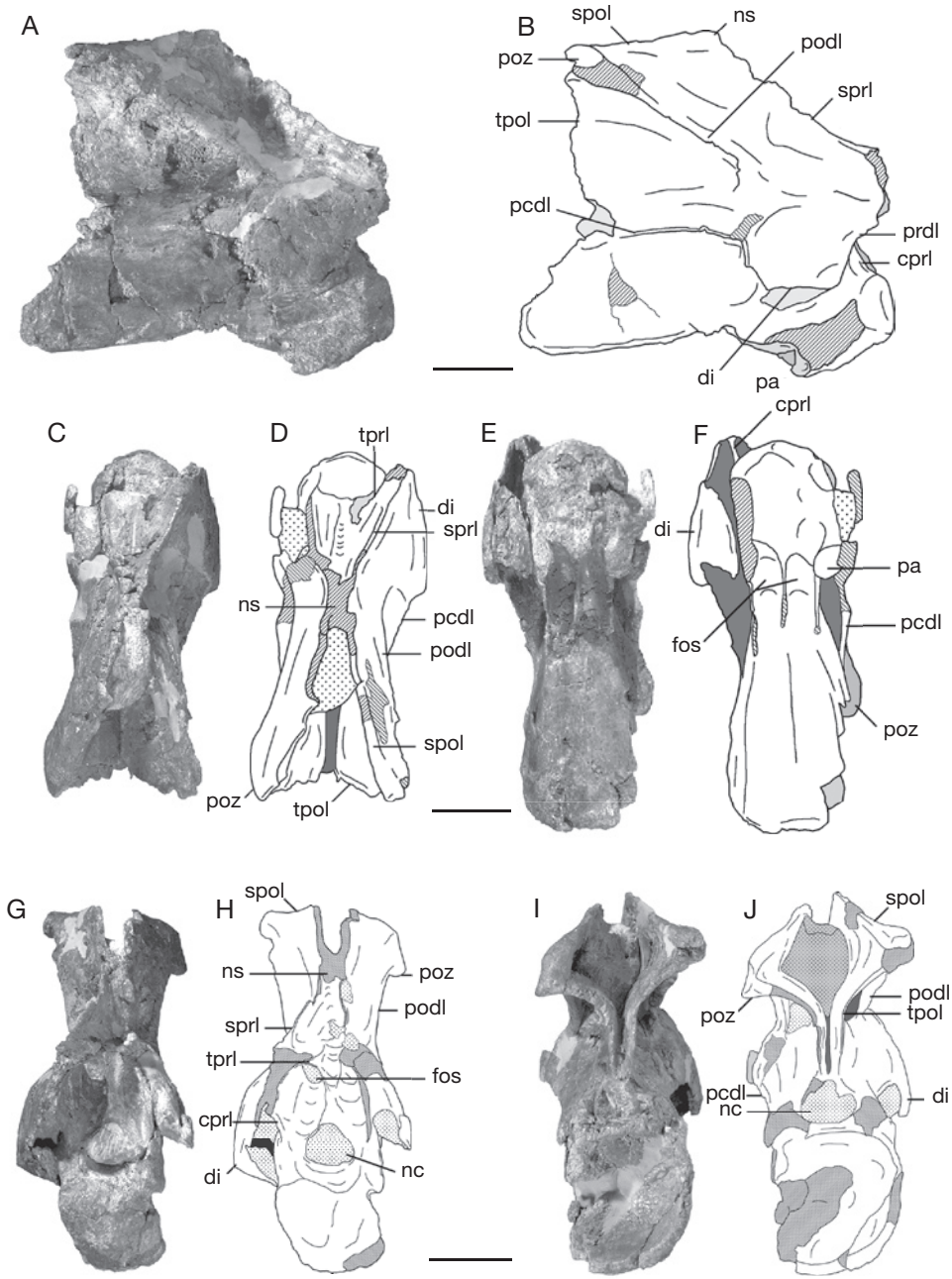

FIG. 9. — *Tazoudasaurus naimi*, cervical vertebra (To1-354): **A**, **B**, right lateral view; **C**, **D**, dorsal view; **E**, **F**, ventral view; **G**, **H**, anterior view; **I**, **J**, posterior view. Abbreviations: **cprl**, centroprezygapophyseal lamina; **di**, diapophysis; **fos**, fossa; **nc**, neural canal; **ns**, neural spine; **pa**, parapophysis; **pcdl**, posterior centrodiapophyseal lamina; **podl**, postzygodiapophyseal lamina; **poz**, postzygapophysis; **prdl**, prezygodiapophyseal lamina; **spol**, spinopostzygapophyseal lamina; **sprl**, spinoprezygapophyseal lamina; **tpol**, intrapostzygapophyseal lamina; **tprl**, intraprezygapophyseal lamina. Scale bars: 5 cm.

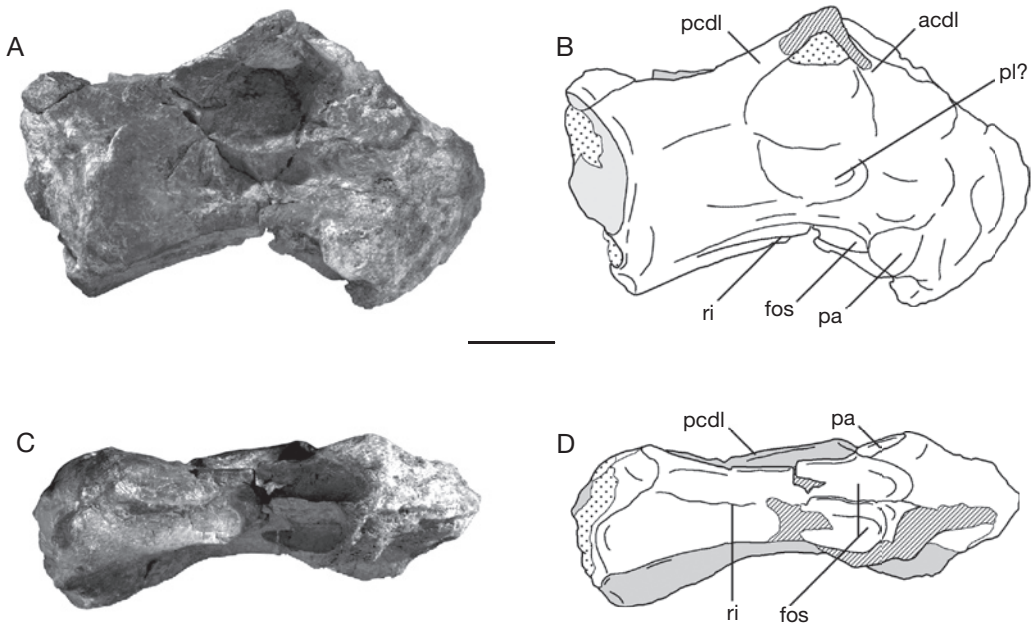

FIG. 10. — *Tazoudasaurus naimi*, cervical vertebra (To1-64): **A**, **B**, right lateral view; **C**, **D**, ventral view. Abbreviations: **acdl**, anterior centrodiapophyseal lamina; **fos**, fossa; **pa**, parapophysis; **pcdl**, posterior centrodiapophyseal lamina; **pl**, pleurocoele: **ri**, ridge. Scale bar: 5 cm.

via a vertical strut, the "anterior midline lamina" of Upchurch & Martin (2002). In *Tazoudasaurus* but also in *Patagosaurus*, the left and right tprl's do not contact each other above the neural canal, and form the lateral walls of a deep furrow which extends posteriorly above the neural canal as far as the neural spine, within the "prespinal fossa" (Fig. 9G, H). According to this conformation, the anterior midline lamina of Upchurch & Martin (2002) is nothing else than the ventromedial portion of the conjoined tprl's. In anterior view the tprl, cprl, and the dorsolateral margin of the neural canal form a dorsoventrally elongate elliptical hollow, that is deeply excavated posteriorly (Fig. 9C, D, G, H). In lateral view, the prdl runs posteroventrally from the prezygapophysis to join the diapophysis (Fig. 9A, B). The transverse process is a broad plate that is located on the anteroventral part of the lateral surface of the neural arch. It curves strongly downwards (Fig. 9G, H), and the acdl is not visible in lateral view. The pcdl extends posteriorly where it merges with the centrum at the level of the neurocentral suture. As the transverse process, the pcdl is also curved ventrally, and the fossa bounded by the acdl and the pcdl below the diapophysis is not visible in lateral view. The podl is the stoutest lamina of the neural arch. It joins the dorsal surface of the transverse process to the anterior margin of the postzygapophysis. It is directed posterodorsally nearly parallel to the sprl, and slopes posteroventrally (Fig. 9I, J). The postzygapophyses are high above the centrum. The articular facets of the postzygapophyses are slightly concave lateromedially and face downwards (Fig. 9I, J). In posterior view, the cervical vertebrae of *Tazoudasaurus* are characterized by the lack of cpol (Fig. 9I, J), which is present in other basal sauropods such as *Omeisaurus*, *Mamenchisaurus* or *Patagosaurus* (Table 2). The only laminae visible on the posterior face of the neural arch originate from the medial margin of the postzygapophyses and project first medially, then ventrally to contact the median dorsal margin of the neural canal (Fig. 9I, J). These laminae are clearly homologous to the tpol as described by Wilson (1999). As with the tprl's, the left and right tpol do not contact each other

TABLE 2. — Distribution of vertebral laminae in various vertebrae of *Tazoudasaurus naimi* and other sauropods, following the nomenclature of Wilson (2002). Abbreviations: **0**, absent; **1**, present; **?**, unknown; **–**, not applicable (parapophyseal laminae are not considered when parapophyses are only located on the centrum); Abbreviations: **ant.**, anterior; **cerv.**, cervical; **dors.**, dorsal; **mid.**, middle; **post.**, posterior; see also abbreviations p. 350. Differences between *Tazoudasaurus* and the other sauropods are in bold.

	acdl	pcdl	prdl	spdl	podl	ppdl	cprl	sprl	tprl	cpol	spol	m.spol	l.spol	tpol	acpl	pcpl	prpl	prsl	posl
Tazoudasaurus																			
Axis	0	1	1	0	1	0	0	0	0	0	1	0	0	1	–	–	–	0	0
Ant. to mid. cerv.	1	1	1	0	1	–	1	1	1	0	1	0	0	1	–	–	–	0	0
Ant dors. juv.	1	1	1	0	1	–	1	1	1	0	?	?	?	1	–	–	0	?	?
Ant. dors.	–	1	1	1	1	1	–	1	1	0	1	0	0	1	–	1?	1	0	0
Mid. dors.	–	1	1	1	1	1	–	1	–	0	1	0	0	1	1	1?	1	0	0
Post. dors.	–	1	1	1	1	1	–	1	–	0	1	0	0	1	1	1?	1	0	0
Patagosaurus **(Bonaparte 1986; Lang com. pers.)**																			
Axis	**1**	1	?	0	1	0	?	?	?	**1**	1	0	0	1	–	–	–	0	0
Ant. to mid. cerv.	1	1	1	0	1	–	1	1	1	**0/1**	1	0	0	1	–	–	–	0	0
Post. cerv.	1	1	1	0	1	–	1	1	1	0	1	0	0	1	–	–	–	0	0
Ant. dors.	–	1	1	?	1	1	–	1	1	0	1	0	0	1	–	1	1	0	0
Mid. dors.	–	1	1	?	1	1	–	1	–	0	1	0	0	–	1	?	1	0	0
Post. dors.	–	1	1	?	1	1	–	1	–	?	1	0	0	–	1	?	1	0	0
Omeisaurus **(He *et al.* 1988)**																			
Axis	**1**	1	1	0	1	0	?	?	0	**1**	1	0	0	1	–	–	–	0	0
Ant. to mid. cerv.	1	1	1	0	1	–	1	1	?	**1**	1	0	0	1	–	–	–	0	0
Post. cerv.	1	1	1	0	1	–	1	1	?	**1**	1	0	0	1	–	–	–	0	0
Ant. dors.	–	1	1	1	1	1	–	1	?	**1**	1	0	0	1	–	1	1	0	0
Mid. dors.	–	1	1	1	1	1	–	1	–	?	1	0	0	1	1	1	1	0	0
Mamenchisaurus **(Ouyang & Ye 2002)**																			
Ant. to mid. cerv.	?	1	1	0	1	–	1	1	1	1	1	0	0	1	–	–	–	0	0
Post. cerv.	1	1	1	0	1	–	1	1	1	1	1	0	0	1	–	–	–	0	0
Ant. dors.	–	1	1	0	1	1	–	1	1	1	1	0	0	1	–	1	1	0	0
Mid. dors.	–	1	1	?	1	1	–	1	–	0	1	0	0	–	1	1	1	0	0
Post. dors.	–	1	1	1	1	1	–	1	–	0	1	0	0	–	1	0	1	0	0
Apatosaurus **(Wilson 1999)**																			
Ant. to mid. cerv.	1	1	1	0	1	–	1	1	1	**1**	1	0	0	1	–	–	–	0	0
Post. cerv.	1	1	1	0	1	–	1	1	1	**1**	1	0	0	1	–	–	–	0	0
Ant. dors.	–	1	1	1	1	1	–	1	–	**0/1**	1	0	0	**1**	**1**	1	1	**1**	**1**
Mid. dors.	–	1	1	1	1	1	–	1	–	**1**	**0**	**1**	**1**	**1**	1	**0**	1	**1**	**1**
Post. dors.	–	1	1	1	1	1	–	1	–	**1**	**0**	**1**	**1**	**1**	1	1	1	**1**	**1**
Camarasaurus																			
Axis	?	1	1	0	1	**1**	**1**	**1**	0	**0**	1	0	0	1	–	–	–	0	0
Ant. to mid. cerv.	1	1	1	0	1	–	1	1	1	**1**	1	0	0	1	–	–	–	0	0
Post. cerv.	1	1	1	0	1	–	1	1	1	**1**	?	0	0	1	–	–	–	0	0
Ant. dors.	1	1	1	1	1	0	1	1	1	1	1	0	0	1	–	0	0	0	0
Mid. dors.	–	1	1	1	1	1	–	1	–	?	1	0	0	1	1	1	1	0	0
Nand sauropod (Wilson & Mohabey 2006)																			
Axis	?	1	1	0	1	**1**	0	**1**	0	**1**	1	0	0	1	?	0	0	0	0

above the neural canal, and form the lateral walls of a deep furrow which extends dorsally and anteriorly above the neural canal. This feature is also present in *Patagosaurus* (pers. obs.). The unbifurcated neural spine is broken distally but its base is only 35 mm long anteroposteriorly (Fig. 9C, D). As in all other sauropods, the spine is formed from a central portion to which are connected the sprl's anteriorly and the spol's posteriorly (Fig. 9C, D). The paired spol's and sprl's enclose medially the postpinal and the prespinal fossae respectively. The sprl's diverge anteriorly and the spol's posteriorly, forming an X in dorsal view.

Dorsal vertebrae

Numerous dorsal vertebrae have been found so far, but only five of them and a dorsal neural arch of a juvenile specimen as well, have been prepared. Three well-preserved articulated middle dorsal vertebrae (To1-38) were figured in the original paper (Allain *et al.* 2004). They are now badly damaged, but are however briefly described below.

Anterior dorsal vertebra

The most anterior dorsal vertebra MHNM To1-69 is very high compared to the cervical vertebrae and other dorsal vertebrae (Table 1; Figs 11, 12). The centrum is slightly damaged both anteriorly and posteriorly but its anterior articular surface was gently convex when the posterior articular is concave (Fig. 11A-D). The latter is markedly more extended transversely and dorsoventrally than the anterior articular surface (Table 1). The anterior articular surface is higher than wide, while the posterior articular surface is wider than high (Table 1). The ventral margin of the concave posterior articular surface projects more posteriorly than the dorsal margin (Fig. 11E-H). The ventral surface of the centrum is arched upwards anteroposteriorly and flat transversely (Fig. 12C), as in the Rutland specimen of *Cetiosaurus* (Upchurch & Martin 2002). A deep fossa is present on the anterodorsal part of the lateral surface of the centrum, and the midline septum between these two fossae is thin (terminology follows Wedel 2003). The parapophysis is positioned dorsally on the neurocentral suture. It is elongated dorsoventrally, more than twice as deep as anteroposteriorly long, and spans the neural arch and the centrum. Thus, the parapophysis intersects the path of the cprl and the acdl, cprl and acpl are not applicable here (Table 2; Wilson 1999).

The neural arch is tall and is more than twice the centrum height (Table 1). The neural arch lamination is as well developed as in other sauropods except for the cpol which is absent (see details below). The articular facets of the prezygapophyses are broken (Fig. 12A, B) but did not project far forwards beyond the anterior end of the articular surface of the centrum (Fig. 11G, H). The prezygapophysis is joined to the diapophysis by a prominent, posterolaterally directed prdl (Fig. 12A, B). It is supported from below by a stout, undivided prpl (Fig. 11A, B). In lateral view, the prpl is intersected at mid-height by a lamina that extends posterodorsally up to the anterior surface of the transverse process (Fig. 11E-H). Altough this lamina does not connect to the parapophysis, it is here interpreted as the ppdl. The ppdl separates the infraprezygapophyseal fossae defined by the prdl, ppdl and prpl, and the infradiapophyseal fossa defined by the ppdl and pcdl. The latter has been termed "lateral opening" (Bonaparte 1986), "infradiapophyseal pneumatopore" (Wilson 2002), or "neural cavity" (Upchurch & Martin 2002). The hyposphene-hypantrum system is weakly developed in To1-69. In anterior view, the prezygapophyses are joined by the tprl's which originate from the ventromedial margin of each prezygapophysis, and meet above the dorsal margin of the neural canal (Fig. 11A, B). The tprl's along with the prpl and the dorsolateral margin of the neural canal define a deep fossa on the anterior surface of the neural arch, similar to that observed in the To1-354 cervical vertebra, but which is absent in the most posterior dorsal (see below To1-156). Within this fossa, a short dorsomedially directed accessory lamina joins the tprl to the prpl (Fig. 11A, B). This accessory lamina is present in the seventh dorsal vertebra of *Omeisaurus* (He *et al.* 1988). The left transverse process is broken distally, but the right one, although damaged, is complete. The transverse processes are directed laterally. In lateral view, the diapophysis is very deep dorsoventrally (Fig. 11G, H), because of the vertical development of the prominent pcdl which supports the transverse process (Fig. 11C, D). The podl is very short and robust (Fig. 11C, D). It originates from the anterolateral corner of the postzygapophysis and is first directed anteriorly, then laterally towards the diapophysis (Fig. 12A, B). Upchurch & Martin (2002: fig. 4b) described an infrapostzygapophyseal accessory lamina in *Cetiosaurus* within the hollow defined by the podl and the pcdl. Such a lamina is absent in *Tazoudasaurus* To1-69 anterior dorsal vertebra. Nevertheless, according to the figures and description of Upchurch & Martin (2002), and to the nomenclature of vertebral laminae of Wilson (1999), this lamina is

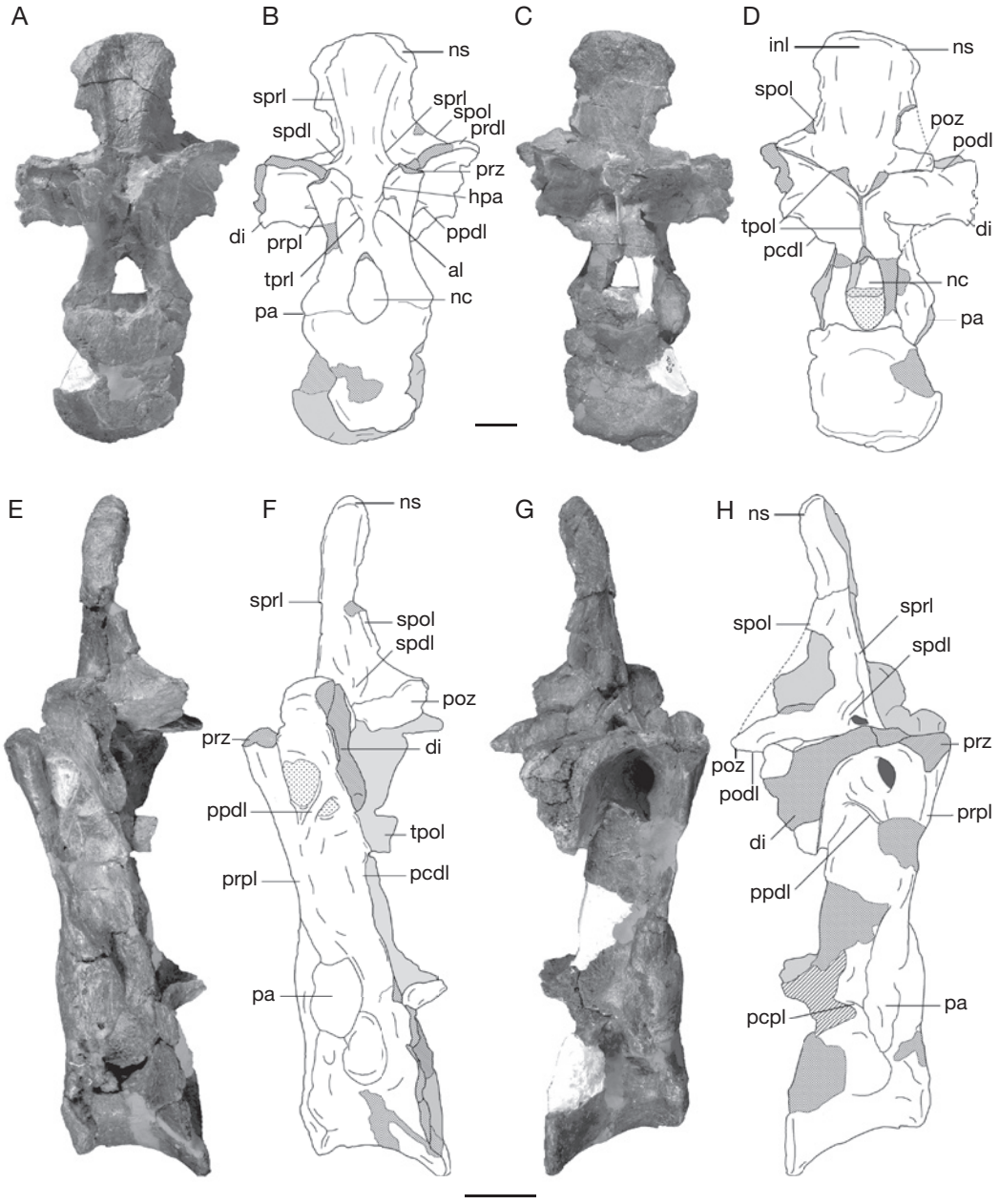

FIG. 11. — *Tazoudasaurus naimi*, anterior dorsal vertebra (To1-69): **A**, **B**, anterior view; **C**, **D**, posterior view; **E**, **F**, left lateral view; **G**, **H**, right lateral view. Abbreviations: **al**, accessory lamina; **di**, diapophysis; **hpa**, hypantrum; **hpo**, hyposphene; **inl**, interspinal ligament; **nc**, neural canal; **ns**, neural spine; **pa**, parapophysis; **pcdl**, posterior centrodiapophyseal lamina; **pcpl**, posterior centroparapophyseal lamina; **podl**, postzygodiapophyseal lamina; **poz**, postzygapophysis; **ppdl**, paradiapophyseal lamina; **prdl**, prezygodiapophyseal lamina; **prpl**, prezygoparapophyseal lamina; **prz**, prezygapophysis; **spdl**, spinodiapophyseal lamina; **spol**, spinopostzygapophyseal lamina; **sprl**, spinoprezygapophyseal lamina; **tpol**, intrapostzygapophyseal lamina; **tprl**, intraprezygapophyseal lamina. Scale bars: 5 cm.

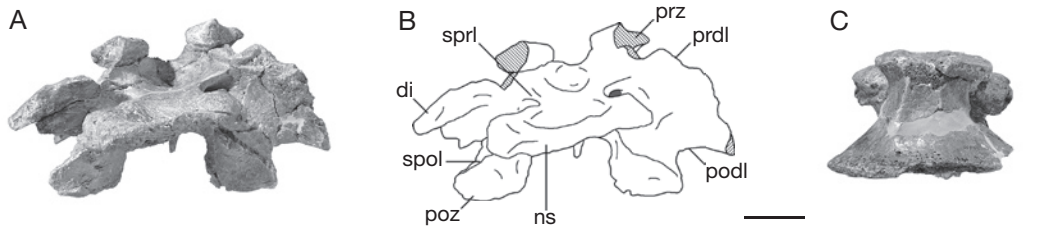

FIG. 12. — *Tazoudasaurus naimi*, anterior dorsal vertebra (To1-69): **A**, **B**, dorsal view; **C**, ventral view. Abbreviations: **di**, diapophysis; **hpa**, hypantrum; **ns**, neural spine; **podl**, postzygodiapophyseal lamina; **poz**, postzygapophysis; **prdl**, prezygodiapophyseal lamina; **prz**, prezygapophysis; **spol**, spinopostzygapophyseal lamina; **sprl**, spinoprezygapophyseal lamina. Scale bar: 5 cm.

not an accessory lamina but the cpol. Although its absence in *Barapasaurus* Jain, Kutty, Roy-Chowdhury & Chatterjee, 1975 needs to be confirmed, it is absent in all dorsal vertebrae of *Patagosaurus* and *Tazoudasaurus*, and in middle and posterior dorsal vertebrae in *Mamenchisaurus youngi* (Table 2). The postzygapophyses are high above the centrum and project backwards beyond the posterior end of the articular surface of the centrum (Fig. 11G, H). The wide articular facets of the postzygapophyses are flat and face ventrally. In posterior view, the postzygapophyses are joined by tpol's which originate from their medial margin, project ventromedially and fuse to a single median lamina (Fig. 11C, D). This single median tpol is 75 mm long and bifurcates again ventrally just above the neural canal. The unbifurcated neural spine raises 155 mm above the postzygapophyses. It is spatulate distally, where it is considerably expanded transversely, being more than five times as broad lateromedially as long anteroposteriorly (Table 1; Fig. 12A, B). Spinodiapophyseal laminae (spdl), spol's and sprl's are all connected to the lateral surfaces of the neural spine, but are not equally developed (Figs 11G, H; 12A, B). The spol is the longest of these three laminae and extends along the posterolateral margin of the neural spine up to the posterolateral corner of the dorsal surface of the postzygapophysis (Fig. 12A, B). The sprl originates on the posterior aspect of the prezygapophysis and stretches slightly medially (Fig. 12A, B), and then vertically along the anterolateral margin of the neural spine to its summit (Fig. 11G, H). The spdl is very reduced, only 33 mm long. It merges laterally into the base of the diapophysis, and is connected anteromedially to the sprl (Fig. 11G, H). It defines with the lower part of the sprl a small but deep hollow which invades the base of the lateral surface of the neural spine.

Middle dorsal vertebrae

The three middle dorsal vertebrae CPSGM To1-38a-c were found in connection (Fig. 13). They are more similar in shape and morphology to the posterior dorsal vertebrae than to the anterior dorsal vertebrae (see below). They differ from the anterior and posterior dorsal vertebrae in having longer centra (Table 1), more posteriorly directed neural spines, and more dorsally directed transverse processes (Fig. 13). The hyposphene-hypantrum articulation is present in the three vertebrae. The neurocentral sutures are clearly visible on the three vertebrae. The neural arch lamination of the middle dorsal vertebrae differs by the presence of more strongly developed spdl, which originates on the posterior half of the dorsal surface of the transverse processes, and extends on the lateral side of the neural spine to which they merge at midlength. The spdl fails to contact the spol. As for the prdl, it is bifurcated anteriorly and contacts both the prezygapophysis and the prpl. The neural spines bear deep scars on their anterior and posterior surfaces for interspinal ligaments.

Posterior dorsal vertebrae

According to the position of its parapophyses and the morphology of its hyposphene-hypantrum system, the vertebra MHNM To1-156 is more posteriorly located in the dorsal series than the three

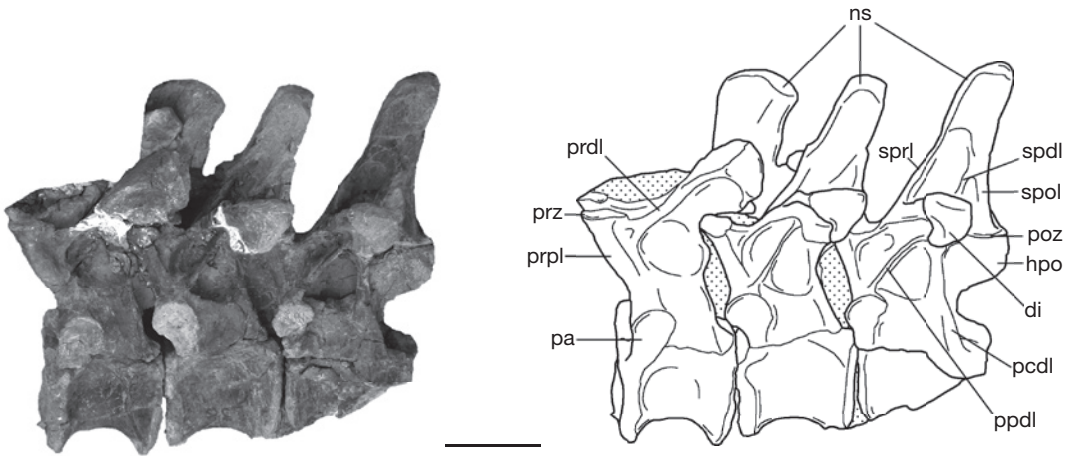

FIG. 13. — *Tazoudasaurus naimi*, mid-dorsal vertebrae (To1-38) lateral view. Abbreviations: **di**, diapophysis; **hpo**, hyposphene; **ns**, neural spine; **pa**, parapophysis; **pcdl**, posterior centrodiapophyseal lamina; **poz**, postzygapophysis; **ppdl**, paradiapophyseal lamina; **prdl**, prezygodiapophyseal lamina; **prpl**, prezygoparapophyseal lamina; **prz**, prezygapophysis; **spdl**, spinodiapophyseal lamina; **spol**, spinopostzygapophyseal lamina; **sprl**, spinoprezygapophyseal lamina. Scale bar: 10 cm.

previously described articulated vertebrae (Fig. 14). The centrum of To1-156 is amphicoelous with a posterior articular surface more concave than the anterior which is nearly flat. It is taller than long, but as tall as wide transversely (Table 1). The ventral surface of the centrum is arched upwards anteroposteriorly and flat to slightly convex transversely (Fig. 14J). Deep fossae invade the dorsal part of the lateral surface of the centrum. They are about 55 mm long and 50 mm high, and are separated by a thin septum. The neural arch is tall, exceeding more than twice the centrum height (Table 1). The parapophysis is positioned dorsally on the neural arch above the neurocentral suture, and is connected to the centrum by the acpl, to the prezygapophysis by the prpl, and to the diapophysis by the ppdl (Fig. 14A, B, E, F). The identification of the pcpl is not obvious, but it is probably present as a faint ridge on the ventral part of the lateral surface of the neural arch (Fig. 14E, F). As in more anterior dorsal vertebrae, the parapophysis is elongated dorsoventrally, more than twice as deep as anteroposteriorly long. The hyposphene-hypantrum complex is well developed in To1-156. Thus, the tprl can not be observed in posterior dorsal vertebrae of *Tazoudasaurus*. Unlike *Patagosaurus* (Bonaparte 1986) and *Barapasaurus* (Jain *et al.* 1979), the prominent anterior surface of the neural arch is flat to nearly convex below the prezygapophyses and is not excavated by a large concavity. The hypantrum is a dorsoventrally very elongated groove (Fig. 14A, B) that is bounded laterally by thin laminae that join the anterolateral corner of the prezygapophysis to the dorsal margin of the neural canal (Fig. 14E-G). The prezygapophyses project slightly forwards beyond the anterior end of the articular surface of the centrum (Fig. 14E, F). The prezygapophysis is joined to the diapophysis by a prominent, posterolaterally directed prdl that bifurcates anteriorly to form an upper and a lower lamina that contact the prezygapophysis and the prpl respectively (Fig. 14E, F).

As in To1-69, the ppdl separate the infraprezygapophyseal fossae defined by the prdl, ppdl and prpl, and the infradiapophyseal fossa defined by the ppdl and pcdl. Both fossae are even deeper than in To1-69. The infradiapophyseal fossae are located dorsal to the neural canal and are at least separated by a thin midline septum of bone, unless they are adjoining. Such excavations have been reported in *Barapasaurus* (Jain *et al.* 1979), *Patagosaurus* (Bonaparte 1986) and perhaps in

Kotasaurus Yadagiri, 1988 (Yadagiri 2001) and *Cetiosaurus* (Upchurch & Martin 2002, 2003).

The transverse processes are directed laterally and are distally less expanded dorsoventrally than in To1-69 (Fig. 14E-G). The podl is very short (Fig. 14E, F) and was first thought to be the cpol. It originates from the anterolateral corner of the postzygapophysis and is directed anteriorly and slightly ventrally, where it merges into the base of the posterior face of the diapophysis (Fig. 14C, D). A deep fossa excavates the neural arch medially to the podl. The postzygapophyses do not project far beyond the posterior end of the articular surface of the centrum (Fig. 14A, B). The articular facets of the postzygapophyses are flat and face ventrally. In posterior view, below the parapophyses, the hyposphene is developed as a median vertical strut, enlarged transversely (Fig. 14C, D). It is connected ventrally to the dorsal margin of the neural canal by a short and thin lamina, the remnant of the tpol, as in diplodocids (Wilson 1999) and in *Omeisaurus* (He *et al.* 1988). In posterior view, two shallow fossae are located laterally to the neural canal, and are themselves bounded laterally by a thick ridge (Fig. 14C, D). It is not clear if this ridge which extends dorsally from the posterior portion of the neurocentral junction is homologous to the cpol.

In dorsal view, unlike the anterior dorsal vertebrae, the neural spine is trapezoid in outline, but remains wider than long (Fig. 14H, I). The sprl originates near the summit of the neural spine and stretches vertically along its anterolateral margin (Fig. 14E, F), but it fails to reach the prezygapophysis, and at the base of the transverse process, it is directed laterally towards the diapophysis (Fig. 14H, I). The spol is wide at its base, where it originates from the dorsal margin of the postzygapophysis (Fig. 14C, D). It extends vertically along the posterolateral margin of the neural spine. The spdl is prominent on the dorsal surface of the transverse process but it is only a faint ridge on the lateral surface of the neural spine (Fig. 14E-I). It stretches only for some centimetres, and it contacts posterodorsally the spol (Fig. 14E-G). The posterior dorsal of *Tazoudasaurus* is characterized by the deep excavation which invades both the base of the neural spine laterally and that of the transverse process dorsally, and leaves only a thin median septum at the level of the neural spine (Fig. 14E, F, H, I). This condition is present in *Patagosaurus* (Bonaparte 1986) and probably in *Barapasaurus* (Jain *et al.* 1979: pl. 98).

Caudal vertebrae

Anterior caudal vertebrae

CPSGM To1-100 is one of the most anterior caudal vertebrae, if it is not the first (Figs 15; 16). As in all sauropods, the centrum is very short anteroposteriorly with a centrum length/height ratio less than 0.5 (Table 1; Fig. 16). The centrum is amphicoelous, but the anterior articular surface is more deeply excavated than the posterior surface (Fig. 15). Both articular surfaces are higher than wide (Table 1). The ventral surface is arched upwards in lateral view and is convex transversely (Fig. 16A, B). The central portion of the centrum is constricted and the lateral surface is deeply concave anteroposteriorly. Thus, the median width of the lateral surface of the centrum is considerably less than the width of the anterior and posterior articular faces (Table 1). The neural arch is situated towards the anterior end of the centrum. The prezygapophyses are broken distally but were projected anterodorsally beyond the anterior end of the centrum. They are connected to the centrum by the cprl and to the diapophysis by the prdl (Figs 15A, B; 16A, B). The postzygapophyses are represented by a small "pinched" area at the base of the lateral surface of the neural spine (Fig. 15A, B). The postzygapophyseal facets face mainly laterally and little ventrally (Fig. 16C, D). Ventrally, the postzygapophyses meet on the midline to form a ridge which extends down to the dorsal margin of the neural canal where it bifurcates (Fig. 16C, D). This structure is likely homologous to the tpol. Dorsally to the postzygapophysis, the spol runs vertically along the posterolateral margin of the neural spine and defines the lateral wall of the postspinal fossa (Fig. 15C, D). The rod-like transverse processes project only laterally and extend from the centrum to the neural arch. The neural spine is broken in its most distal part, but it is a compressed vertical plate (Fig. 15C, D).

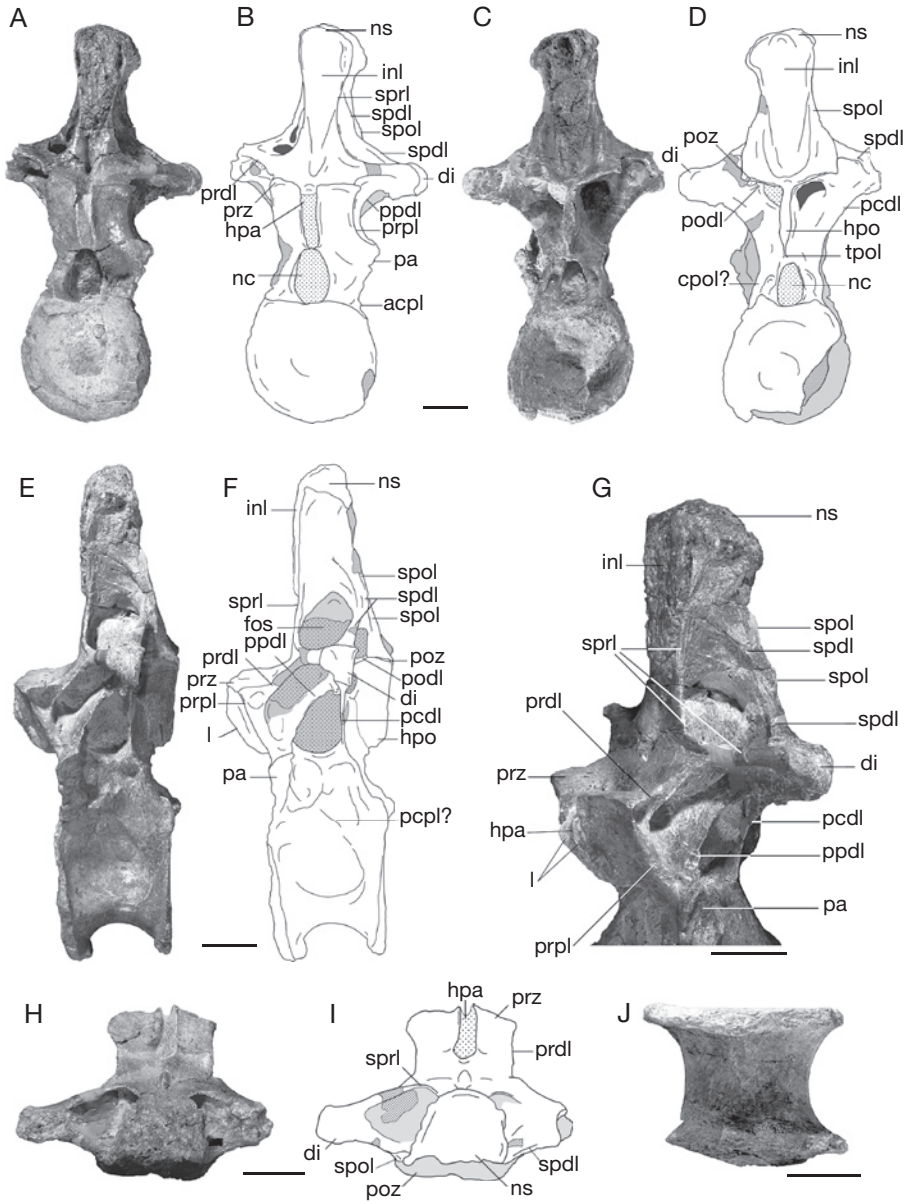

FIG. 14. — *Tazoudasaurus naimi*, posterior dorsal vertebra (To1-156): **A**, **B**, anterior view; **C**, **D**, posterior view; **E**, **F**, left lateral view; **G**, detailed view of the laminae in right anterolateral view; **H**, **I**, dorsal view; **J**, ventral view. Abbreviations: **acpl**, anterior centroparapophyseal lamina; **cpol**, centropostzygapophyseal lamina; **di**, diapophysis; **fos**, fossa; **hpa**, hypantrum; **hpo**, hyposphene; **inl**, interspinal ligament; **l**, lamina; **nc**, neural canal; **ns**, neural spine; **pa**, parapophysis; **pcdl**, posterior centrodiapophyseal lamina; **pcpl**, posterior centroparapophyseal lamina; **podl**, postzygodiapophyseal lamina; **poz**, postzygapophysis; **ppdl**, paradiapophyseal lamina; **prdl**, prezygodiapophyseal lamina; **prpl**, prezygoparapophyseal lamina; **prz**, prezygapophysis; **spdl**, spinodiapophyseal lamina; **spol**, spinopostzygapophyseal lamina; **sprl**, spinoprezygapophyseal lamina; **tpol**, lamina intrapostzygapophyseal lamina. Scale bars: 5 cm.

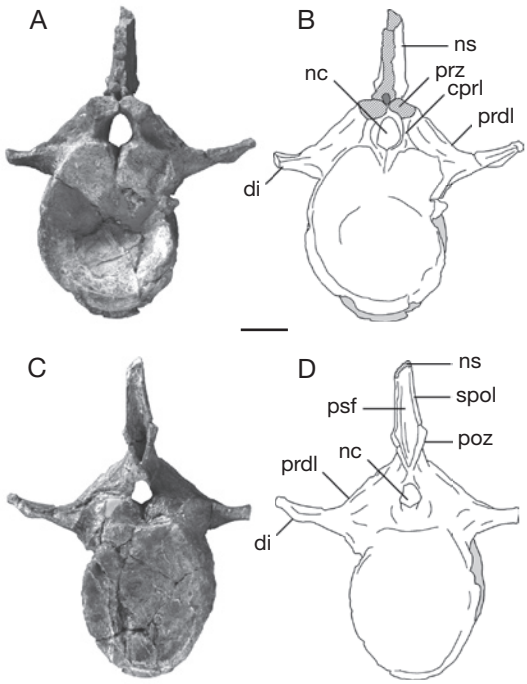

FIG. 15. — *Tazoudasaurus naimi*, anterior caudal vertebra (To1-100): **A**, **B**, anterior view; **C**, **D**, posterior view. Abbreviations: **cprl**, centroprezygapophyseal lamina; **di**, diapophysis; **nc**, neural canal; **ns**, neural spine; **poz**, postzygapophysis; **prdl**, prezygodiapophyseal lamina; **prz**, prezygapophysis; **psf**, postspinal fossa; **spol**, spinopostzygapophyseal lamina. Scale bar: 5 cm.

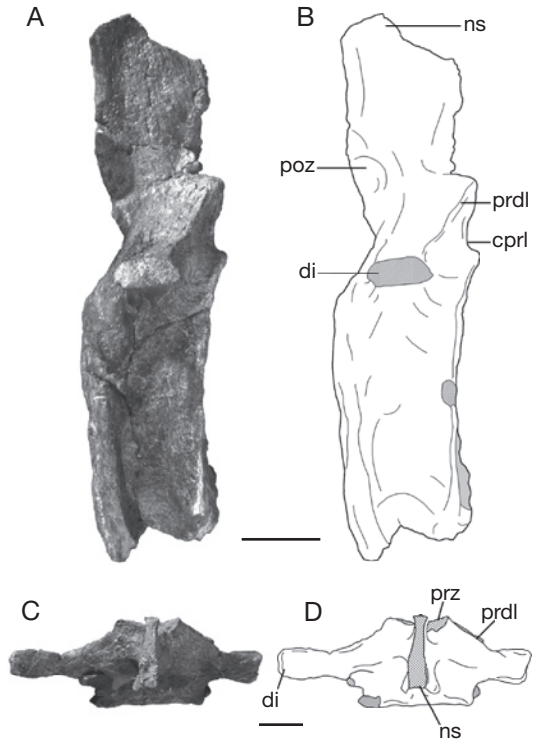

FIG. 16. — *Tazoudasaurus naimi*, anterior caudal vertebra (To1-100): **A**, **B**, right lateral view; **C**, **D**, dorsal view. Abbreviations: **cprl**, centroprezygapophyseal lamina; **di**, diapophysis; **ns**, neural spine; **poz**, postzygapophysis; **prdl**, prezygodiapophyseal lamina; **prz**, prezygapophysis. Scale bars: 5 cm.

Middle and distal caudal vertebrae

Numerous caudal vertebrae of *Tazoudasaurus* have been found in articulation (Fig. 17) or isolated (Fig. 18). The three caudal vertebrae MHNM To1-303a, b and c have thin transverse processes (Fig. 17) and probably belong to proximal part of the middle series of the tail. The other caudal vertebrae (Fig. 18) lack transverse processes, although a faint ridge is present on the lateral side of the upper part of the centrum of MHNM To1-288 (Fig. 18C, D). The centrum length/height ratio is 0.6 for middle caudal vertebrae To1-288, 1.0 for posterior middle caudal vertebrae MHNM To1-88 (Fig. 18A, B), and more than 2.0 for distal caudal vertebrae MHNM To1-317 and MHNM To1-357 (Fig. 18E-H). For the three articulated proximal middle caudal vertebrae To1-303, this ratio is nearly equals to 1.0 and thus significantly greater than the ratio of the more posterior caudal vertebra To1-288. This is possibly due to the immaturity of this specimen and could suggest allometric growth of the caudal vertebrae. All the middle and distal centra are amphicoelous, lacking pleurocoels and ventral excavations. The central portion of the centrum is slightly constricted, and the lateral surface of the centrum is concave anteroposteriorly, although there is a horizontal ridge situated at approximately midheight of the lateral surface in the middle caudal To1-288 (Fig. 18C, D). The autapomorphic deep groove found on the ventral surface of the caudals of *Vulcanodon* Raath, 1972 has not been observed in *Tazoudasaurus* (Cooper 1984). The chevron facets are weakly developed and face posteroventrally. The middle caudal vertebrae possess neural arches situ-

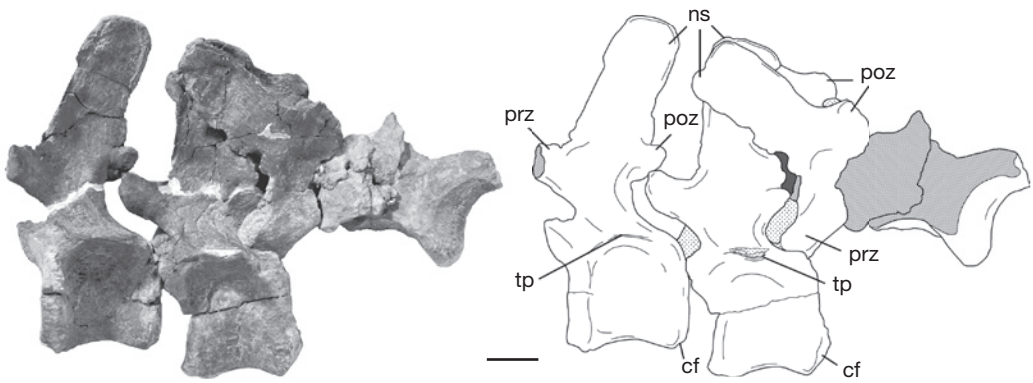

FIG. 17. — *Tazoudasaurus naimi*, anterior mid-caudal vertebrae (To1-303), left lateral view. Abbreviations: **cf**, chevron facet; **ns**, neural spine; **poz**, postzygapophysis; **prz**, prezygapophysis; **tp**, transverse process. Scale bar: 5 cm.

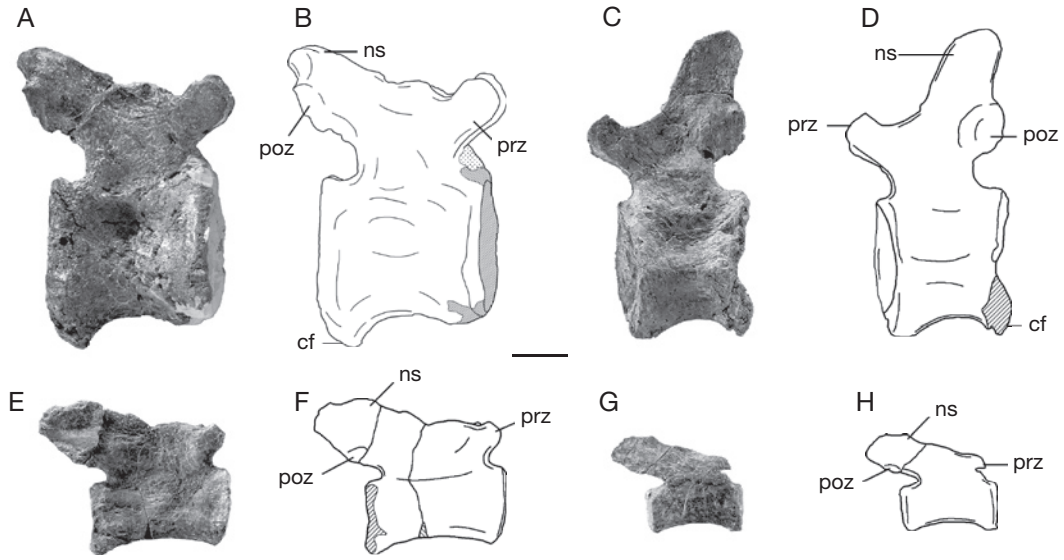

FIG. 18. — *Tazoudasaurus naimi*, caudal vertebrae: **A**, **B**, posterior mid-caudal vertebra (To1-88) in right lateral view; **C**, **D**, mid-caudal vertebra (To1-288) in left lateral view; **E**, **F**, distal caudal vertebra (To1-317) in right lateral view; **G**, **H**, distal caudal vertebra (To1-357) in right lateral view. Abbreviations: **cf**, chevron facet; **ns**, neural spine; **poz**, postzygapophysis; **prz**, prezygapophysis. Scale bar: 5 cm.

ated towards the anterior end of the centrum, when the neural arch of the posterior caudal vertebrae is placed on approximately the center of the centrum. The neural arches are laterally compressed. The prezygapophyses are more anteriorly projected in middle caudal vertebrae than in distal caudal vertebrae. The prezygapophyseal facets face medially. The postzygapohyses are located at the base of the neural spine and face laterally. They are nearly imperceptible in distal caudal vertebrae. Prespinous and postspinous fossae are found in middle caudal series but disappear in distal caudal vertebrae. The blade-like neural spines are directed mainly dorsally and slightly posteriorly in middle caudal vertebrae, while they project strongly backwards in the distal caudal vertebrae (Fig. 18E-H).

FIG. 19. — *Tazoudasaurus naimi*, chevrons: **A**, proximal chevron (To1-187) in posterior view; **B**, same in lateral view; **C**, distal chevron (To1-182) in dorsal view; **D**, same in ventral view; **E**, middle chevron (To1-217) in posterior view; **F**, same in dorsal view; **G**, same in lateral view. Scale bars: 5 cm.

CHEVRONS

As for the caudal vertebrae, numerous chevrons have been recovered in Toundoute that fall into three different types (Fig. 19). In all chevrons the haemal canal is closed dorsally by a bridge of bone (Fig. 19C, F). This proximal bridge articulates with the caudal vertebrae through two facets. The anterior facet is perpendicular to the long axis of the chevron, whereas the posterior facet faces posterodorsally. Thus, in articulation with the caudal vertebrae, the chevrons are directed mainly ventrally and slightly posteriorly.

In anterior and posterior views, the proximal chevron MHNM To1-187 is triangular in outline because of its very short distal blade (Fig. 19A). The haemal canal is also triangular and occupies 36% of chevron length. The posterior articular facet of the proximal bridge is excavated by two lateral shallow fossae. The distal blade and the lateral rami of the haemal canal are compressed laterally. In lateral view, the distal end of the blade is more expanded anteroposteriorly than the proximal articular end (Fig. 19B). The distal blade of the middle chevrons MHNM To1-217 is considerably longer than To1-187. The haemal canal is vertically elongate but is only 28% of the chevron length. Below the haemal canal, the blade is wider transversely than long anteroposteriorly, while it is longer than wide distally (Fig. 19E-G). The distal chevron CPSGM To1-182 is forked and thus has distinct anterior and posterior prongs (Fig. 19C, D). It is bridged proximally as in *Barapasaurus*, whereas distal chevrons are open proximally in *Omeisaurus* (Wilson & Sereno 1998). The anterior and posterior flattened prongs are not fused distally. This represents a derived state only known within Titanosauria such as *Opisthocoelicaudia* Borsuk-Bialynicka, 1977 and *Alamosaurus* Gilmore, 1922 (Wilson 2002). Thus, proximally bridged and distally open distal chevrons should be regarded as an autapomorphy of *Tazoudasaurus*.

PECTORAL GIRDLE

Coracoid

The complete right coracoid of a large specimen of *Tazoudasaurus* is the only bone of the pectoral girdle found and prepared so far in Toundoute (Fig. 20). The coracoid is a massive element which has an oval outline in lateral view. It is more expanded dorsoventrally than anteroposteriorly. The coracoid is convex on its lateral surface and correspondingly concave medially. It thickens ventrally in the glenoid area. The coracoid foramen is very large and is located at mid-height, 2 cm anterior from the scapula-coracoid articulation. The ventral margin of the coracoid lacks the notch located anterior to the glenoid observed in many sauropods such as *Cetiosaurus* (Upchurch & Martin 2003), *Opistho coelidaudia* (Borsuk-Bialynicka 1977) or *Suuwassea* Harris & Dodson, 2004 (Harris & Dodson 2004). The flat glenoid facet faces mainly posteroventrally and very slightly medially.

TABLE 3. — Measurements (in mm) of forelimb elements of *Tazoudasaurus naimi*. Abbreviations: **e**, estimated; **L**, length; **Prow**, transverse width of proximal end; **Prol**, anteroposterior length of proximal end; **Medw**, transverse width of the shaft at midlength; **Medl**, anteroposterior length of the shaft at midlength; **Disw**, transverse width of distal end; **Disl**, transverse length of distal end.

Specimen	L	Prow	Prol	Medw	Medl	Disw	Disl
Humerus							
To1-93, left	185	49	12	23	19	41	14
To1-48, right	185e	51	–	23	17	41	23
Pt1, left	1030	380	111	150	87	300	144
Ulna							
To1-374, right	220	47		26	24	36	
To1-375, right	720	172		87	68	100	
Pt24, left	730	166		90	77	110	

FORELIMB

Humerus

At least seven humeri of *Tazoudasaurus* have been found in both bone beds of the Toundoute series. Only three of them are complete: one belongs to an adult individual (MHNM Pt1) and the two others to one juvenile individual described in a later section (CPSGM To1-48; CPSGM To1-93). The humerus is straight in anterior and lateral views and transversely expanded both proximally and distally (Fig. 21A-F). The proximal end is slightly broken medially, but is rounded proximally and compressed anteroposteriorly. Its transverse width is only 37% of the length of the humerus (Table 3), which is slightly less than in other sauropods. There is no supracoracoideus process on the lateral corner of the proximal end (Fig. 21G, H). The anterior face of the proximal end is shallowly concave, and bounded laterally by the deltopectoral crest (Fig. 21A, B). The latter extends down the anterolateral margin over 510 mm and remains relatively narrow throughout its length. Ventral to the low deltopectoral crest, the humeral midshaft is elliptical in cross section, with a long axis oriented transversely (Table 3). The anterior surface of the distal end of the humerus is shallowly concave, whereas the posterior surface which has been crushed must be convex. A prominent crest, which is 110 mm long, runs over the anterolateral margin of the humerus just above the radial condyle (Fig. 21A-D). The distal articular surface is rugose and forms low condylar areas for the radius and ulna. The distal end is rotated about 15° counterclockwise with respect to the proximal end.

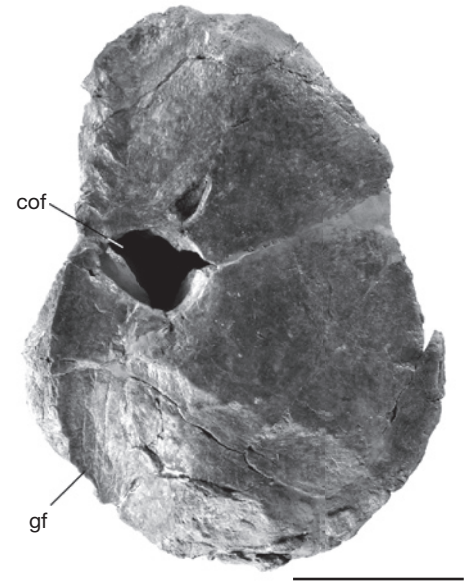

FIG. 20. — *Tazoudasaurus naimi*, right coracoid in lateral view. Abbreviations: **cof**, coracoid foramen; **gf**, glenoid fossa. Scale bar: 10 cm.

Ulna

At least three ulnae of *Tazoudasaurus* haven been recovered in Toundoute. They belong to three different individuals: two of which are adult (MHNM To1-375; MHNM Pt24) and one of which is juvenile (To1-374, see below). The right ulna Pt24 was found near

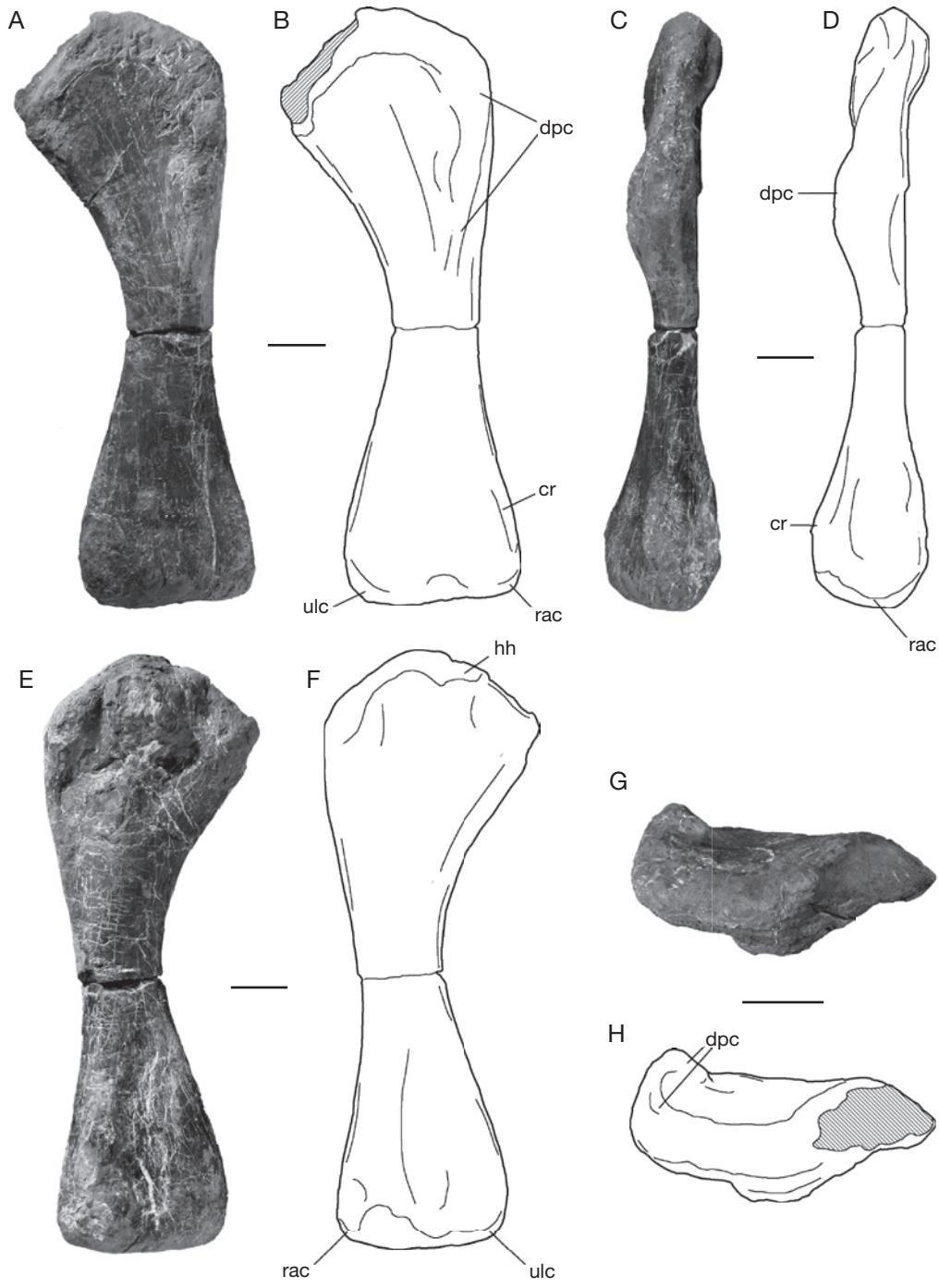

FIG. 21. — *Tazoudasaurus naimi*, left humerus (Pt-1): **A**, **B**, anterior view; **C**, **D**, lateral view; **E**, **F**, posterior view; **G**, **H**, proximal view. Abbreviations: **cr**, crest; **dpc**, deltopectoral crest; **hh**, humeral head; **rac**, radial condyle; **ulc**, ulnar condyle. Scale bars: 10 cm.

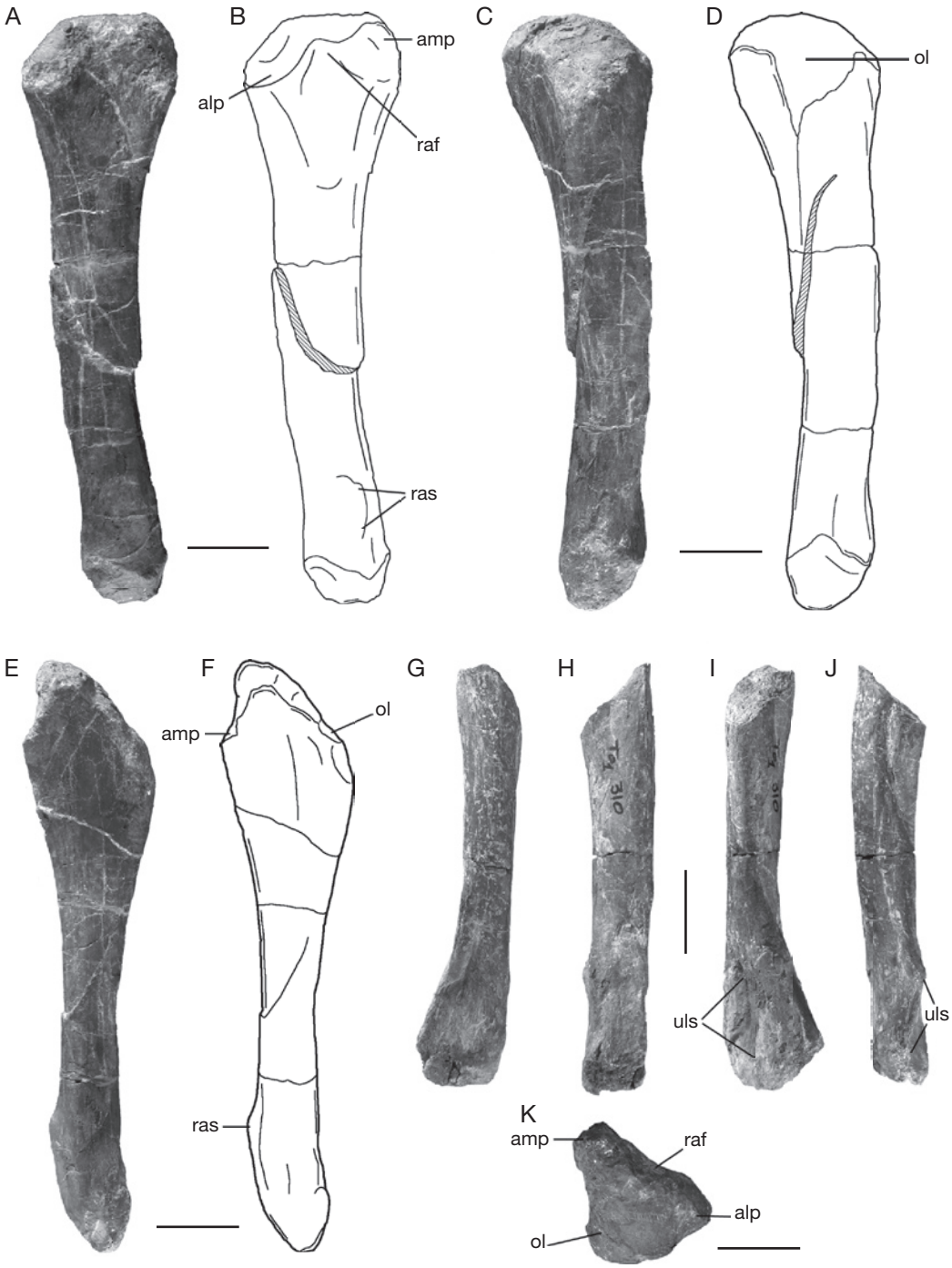

FIG. 22. — *Tazoudasaurus naimi*: **A**-**F**, **K**, right ulna (Pt-24); **G**-**J**, left radius; **A**, **B**, **G**, anterior views; **C**, **D**, **I**, posterior views; **E**, **F**, **J**, medial views; **H**, lateral view; **K**, proximal view. Abbreviations: **alp**, anterolateral process of the ulna; **amp**, anteromedial process of the ulna; **ol**, olecranon area; **raf**, radial fossa; **ras**, radial articular surface; **uls**, ulnar articular surface. Scale bars: 10 cm.

the humerus Pt1. It is a robust bone with an expanded proximal end (Fig. 22). As in other sauropods, the proximal end is triradiate, with both anterolateral and mediolateral processes which project from the olecranon region and delimit the radial fossa. The latter seems shallow due to the break of the distal part of both processes (Fig. 22K). The proximal articular surface lacks an olecranon (Fig. 22A-D), but the olecranon region is wider than in *Vulcanodon* (Cooper 1984: fig. 8). Although it is distally broken, the anterolateral process is clearly shorter than the mediolateral process. The latter is shorter than in *Vulcanodon* (Cooper 1984). The medial surface of the anteromedial process is slightly concave, whereas the lateral surface of the anterolateral process is slightly convex (Fig. 22K). Below the proximal end, the shaft of the ulna is subtriangular in cross section, and become elliptical with a laterally directed great axis towards the distal end (the directional terms used here assume one is viewing the proximal end of the ulna such that the olecranon region is pointing directly posteriorly). A prominent bump (Fig. 22A, B, E, F) appears on the anterior surface of the shaft of the ulna at about 18 cm above the distal articular surface and marks the contact area of the radius. The distal end is only slightly expanded and has a rugose articular surface.

Radius

Only one incomplete left radius (MHNM To1-310) has been found in Toudounte so far (Fig. 22G-J). The proximal end is missing. The shaft of the radius is only slightly curved medially and posteriorly. The distal end is strongly expanded transversely and flattened anteroposteriorly. In distal view, the articular surface is almost rectangular and gently convex mediolaterally. The long roughened surface of the posterior and lateral portion of the distal radial shaft marks the contact area with the ulna. A distinct process directed posteriorly borders its lateral margin (Fig. 22H, J).

MANUS

The lower bone-bed of the Toundoute series has yielded a nearly complete articulated distal left forefoot (MHNM To2-112). Although it clearly belongs to a small individual, it is described here rather than in the section dealing with juvenile specimens. This left forefoot was discovered as an articulated group of five metacarpals, 10 phalanges (one phalanx is missing, see below), one carpal and the distal ends of the ulna and the radius (Figs 23; 24A; Table 4). Unfortunately, the block in which the bones were embedded was incomplete in its median part and the exact number of carpals can not be determined. In its present position, the manus is flexed so that the distal articular surfaces of the ulna and the radius are nearly perpendicular to the proximal articular surfaces of the carpal and the metacarpals, but the different elements have not been shifted from their natural position (Fig. 23A, B).

A "traditional" saurischian manus orientation is assumed here (Wilson & Sereno 1998 *contra* Bonnan 2003). Thus, the external part of the manus faces mainly laterally and the distal end of the radius articulates against flat anterior margin of the distal end of the ulna and is mainly anterior and slightly lateral to it (Fig. 23). In this configuration, the long axis of the distal end of the ulna is mediolaterally directed and the anterolateral process of the proximal ulna would be directed only laterally (see Fig. 39). For convenience, in the following descriptions, the outward-facing surfaces of the metacarpals will be regarded as anterior, and the inward-facing surfaces as posterior. The only preserved carpal articulates with the radius proximally and with metacarpals I and II distally, and probably represents the distal carpal 1. The carpal is blocked-shaped. It is roughly rectangular in outline with a prominent and slightly pinched posteromedial process that is unknown in other sauropods (Fig. 23A, B). The proximal articular surface is flat and rugose. The distal articular surface bears at least one shallow and smooth concave facet above the metacarpal II. The presence of a second facet for the articulation of metacarpal I is likely but can not be observed as this portion of the distal articular surface is slightly eroded.

The metacarpals make a 45° angle with the horizontal and are held off the ground while the phalanges remain in contact with the substrate, so that the pose of the manus is digitigrade (*s.l.*). Nevertheless, as the proximal ends of the first

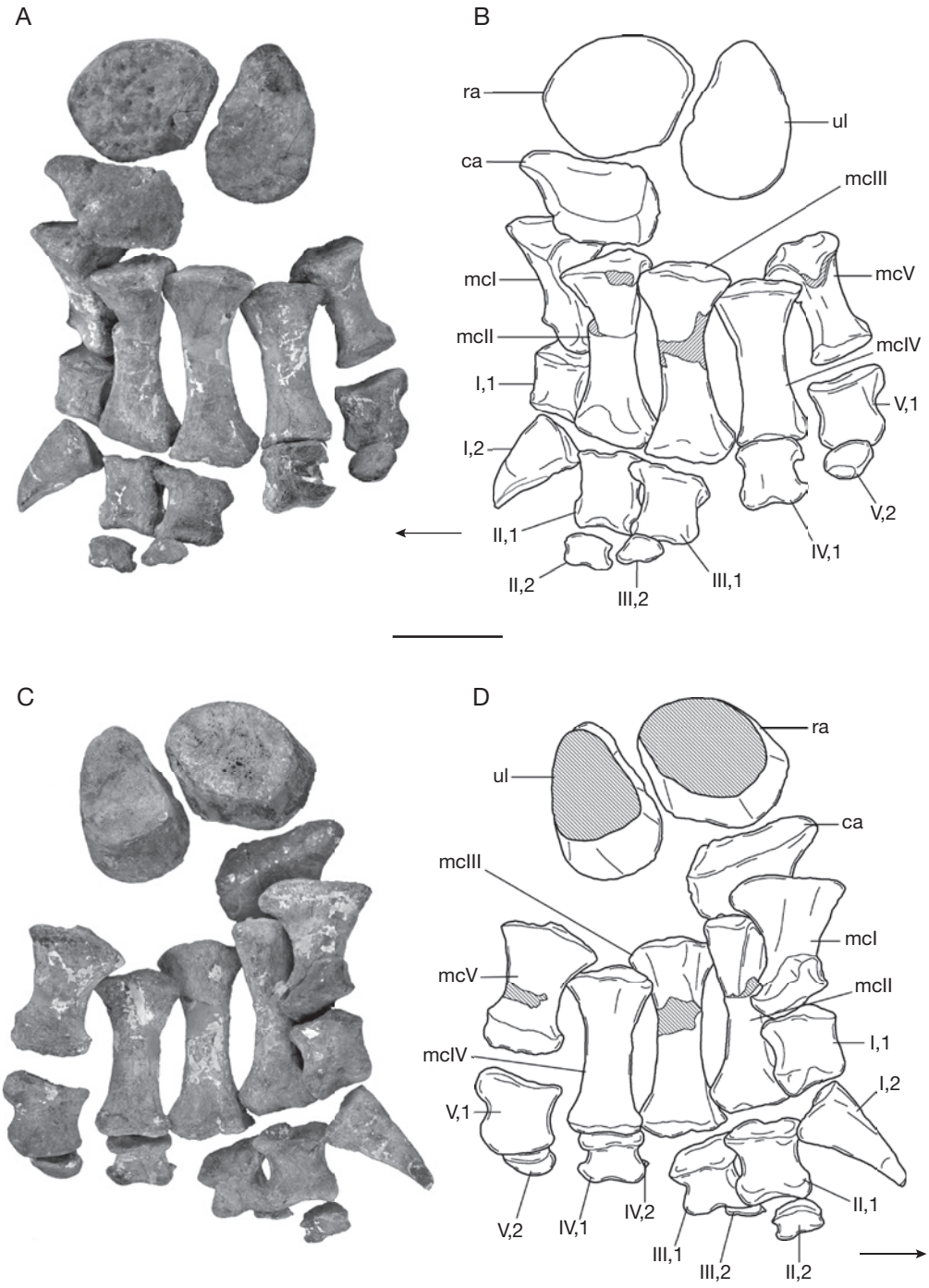

FIG. 23. — *Tazoudasaurus naimi*, left manus (To2-112): **A**, **B**, lateral view; **C**, **D**, medial view. Abbreviations: **ca**, carpal; **mc**, metacarpal (I-V) **ra**, radius; **ul**, ulna; arabic numerals indicate phalanges. Arrows indicate the anterior direction. Scale bar: 5 cm.

phalanges do not contact the substrate, the manus posture in *Tazoudasaurus* could be more precisely termed sub-unguligrade (Carrano 1997). Such a posture is consistent with the orientation of the distal articular surfaces of the metacarpals. The latter face only distally in *Tazoudasaurus* contrary to neosauropods, the same articular surfaces of which extend dorsally on the anterior surface of the metacarpals which are nearly vertically held. In proximal view, the articular surfaces of the metacarpals form a composite arc of slightly less than 90° (Fig. 24A). This arc is of approximately 90° even if the proximal metacarpals are closely abutted following their shape (Fig. 24B). Thus, the metacarpus has a spreading configuration rather than a semi-tubular configuration (see discussion below). The distal and proximal ends of the metacarpals are expanded relative to their shaft. The resultant hourglass shape of the metacarpals precludes their proximal part from being tightly abutted along their proximal shaft. Thus, only the bases of the metacarpals are in contact and a significant space remains between the proximal halves of the articulated metacarpals, as seen in prosauropods, *Shunosaurus* and *Omeisaurus* (Wilson & Sereno 1998). This configuration is enhanced by the lack of intermetacarpal articular surfaces on the proximal half of the metacarpals, which are present in neosauropods and possibly in *Cetiosaurus* (Upchurch & Martin 2003). The roughened proximal articular surfaces of metacarpals I and V are positioned above the articular surfaces of metacarpals II-IV. They are subtriangular and slightly convex mediolaterally. Metacarpal III is the longest, while metacarpals I and V are more robust and are only 70% of the length of metacarpal III unlike in Macronaria (Table 4). The shaft of each metacarpal is straight. The distal articular ginglymus of metacarpals II, III and IV is symmetrical with very shallow collateral fossae. The articular surfaces are only poorly subdivided and face completely distally. In contrast, the ginglymus of metacarpals I and V are asymmetrical. The long axis of the subdivided distal articular surface of metacarpal I is nearly perpendicular to that of the proximal articular surface. The medial condyle is expanded into a posteromedial process, but is more reduced distally than the lateral one so that the articular surface is bevelled proximodistally relative to the axis if the shaft and faces slightly medially. The large ginglymus of the metacarpal V is not subdivided. It is asymmetrical with a well-expanded posterolateral process.

The phalangeal formula of the manus is 2-3-2-2-2 (the ungual phalanx of digit IV is preserved but not figured in Fig. 23). Thus, the number of phalanges in *Tazoudasaurus* is less than in prosauropods which retain four phalanges in digit III and three in digit IV (Galton & Upchurch 2004a; Wilson 2005b), but more than in any other known sauropod, the second digit probably retaining three phalanges (see below). The first phalanx of each digit is almost as long proximodistally as broad transversely (Table 4). The proximal articular surface is undivided, shallowly concave, and has a semi-circular outline with a nearly straight ventral margin and a rounded dorsal margin. The distal articular surfaces are as expanded mediolaterally as their corresponding proximal articular surfaces, except for the first phalanx of the digit V the proximal articular of which is strongly expanded laterally (Table 4). On the other hand, the distal ginglymi are considerably more anteroposteriorly compressed, except for the first digit, and the condyles have developed into two separate L-shaped lobes. The second digit retains a very short second phalanx with a clearly subdivided distal articular surface which suggests that an ungual phalanx was also present in digit II, although it has not been recovered. The unguals of digits III, IV, and V still have a relatively large and concave proximal articular surface. The unguals IV and V are oval in shape, while the ungual III has a sigmoid distal margin and reminds of a vestigial non-ungual phalanx (Fig. 23A). Ungual V is far from reduced relative to the unguals III and IV and is even anteroposteriorly expanded distally. The pollex ungual is massive and strongly recurved distally. It is shorter than the metacarpal I and its concave proximal articular surface is higher than broad (Table 4). In articulation with the manus, it is oriented medially (Fig. 23). Nail grooves are present on each side of the claw, the medial one being in more dorsal position than the lateral.

TABLE 4. — Measurements (in mm) of manus elements of *Tazoudasaurus naimi* (To2-112). Abbreviations: **L**, length; **Prow**, maximum transverse width of proximal end; **Proh**, maximum anteroposterior length/height of proximal end; **Disw**, maximum transverse width of distal end; **Dish**, maximum transverse length/height of distal end.

To2-112	L	Prow	Proh	Disw	Dish
Ulna	–	–	–	49	74
Radius	–	–	–	67	54
Carpal I	24	62	35	69	38
Metacarpal I	66	40	49.5	43	25
Metacarpal II	89	41	43	38	28
Metacarpal III	92	43	31	38	25
Metacarpal IV	78	43	28	34	21
Metacarpal V	61	46	40	42	36
Phalanx I,1	33	36	29	33	25
Phalanx I,2	54	26	33	–	–
Phalanx II,1	38	35	24	36	15
Phalanx II,2	16	24	13	24	6
Phalanx III,1	38	39	22	33	12
Phalanx III,2	12	22	10	22	5
Phalanx IV,1	29	30	18	32	12
Phalanx IV,2	11	17	11	18	4
Phalanx V,1	40	39	21	34	14
Phalanx V,2	20	22	11	18	9

In addition to this complete distal left forefoot, another manual ungual belonging to an adult specimen has been recovered in the upper bonebed (To1-122). It was first thought to be a pedal ungual phalanx, but it is very similar in shape to the ungual of the digit V of the manus described above except that its length and proximal width are respectively 330% and 400% that of To2-112. The proximal articular surface is 90 mm wide and only 39 mm high. It is smooth and concave and is slightly inclined anterodorsally. The medial margin of the ungual is short and perpendicular to the proximal articular surface, while its lateral margin is longer and directed anteromedially relative to the proximal articular surface, so that the bone has a roughly triangular outline in dorsal and ventral views. The distal end is thickened dorsoventrally as in the juvenile specimen.

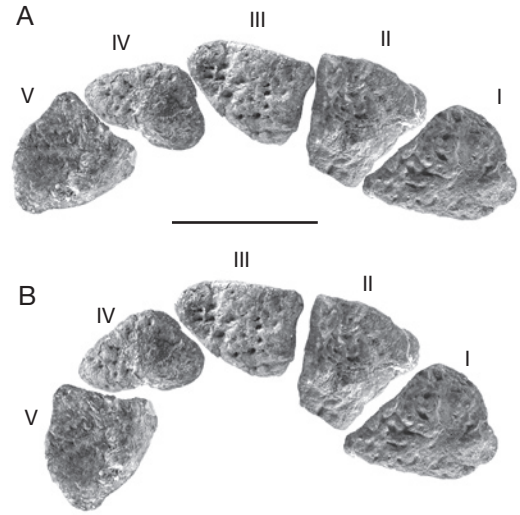

FIG. 24. — *Tazoudasaurus naimi*, left manus (To2-112): **A**, metacarpals as found articulated in proximal view; **B**, metacarpals articulated in a more tubular structure in proximal view. Scale bar: 5 cm.

PELVIC GIRDLE

Ilium

Only a left ilium (MHNM To1-373) of *Tazoudasaurus* has been recovered so far (Fig. 25; Table 5). The ilium is complete except a portion missing from the dorsal margin of the iliac blade. The preacetabular process curved forwards as in other sauropods but does not taper distally and is rounded in outline (Fig. 25A, B). It is directed anterodorsally but not deflected laterally as seen is neosauropods (Wilson & Sereno 1998), and only slightly curved

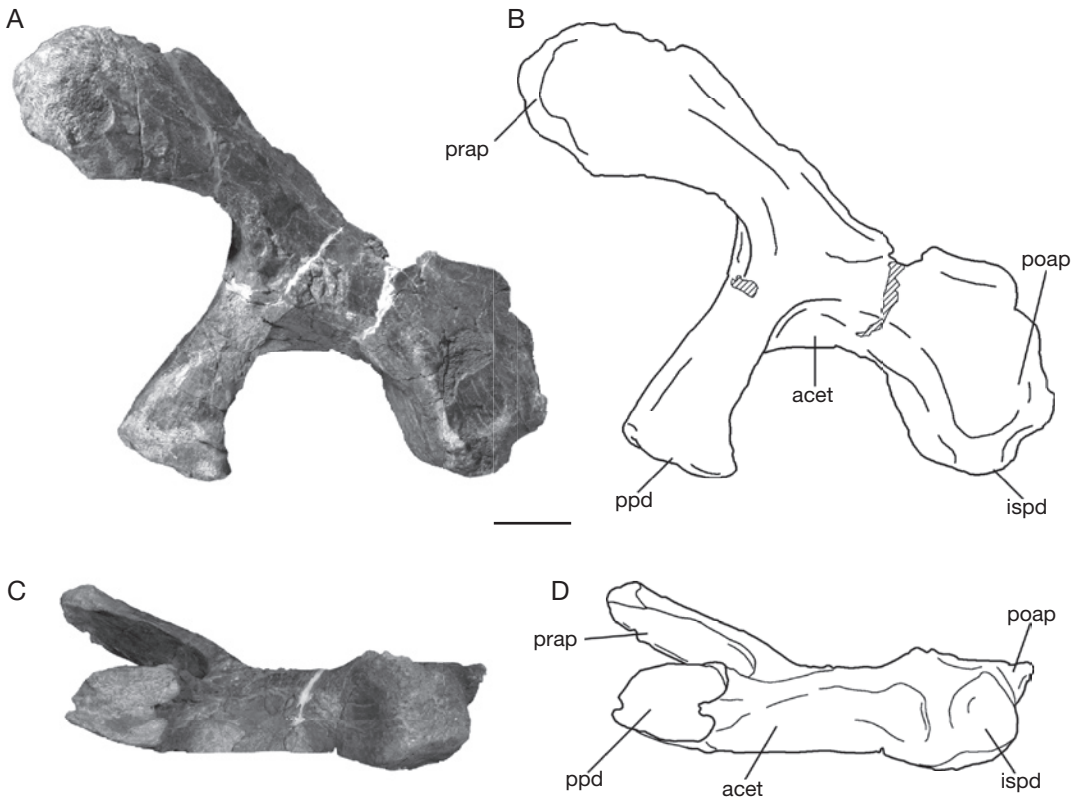

FIG. 25. — *Tazoudasaurus naimi*, left ilium (To1-373): **A**, **B**, lateral view; **C**, **D**, ventral view. Abbreviations: **acet**, acetabulum; **ispd**, ischial peduncle; **poap**, postacetabular process; **ppd**, pubic peduncle; **prap**, preacatabular process. Scale bar: 10 cm.

outward (Fig. 25C, D). The ventral margin of the preacetabular process is slightly concave in lateral view. The iliac blade is concave anteroposteriorly and convex dorsoventrally. If the dorsal margin of the preacetabular and postacetabular processes is convex in lateral view, it is not clear if it the case of that of the iliac blade. It is likely that the iliac blade was only slightly dorsally concave in *Tazoudasaurus*, compared with the strong convexity seen in *Patagosaurus* (Bonaparte 1986) and neosauropods. The pubic peduncle is prominent, directed anteroventrally, and triangular in cross section. The ischial peduncle is reduced but still below the distal margin of the postacetabular process contrary to the condition observed in neosauropods (Upchurch 1998). It is subcircular and faces posteroventrally. The medial surface of the ilium is damaged but bears deep scars where sacral ribs attached.

Pubis

At least three pubes of *Tazoudasaurus* have been found in Toundoute, from both localities To1 and To2 (CPSGM To1-103, MHNM To2-10 and CPSGM Pt2). They belong to three different adult individuals but only one is complete and described here (To1-103; Fig. 26; Table 5). As previously stated by Allain *et al.* (2004), the pubis of *Tazoudasaurus* is very similar to that of *Vulcanodon*, both in shape and proportions. The pubis is relatively slender compared with that of more advanced sauropods. Its lateral margin is concave laterally in anterior and posterior views (Fig. 26A-D). The iliac

TABLE 5. — Measurements (in mm) of pelvis elements of *Tazoudasaurus naimi*. Abbreviation: **e**, estimated.

Bone/Dimension	Measurements	
Ilium (To1-373)		
Length	675	
Length of the iliac blade	795	
Length of the pubic peduncle	270	
Diameter of acetabulum	265	
Length of the distal end of the pubic peduncle	175	
Width of the distal end of the pubis peduncle	197	
Length of the distal end of the ischial peduncle	97	
Width of the distal end of the ischial peduncle	144	
Pubis (To1-103)		
Length	610	
Maximum width of the proximal end	235	
Length of the iliac peduncle	111	
Width of the iliac peduncle	150	
Width of the distal end	180	
Heigth of the distal end	98	
Minimum width of the pubic blade	123	
Length of the acetabulum	120	
Ischium	**To1-378**	**To1-379**
Lenght	–	285e
Width across proximal end	394	94
Length of the pubic peduncle	178	50
Length of the iliac peduncle	176	52
Length of chord across acetabular margin	122	37
Minimum width of the ischial blade	–	33
Width of the distal end	–	57e

articular surface is rough and not very well defined. It appears to be anteriorly deflected (Fig. 26A, B, E, F). The anterior margin of the iliac peduncle is confluent with the pubic apron and the ambiens process is absent. The broad and smooth acetabulum lies posteromedial to the iliac peduncle (Fig. 26I, J). The puboischial plate is damaged anteriorly near the pubic symphysis. It is pierced by a large anteroventrally elongate obturator foramen which is not completely visible in anterior view. The length of the articulation for the ischium is less than one third the total pubis length. The pubic apron has a transverse orientation as in *Vulcanodon* and the symphysis is straight. Its lateral margin is thicker than the medial margin (Fig. 26G, H). A prominent and long crest runs on the posterior surface of blade of the pubis from the lateral wall of the obturator foramen (Fig. 26C, D). The distal end of the pubis is expanded anteroposteriorly, especially along its lateral margin. It has a convex rugose surface and a triangular outline.

Ischium

Two incomplete adult ischia (CPSGM To1-4; MHNM To1-378) and one juvenile ischium (To1-379, see below) have been recovered in Toundoute. To1-378 which is described here was lying under the left ilium. Only the proximal part of this ischium is complete, most of the ischial blade and the distal end are missing (Fig. 27; Table 5). The mildly convex proximal end of the iliac peduncle is elliptical in outline, with the long axis of this ellipse directed anteroposteriorly. The pubic peduncle is as long as the iliac peduncle and is triangular in outline, with its ventral expansion forming the apex. The acetabular surface slopes medially and has an upstanding medial rim (note that Cooper [1984: fig. 18c] has probably mislabelled a lateral view of the left ischium as a "medial" view of the "right" ischium). The preserved portion of the ischial blade is in the same plane as the proximal plate. The blade is directed posteroventrally, and it is thicker posterodorsally than anteroventrally. A prominent groove extends

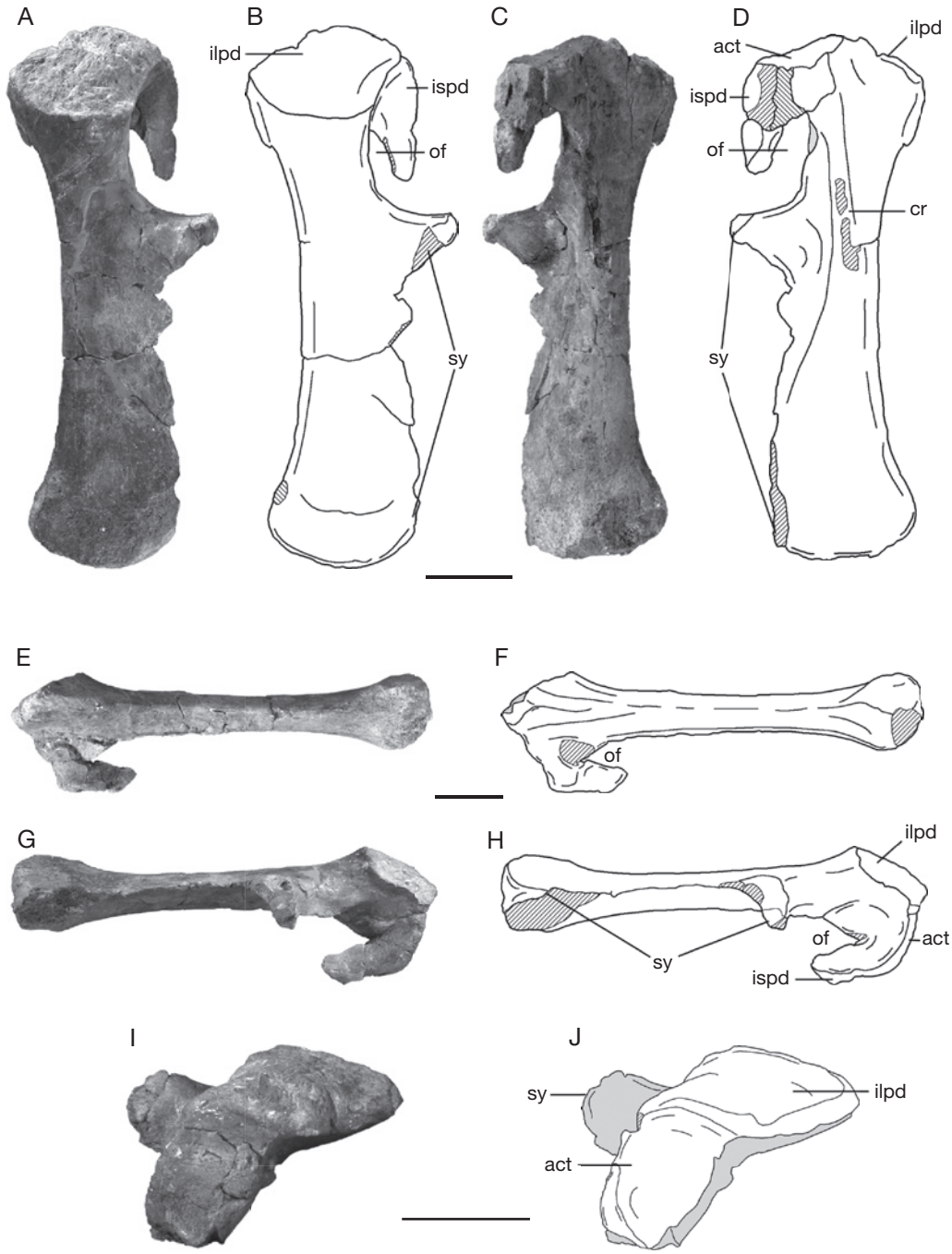

FIG. 26. — *Tazoudasaurus naimi*, right pubis (To1-103): **A**, **B**, anterior view; **C**, **D**, posterior view; **E**, **F**, lateral view; **G**, **H**, medial view; **I**, **J**, proximal view. Abbreviations: **act**, acetabulum; **cr**, crest; **ilpd**, iliac peduncle; **ispd**, ischiac peduncle; **of**, obturator foramen; **sy**, symphysis. Scale bars: 10 cm.

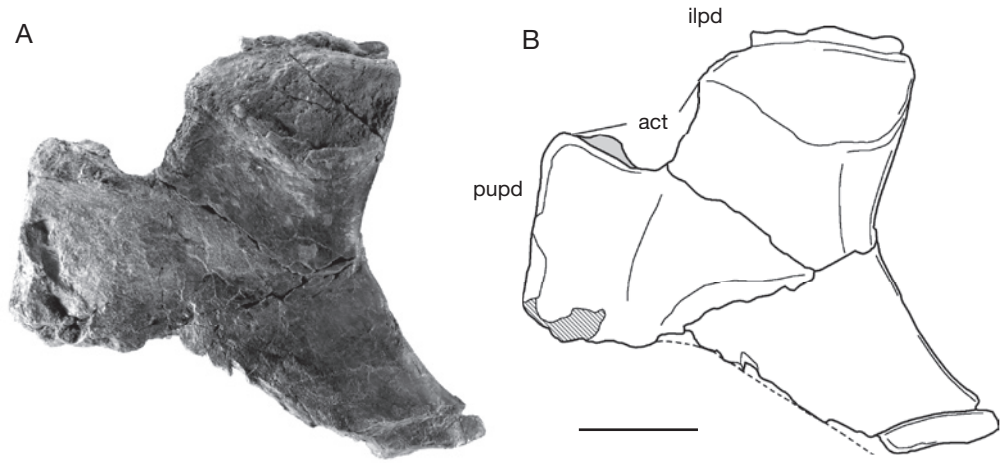

FIG. 27. — *Tazoudasaurus naimi*, right ischium (To1-378): **A**, **B**, medial view. Abbreviations: **act**, acetabulum; **ilpd**, iliac peduncle; **pupd**, pubic peduncle. Scale bar: 5 cm.

along the laterodorsal margin of the proximal part of the blade. In lateral view, the distal shaft is slightly curved and its long axis, if extrapolated forwards, would pass through the most ventral point of the acetabulum. The angle between the blade and the iliac peduncle is greater than that between the blade and the pubic peduncle.

HINDLIMB

Femur

Five femora belonging to five different individuals have been found in Toundoute (CPSGM To1-4, CPSGM To1-105, MHNM To1-256, MHNM To1'-381 and CPSGM To2-9). The longest of these femora (To1'-381) is about 1230 mm, but is not fully prepared. The only complete femur, To1-256, belongs to a juvenile individual, but is crushed anteroposteriorly (see description below). Thus, the adult femur description that follows is based on the various specimens available.

The femora of *Tazoudasaurus* are straight and anteroposteriorly compressed. The head of the femur of To1'-381 is bulbous and sub-circular in proximal view. It extends little beyond the medial border of the femoral shaft. The femoral head is directed dorsomedially. As in *Vulcanodon*, the lesser trochanter is preserved as a developed ridge on the lateral edge of the shaft of the femur (Fig. 3). In adult specimens, the fourth trochanter is reduced to a low ridge. It lies at the posteromedial margin of the shaft, and extends beyond the mid-length of the femur. The *Tazoudasaurus* femora exhibit an elliptical midshaft cross section. The distal end of the femur is badly damaged in every specimen, but it seems that the fibular condyle is larger than the tibial condyle.

Tibia

The upper bone bed of Toundoute series has yielded at least three tibiae (MHNM To1-76, MHNM To1'-380 and MHNM To1'-382). To1-76 belongs to a juvenile individual (see below). The right tibia To1'-380 was found beneath the largest known femur of *Tazoudaurus* (To1'-381), which was itself near the proximal part of a left tibia (To1'-382). These three bones belong to the same adult individual (Fig. 4), and the tibia/femur length ratio is around 0.58, which is typical for the Sauropoda (McIntosh, 1990).

The tibia of *Tazoudasaurus* is strongly reminiscent of that of *Vulcanodon* and shares with it features unknown in other sauropods (Fig. 28). The proximal end is strongly expanded anteroposteriorly, and its length is more than twice its mediolateral width (Table 6). This symplesiomorphic condition is unique within sauropods. In

TABLE 6. — Measurements (in mm) of hindlimb elements of *Tazoudasaurus naimi*. Abbreviations: **e**, estimated; **L**, length; **Prow**, transverse width of proximal end; **Prol**, anteroposterior length of proximal end; **Medw**, transverse width of the shaft at midlength; **Medl**, anteroposterior length of the shaft at midlength; **Disl**, transverse length of distal end; **Disw**, transverse width of distal end.

Specimen	L	Prow	Prol	Medw	Medl	Disw	Disl
Femur							
To1-04, left	1150e	–	–	150	80	300	–
To1-105, right	495	137	–	80	52	138	–
To1-256, right	290	88	–	45	25	94	–
To1-381, right	1230e	290e	–	200e		330e	
Tibia							
To 1-76, left	250	45	109	23	44	43	64
To1-380, right	710	138	360	52	143	205	182
Fibula							
To1-42, right	730	150	–	–	–	146	–
To1-43, left	730e	–	–	–	–	155	–
To1-377, left	530	133	–	68	46	126	–

other sauropods, the proximal end of the tibia is either transversely expanded as in *Mamenchisaurus* Young, 1954 (Ouyang & Ye 2002), *Shunosaurus* (Zhang 1988), *Omeisaurus* (He *et al.* 1988), and *Cetiosaurus* (Upchurch & Martin 2003) or subcircular as in neosauropods but also *Patagosaurus* (*contra* Wilson 2002, 2005a). The stout cnemial crest is 10 cm long, and is directed mainly anteriorly and very slightly laterally (Fig. 28A-D). In lateral view, the proximal end is convex anteroposteriorly (Fig. 28E, F). It tapers posteriorly to form a process which points posteroventrally (Fig. 28G, H). Between this process and the cnemial crest, the lateral margin of the proximal end forms a broad projection which extends distally and gradually merges with the shaft. The shaft of the tibia is strongly flattened transversely (Table 6): its mediolateral width at midlength is only 36% of its anteroposterior length (38% in *Vulcanodon*). The distal breadth of the tibia is considerably more than twice its midshaft breadth. In this respect, *Tazoudasaurus* possesses the derived state present in Titanosauria (Wilson, 2002) but also in *Vulcanodon*. In the two Toarcian African sauropods, the midshaft/distal tibial breadth ratio is around 0.25. The distal end is expanded both anteroposteriorly and especially transversely, and has a rectangular outline with subequal anteroposterior and transverse diameters (Fig. 28I, J). As in other sauropods, the posteroventral process of the tibia is reduced, and does not extend laterally towards the calcaneum. Thus, the posterior fossa of the astragalus must be visible posteriorly.

Fibula

To1 locality has yielded three fibulae. CPSGM To1-33 and CPSGM To1-42 belong to the same adult individual and were mentioned in the original publication (Allain *et al.* 2004). The presence of a prominent crest on the lateral surface of the proximal end of the right fibula To1-42, was used as a diagnostic character of *Tazoudasaurus*. It appears now that this crest is a preservational artefact. The description which follows, therefore, is based solely on the left fibula MHNM To1-377 (Fig. 29).

The *Tazoudasaurus* fibula is similar to those of other sauropods, with a transversely compressed proximal end, and a long and straight slender shaft. The medial surface of the proximal end is marked by the broad triangular striated area, for articulation with the tibia. The inturned anterior trochanter of the proximal end described in *Vulcanodon* (Cooper, 1984) is present in *Tazoudasaurus* as well (Fig. 29A D), but it seems stouter than in the Zimbabwean specimen and does not bear a deep depression on its anterolateral surface, which is only very slightly concave. The medial surface of the fibula is nearly flat.

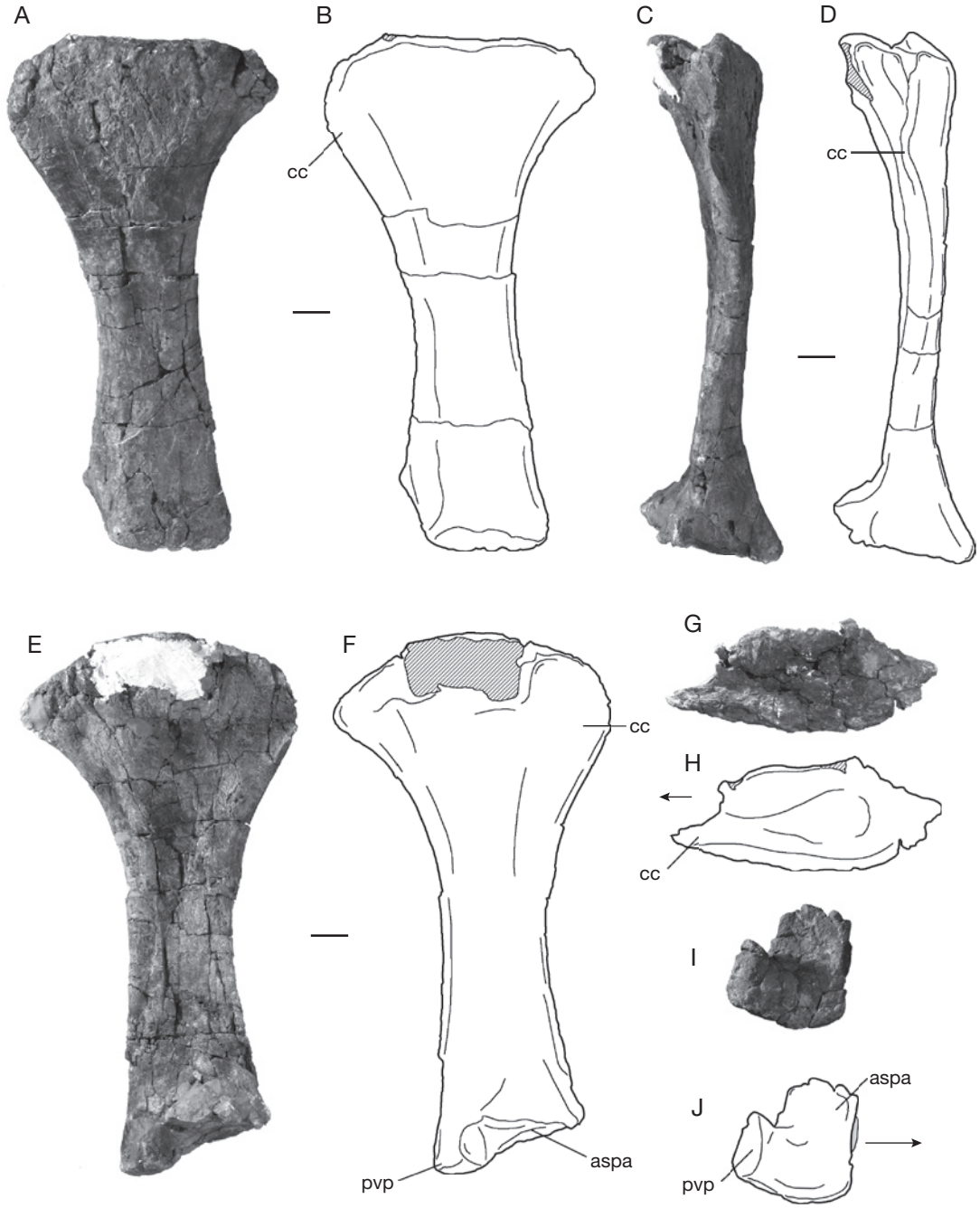

FIG. 28. — *Tazoudasaurus naimi*, right tibia (To1-380): **A**, **B**, medial view; **C**, **D**, anterior view; **E**, **F**, lateral view; **G**, **H**, proximal view; **I**, **J**, distal view. Abbreviations: **aspa**, articular surface for the ascending process; **cc**, cnemial crest; **pvp**, posteroventral process. Black arrow is directed anteriorly. Scale bars: 5 cm.

FIG. 29. — *Tazoudasaurus naimi*, left fibula (To1-377): **A**, **B**, lateral view; **C**, **D**, medial view; **E**, **F**, anterior view; **G**, **H**, posterior view; **I**, proximal view; **J**, distal view. Abbreviations: **asa**, astragalar articular surface; **at**, anterior trochanter; **caa**, calcaneal articular surface; **cr**, crest; **lt**, lateral trochanter; **tas**, tibial articular surface. Scale bars: 10 cm.

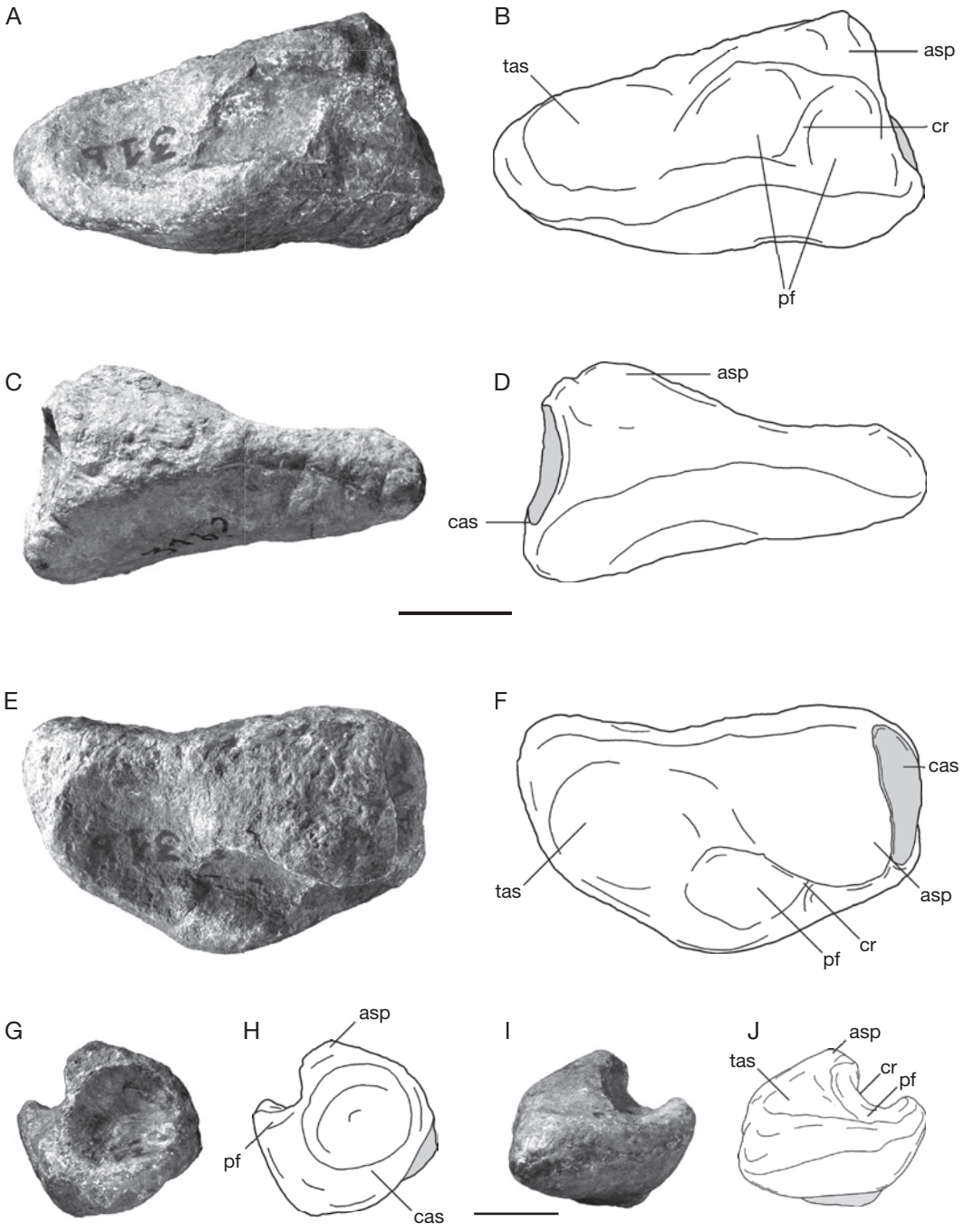

FIG. 30. — *Tazoudasaurus naimi*, right astragalus (To1-31): **A**, **B**, posterior view; **C**, **D**, anterior view; **E**, **F**, proximal view; **G**, **H**, lateral view; **I**, **J**, medial view. Abbreviations: **asp**, ascending process of the astragalus; **cas**, calcaneal articular surface; **cr**, crest; **pf**, posterior fossa; **tas**, tibial articular surface. Scale bars: 5 cm.

A large bulge is present at approximately mid-length on the lateral side of the shaft of *Tazoudasaurus* fibula and interpreted as the lateral trochanter. Such a trochanter is considered to be a synapomorphy of Eusauropoda (Wilson & Sereno 1998; Wilson 2002; Norman *et al.* 2004b), but in fact it has been described but not figured for *Vulcanodon* (Cooper 1984; Raath 1972). Towards the distal end, the anterior margin of the shaft forms an acute vertical crest, whereas the corresponding posterior margin is somewhat thicker and more rounded (Fig. 29E, F). The distal articular surface is convex. It expands both medially where it contacts the astragalus (Fig. 29G, H), and anterodorsally where it tapers to a point and has a hook-like profile (Fig. 29A, B).

Tarsus

Astragalus

Two astragali have been recovered in Toundoute, one belonging to an adult individual (CPSGM To1-31; Fig. 30) and the other to a juvenile (To1-135; Fig. 43). The astragalus of *Tazoudasaurus* is strongly reminiscent of that of *Vulcanodon* (Cooper 1984). In proximal view, the astragalus is more rectangular than triangular in outline, although it is widest laterally than medially. Its anterior margin is slightly concave transversally, whereas the posterior one is markedly convex (Fig. 30E, F). In anterior view, the medial side of the astragalus is reduced, and the astragalus appears wedge-shaped, but to a lesser extent than in neosauropods (Wilson & Sereno 1998) because of the slight transversal concavity of the ventral articular surface (Fig. 30C, D). This latter is rugose and pitted. Anteriorly, the thick ascending process rises towards the lateral side with a slanting upper surface. It is directed weakly dorsally and strongly posteriorly, so that it extends to the posterolateral margin of astragalus (Fig. 30E, F). The lateral fibular articular surface is large and circular. Contrary to that of *Vulcanodon*, it is markedly concave and smooth (Fig. 30G, H). The posterior fossa of the astragalus is divided unequally by a rounded crest that extends posteromedially as far as the posterior tongue, as in other sauropods including *Vulcanodon*. Foramina have been reported in the posterior fossa of various sauropods (Wilson & Sereno 1998; Bonnan 2005), but are absent in *Tazoudasaurus* and *Vulcanodon*. The medial posterior sub-fossa is broader than the lateral. The posterior fossa is separated from the tibial articular surface by another crest extending posteromedially from the medial side of the ascending process (Fig. 30E, F, I, J). The tibial articular surface is shallowly concave and occupies most of the medial side of the astragalus proximally.

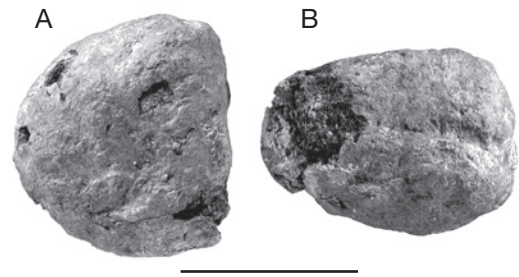

Fig. 31. — *Tazoudasaurus naimi*, left(?) calcaneum (To1-356): **A**, dorsal view; **B**, medial view. Scale bar: 5 cm.

Calcaneum

As other known sauropod calcanea, the calcaneum of *Tazoudasaurus* (MHNM To1-356) is rugose, globular in shape, and has few distinguishing characteristics (Fig. 31). The anteromedial expansion of the calcaneum seen in *Vulcanodon* is absent in *Tazoudasaurus*. The proximal articular surface, which receives the distal end of the fibula, is flat and smooth (Fig. 31A). The medial surface of the calcaneum, which articulates with the astragalus, is flat and slightly roughened (Fig. 31B), but the the condition of this articulation is not clear. The lateral, distal anterior and posterior surfaces of the calcaneum are strongly convex and rugose.

Pes

Numerous elements of the pes of different individuals of *Tazoudasaurus* have been recovered in Toundoute but none of them have been found in articulation, rendering difficult identification of the elements, especially the pedal phalanges. Metatarsals I, II, IV and V have been tentatively identified as well as unguals of at least three digits (Figs. 32-36).

FIG. 32. — *Tazoudasaurus naimi*, metatarsals: **A**-**D**, left metatarsal I (To1-22); **A**, dorsal view; **B**, ventral view; **C**, medial view; **D**, proximal view; **E**-**H**, left(?) metatarsal II (To1-265); **E**, dorsal view; **F**, ventral view; **G**, lateral view; **H**, proximal view; **I**-**L**, right metatarsal IV (To1-13); **I**, dorsal view; **J**, ventral view; **K**, medial view; **L**, proximal view. Abbreviation: **bu**, bump. Scale bars: 5 cm.

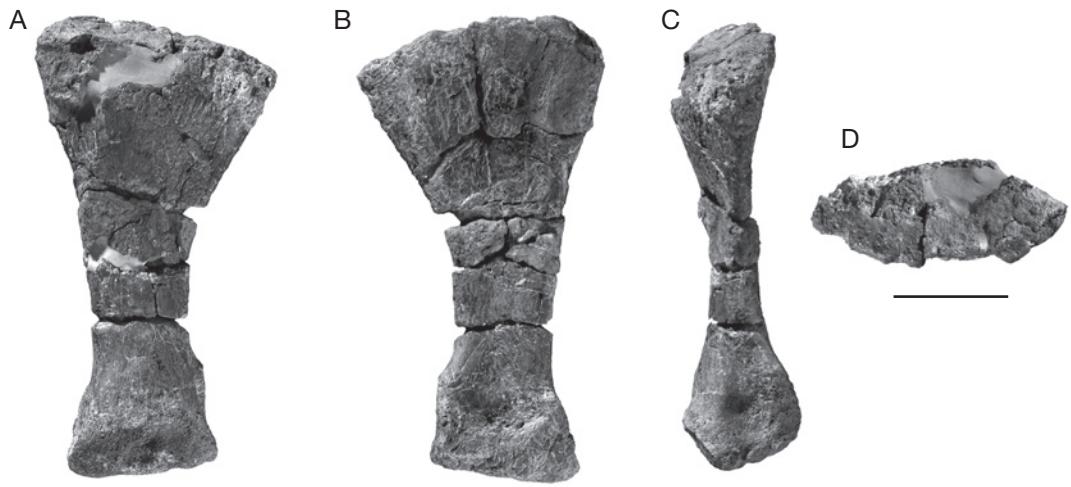

FIG. 33. — *Tazoudasaurus naimi*, right metatarsal V (Pt-25): **A**, dorsal view; **B**, ventral view; **C**, medial view; **D**, proximal view. Scale bar: 5 cm.

Metatarsals

Metatarsal I (MHNM To1-22) is the stoutest element of the pes (Fig. 32 A-D). Its minimum shaft width is 35% of its length, whereas it is less than 25% in other metatarsals. Its triangular proximal articular surface is deeper than wide (Fig. 32D), due to the presence of a ventral keel which extends anteriorly as far as the mid-shaft (Fig. 32B, C). The proximal articular surface faces slightly ventrally and is deeply concave. The shaft is nearly straight medially and strongly concave laterally (Fig. 32A). The distal articular surface is well developed and asymmetrical with a much enlarged lateral condyle and a deep collateral fossa.

In dorsal view, the proximal and distal ends of the metatarsal II (CPSGM To1-265) are well expanded (Fig. 32E). The proximal end is strongly asymmetrical; its flat dorsal surface expands medially while the flat ventral surface is expanded laterally (Fig. 32H). Both the medial and lateral sides of the proximal end are strongly concave, probably to receive metatarsals I and III respectively. This suggests that at least the first three metatarsals were closely appressed in *Tazoudasaurus*, as seen in *Vulcanodon* (Cooper 1984). The proximal articular surface of the metatarsal II is slightly convex. The shaft of the metatarsal II is straight. Deep collateral fossae invade the lateral and medial sides of the asymmetrical distal articular surface, which extends on the dorsal surface of the shaft and faces slightly laterally (Fig. 32E, G).

Metatarsal IV is known from three different specimens, two of them belonging to the same individual (MHNM To-13; MHNM To1-197). The proximal end of the metatarsal IV is as strongly expanded as that of *Vulcanodon*, but it is not as asymmetrical. The proximal surface is slightly concave (Fig. 32L) and its dorsoventral depth is only 25% of its transversal width. A well-developed bump lies on the medial part of the anterior surface of the proximal end of the metatarsal IV (Fig. 32I, K) in each of the three recovered metacarpals IV. This bump is unknown in other sauropods and is considered here as an autapomorphy of *Tazoudasaurus*. The posterior surface of the proximal end of the metatatarsal IV is transversely concave (Fig. 32J). At midlenght its shaft becomes straight and has an oval cross section. The distal articular surface is not subdivided, but it is expanded both transversely and dorsoventrally, so that the distal end is deeper than the proximal end (Fig. 32K). The lateral collateral pit is more strongly developed than the medial.

Metatarsal V (MHNM Pt-25) is similar in shape to the metatarsal IV (Fig. 33) but its proximal end is more medially expanded (Fig. 33A, B). The concave proximal articular surface faces posterodorsally, and

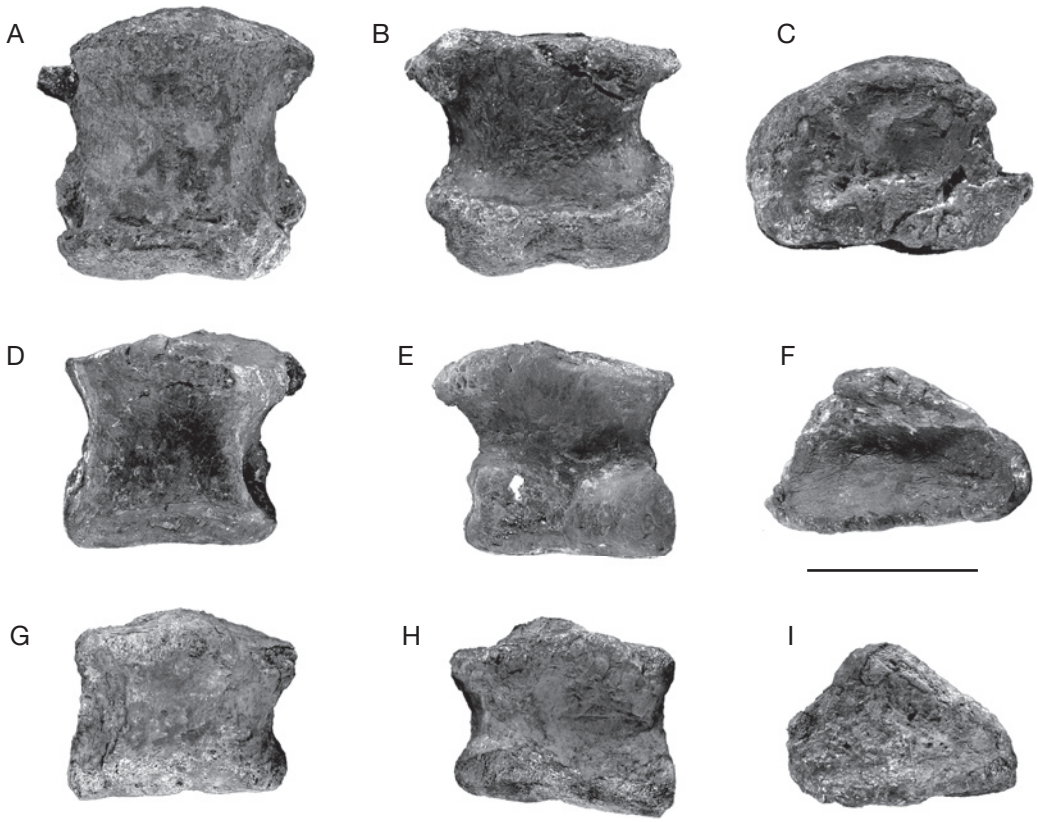

FIG. 34. — *Tazoudasaurus naimi*, pedal phalanges: **A**-**C**, pedal phalanx (To1-121); **A**, dorsal view; **B**, ventral view; **C**, proximal view; **D**-**F**, pedal phalanx (To1-137); **D**, dorsal view; **E**, ventral view; **F**, proximal view; **G**-**I**, pedal phalanx (To1-158); **G**, dorsal view; **H**, ventral view; **I**, proximal view. Scale bar: 5 cm.

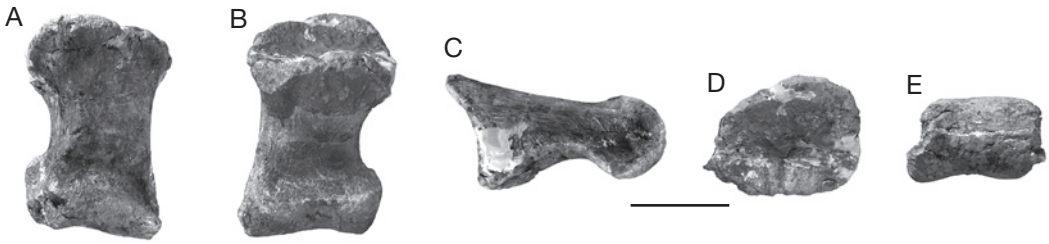

FIG. 35. — *Tazoudasaurus naimi*, left pedal phalanx (To1-67): **A**, dorsal view; **B**, ventral view; **C**, medial view; **D**, proximal view; **E**, distal view. Scale bar: 5 cm.

its depth is only 20% its transverse width (Fig. 33C, D) The distal condyle is undivided and expands dorsoventrally (Fig. 33C). The collateral fossae are shallower than in metatarsals II and IV.

Pedal phalanges

Numerous pedal phalanges have been recovered in Toundoute, but their position in the pes is difficult to determine and the phalangeal formula

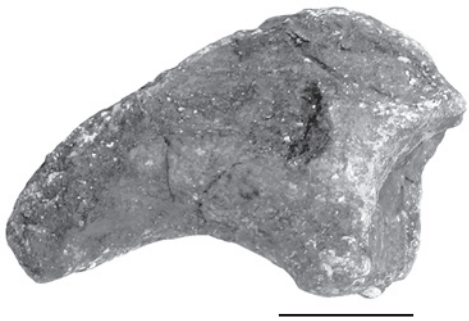

FIG. 36. — *Tazoudasaurus naimi*, ungual phalanx I in lateral view (To1-94). Scale bar: 5 cm.

FIG. 37. — *Tazoudasaurus naimi*, ungual phalanges: **A**, **C**, **E**, ungual phalanx IV (To1-14); **A**, dorsal view; **C**, lateral view; **E**, proximal view; **B**, **D**, **F**, ungual phalanx III (To1-114); **B**, dorsal view; **D**, lateral view; **F**, proximal view. Scale bar: 5 cm.

of *Tazoudasaurus* remains unknown (Figs 34; 35). One of the phalanges is significantly longer proximodistally than broad transversely (Fig. 35), a condition unknown in eusauropods but retained by prosauropods and *Vulcanodon*. This suggests that this phalanx is probably the first phalanx of the second or third digit. Other phalanges are broader than long and are probably more distal (Fig. 34). As in *Vulcanodon*, all the phalanges have deep collateral fossae and well-developed distal articular surface, suggesting a considerable digital flexibility in the pes (Wilson & Sereno 1998).

Ungual phalanges

The ungual phalanx of the first pedal digit (MHNM To1-94) is badly preserved but is distinctly transversely compressed and sickle-shaped, as in other sauropods (Fig. 36). It is also significantly longer than the unguals of the other pedal digits. The other pedal unguals of *Tazoudasaurus* are reminiscent of those seen in *Vulcanodon* (Fig. 37), which are unique among saurischians in being particularly dorsoventrally flattened. According to the shape of the articulated unguals described in *Vulcanodon* (Raath 1972; Cooper 1984), the two unguals of *Tazoudasaurus* described here probably belong to the digit III and IV of the pes. However, the pedal ungual of the digit II of *Vulcanodon* is strongly asymmetrical (Cooper 1984), a feature which is not observed in the two recovered unguals of *Tazoudasaurus* (Fig. 37). Ungual III of *Tazoudasaurus* (CPSGM To1-114) is symmetrical and only slightly recurved ventrally (Fig. 37B, D, F). The proximal articular surface is concave and twice as broad as deep (Fig. 37F), and faces slightly ventrally (Fig. 37D). The dorsal surface is convex both transversely and anteroposteriorly, and bears laterally two deep longitudinal grooves (Fig. 37B). In lateral view, ungual IV of *Tazoudasaurus* (MHNM To1-14) is more curved than the ungual III (Fig. 37C) but remains symmetrical. Its proximal articular surface is deeper dorsoventrally and faces only posteriorly. The distal tip of both unguals is blunt distally.

EARLY JUVENILE *TAZOUDASAURUS* BONES

Among the several hundred bones collected in Toundoute, some very small elements are perfectly preserved and can be confidently assigned to *Tazoudasaurus*. Because juvenile material of sauropods is relatively rare in the fossile record (Norman *et al.* 2004b), some bones of these early juvenile sauropods are described below. A detailed ontogenetic

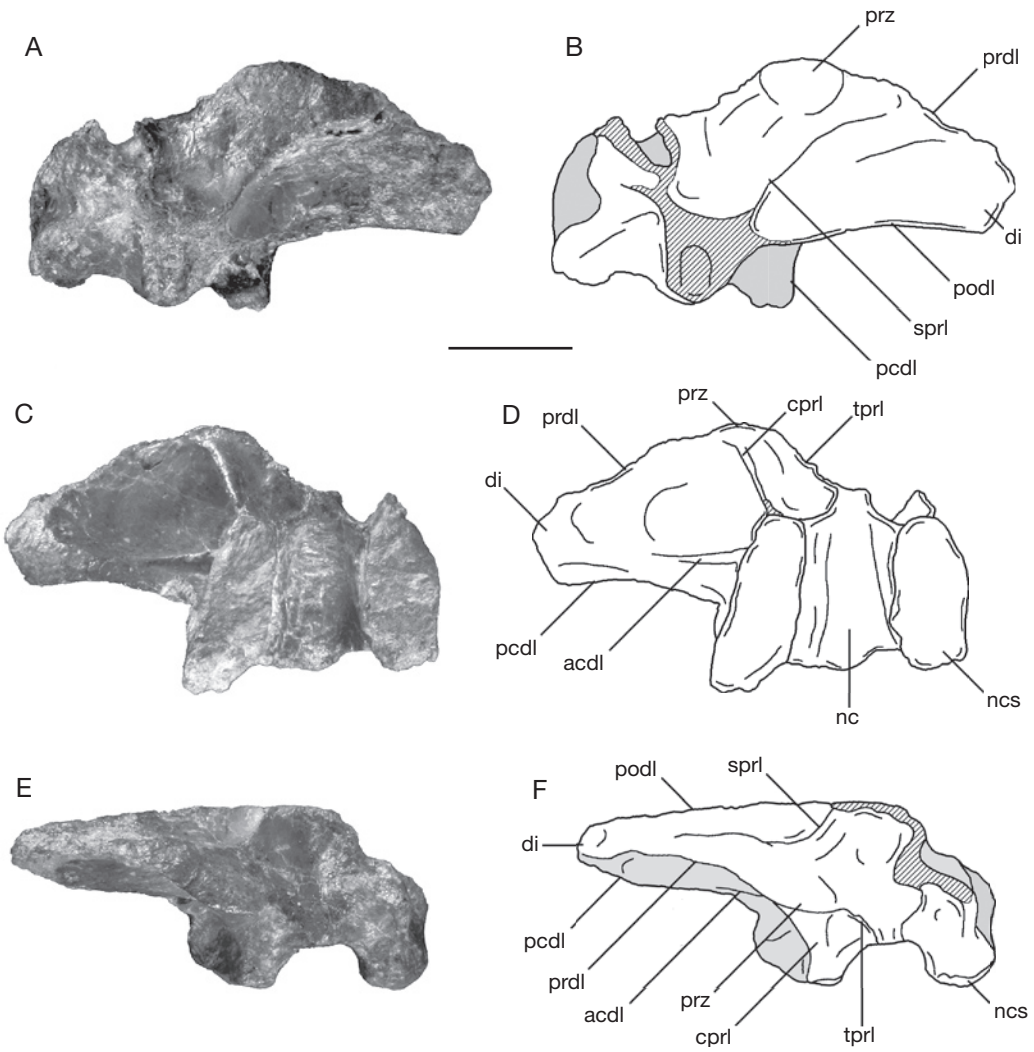

FIG. 38. — *Tazoudasaurus naimi*, dorsal neural arch of a juvenile individual (To1-383): **A**, dorsal view; **B**, ventral view; **C**, posterior view. Abbreviations: **acdl**, anterior centrodiapophyseal lamina; **cprl**, centroprezygapophyseal lamina; **di**, diapophysis; **nc**, neural canal; **ncs**, neurocentral suture; **pcdl**, posterior centrodiapophyseal lamina; **podl**, postzygodiapophyseal lamina; **prdl**, prezygodiapophyseal lamina; **prz**, prezygapophysis; **sprl**, spinoprezygapophyseal lamina; **tprl**, intraprezygapophyseal lamina. Scale bar: 5 cm.

and histological study is beyond the scope of this paper.

ANTERIOR DORSAL NEURAL ARCH

The incomplete neural arch of an anterior dorsal vertebra of a juvenile individual (MHNM To1-383) has been recovered in Toundoute (Fig. 38). The left transverse process, the neural spine and the postzygapophyses are missing. The interdigitating neurocentral suture is clearly visible in ventral view (Fig. 38C, D), confirming the immaturity of the specimen. The parapophyses are not present on the neural arch and thus were located on the centrum, suggesting this was probably an anterior dorsal

neural arch. The neural arch lamination is as well developed as in the adult specimen To1-69. Four diapophyseal laminae (acdl, pcdl, prdl, podl), and four zygapophyseal laminae (cprl, sprl, tprl, tpol) have been identified on the centrum (Table 2), and the cpol is absent. The spinodiapophyseal lamina, which is very reduced in the anterior dorsal vertebra of the adult (see above), is absent in this juvenile vertebra. The articular facets of the prezygapophyses face dorsally (Fig. 38A, B). The hyposphene-hypantrum system is not developed in To1-383, and the tprl's do not fuse to each other above the neural canal (Fig. 38E, F). Each tprl defines with the cprl and the dorsolateral margin of the neural canal a deep fossa on the anterior surface of the neural arch as in To1-69, but without additional lamina inside the fossa (Fig. 38E, F). The transverse process is directed laterally. The tpol's meet above the neural canal but extend laterally to the neural canal, and thus form an X, in posterior view.

Left humerus

The left juvenile humerus (MHNM To1-93) is only 18% the length of the largest known adult humerus (Pt-1) (Fig. 39A-J; Table 3). Its circumference/length ratio (0.35) is slightly less than that of the adult (0.39). The proximal end is less expanded transversely and is 13% of the adult proximal width. Similarly, the distal end is less expanded anteroposteriorly with a length which is only 8% of the length of To1-193 while it is 14% in Pt1. In medial view, the humerus is slightly sigmoidal (Fig. 39E, F). Its lateral margin is nearly straight on its entire length in anterior and posterior views (Fig. 39A-D). The proximal end is compressed anteroposteriorly. Its anterior surface is more concave than in the adult specimen (Fig. 39A, B, I, J). The deltopectoral crest extends down the anterolateral margin of the humerus over 82 mm, which represents 44% of the total length of the bone (49% in Pt-1), and is slightly more prominent than in the adult humerus. The crest running over the anterolateral margin of the distal end of the humerus is absent in the juvenile specimen (Fig. 39G, H). As in Pt-1, the distal end is rotated about 15° anticlockwise with respect to the proximal end.

Left ulna

The juvenile left ulna MHNM To1-374 is better preserved than the adult ulna (Pt-24) described above. It is a slender bone, which is 30% the length of the largest known adult ulna (Pt-24) (Fig. 40A F; Table 3). Its circumference/length ratio (0.37) is not substantially different than that of the adult (0.34). The proximal end is triradiate, but one of the processes is broken distally. This bone was first thought to be a right ulna, but according to the complete left manus found articulated with a distal radius and ulna (Fig. 23), it would appear to be the left ulna, the anteromedial process of which is broken (Fig. 40A, C, E). The anterolateral process is more developed than in the adult specimen and in *Vulcanodon* and must be only slightly shorter than the anteromedial process. The radial fossa is deeper than in the adult specimen. The proximal articular surface lacks an olecranon (Fig. 40A-D). The medial surface of the anteromedial process is slightly concave, whereas the lateral surface of the anterolateral process is slightly convex (Fig. 40E). Below the proximal end, the shaft of the ulna is subtriangular in cross section, with the apex directed anteriorly. The shaft of the ulna is concave laterally and medially and straight posteriorly. The distal end is elliptical with an almost laterally directed long axis. A small bump and roughened ridges mark the contact of the radius on the lateral side of the anterior surface of the ulna, but these are not as prominent as in the adult specimen (Fig. 40A). The rugose distal articular surface of the ulna is expanded transversely.

Right ischium

The maximum width across the proximal end of the right juvenile ischium MHNM To1-379 is 24% that of the adult specimen (Table 5). Only the distal-most part of the ischium is missing (Fig. 41). The mildly convex proximal end of the iliac peduncle is elliptical in outline, with the long axis of this ellipse directed anteroposteriorly. The pubic peduncle is as long as the iliac peduncle and is also elliptical in outline. The acetabular surface slopes medially and has an upstanding medial rim (Fig. 41C, D). As in the adult specimen, the blade of the ischium is thicker posterodorsally than anteroventrally where

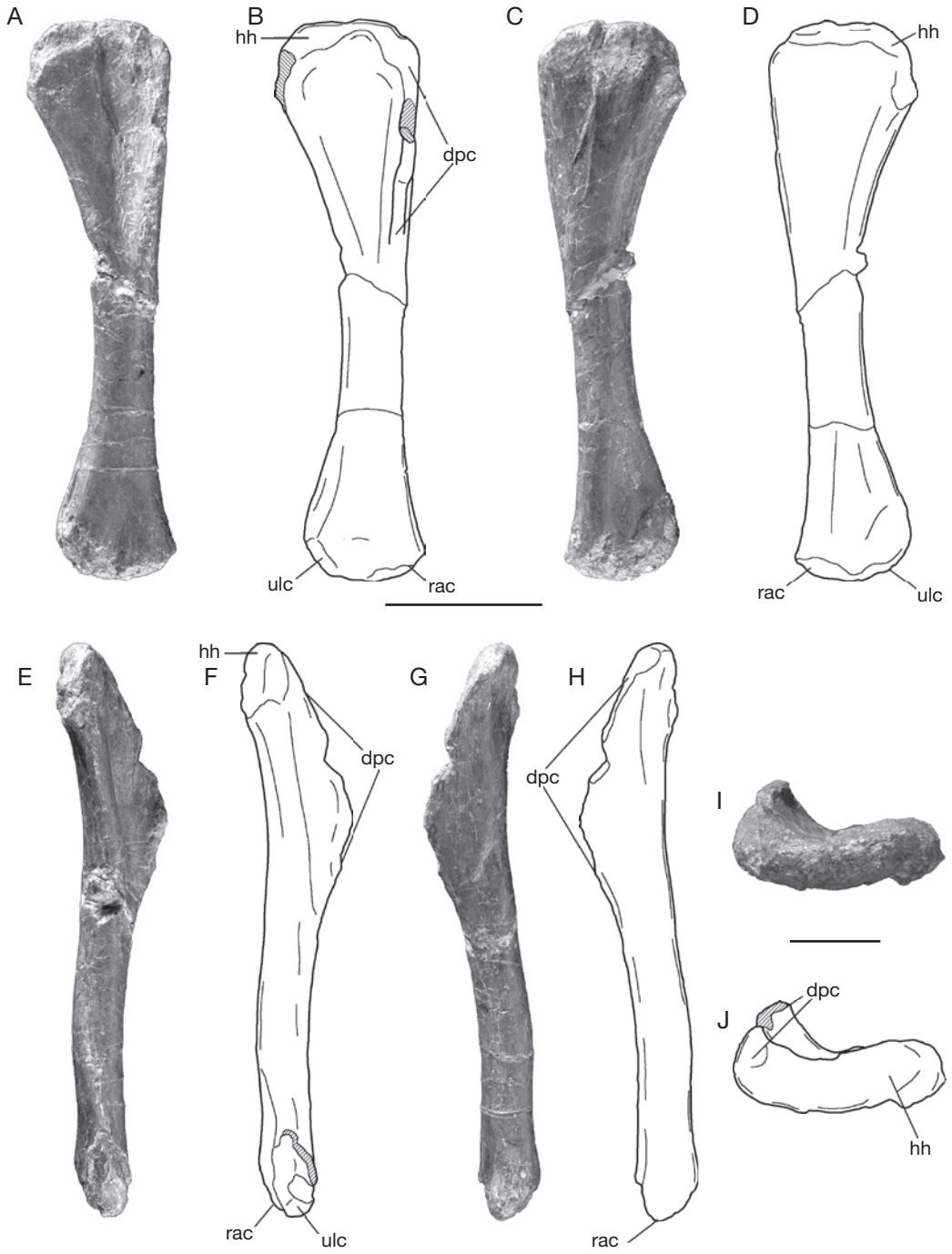

FIG. 39. — *Tazoudasaurus naimi*, left humerus of a juvenile individual (To1-93): **A**, **B**, anterior view; **C**, **D**, posterior view; **E**, **F**, medial view; **G**, **H**, lateral view; **I**, **J**, proximal view. Abbreviations: **dpc**, deltopectoral crest, **hh**, humeral head; **rac**, radial condyle; **ulc**, ulnar condyle. Scale bars: 5 cm.

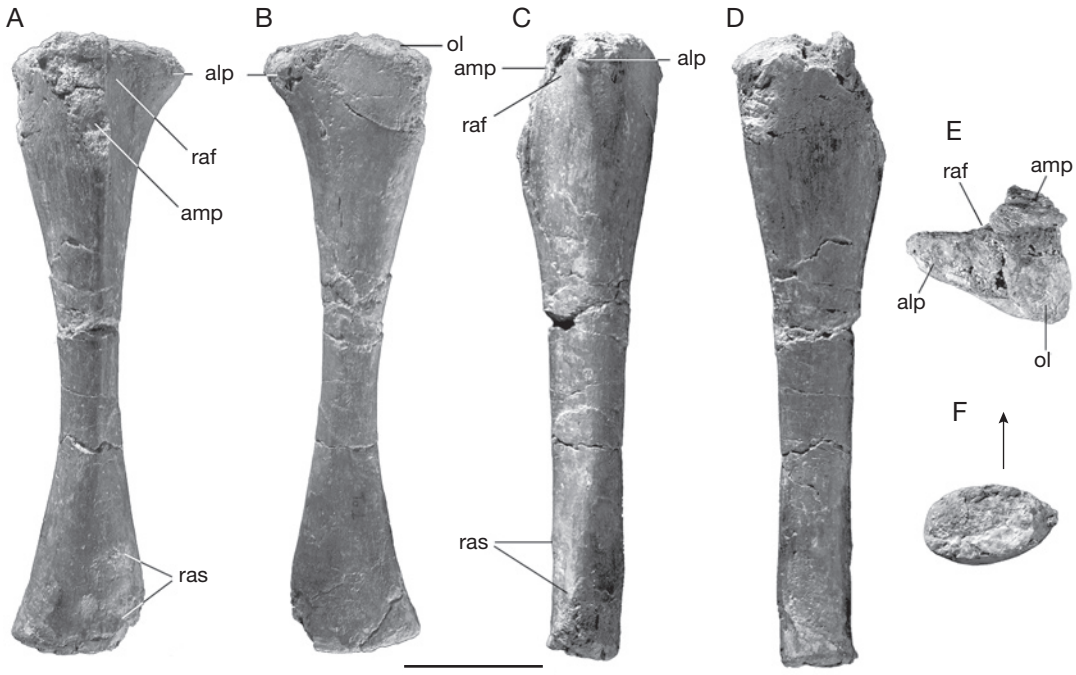

FIG. 40. — *Tazoudasaurus naimi*, left ulna of a juvenile individual (To1-374): **A**, anterior view; **B**, posterior view; **C**, lateral view; **D**, medial view; **E**, proximal view; **F**, distal view. Abbreviations: **alp**, anterolateral process of the ulna; **amp**, anteromedial process of the ulna; **ol**, olecranon area; **raf**, radial fossa; **ras**, radial articular surface. Arrow indicates the anterior direction. Scale bar: 5 cm.

it is articulated with the left ischium. The ischial blade is thus triangular in cross section. A prominent groove extends along the laterodorsal margin of the proximal part of the blade (Fig. 41A, B). Unlike the adult specimen, the angle between the blade and the pubic peduncle is greater than that between the blade and the iliac peduncle, implying that the ischium was more ventrally directed in juvenile individuals. The distal blade is slightly twisted laterally relative to the plane of the proximal plate, but both ischia would meet on an angle, forming a triangle in distal view, unlike macronarians (Wilson & Sereno 1998). The distal end of the ischium is expanded ventromedially.

FEMUR

The right juvenile femur (MHNM To1-256) is 24% the length of the longest femur To1'-381. Although it is complete, this femur is severely crushed anteroposteriorly, and thus lost its shape in its distal half (Fig. 42). The juvenile femur is straight and anteroposteriorly compressed. The head of the femur is directed dorsomedially (Fig. 42A, B). The lesser trochanter is clearly visible and extends as a developed ridge on the anterolateral margin of the femur, terminating about 104 mm below the femoral head (Fig. 42A-E). The fourth trochanter, which lies at the posteromedial margin of the femur, is more prominent than in the adult specimen (Fig. 42C-F). A deep intercondylar groove separates the fibular and rounded tibial condyles (Fig. 42C, D). Poor preservation prevents any assessment of the extent of the distal condyles.

LEFT TIBIA

The juvenile left tibia (MHNM To1-76) is 35% the length of the largest known tibia of *Tazoudasaurus* (To1'-380) (Fig. 43). The circumference/length ratio of the juvenile tibia (0.48) is equivalent to that of the adult (0.49). The shaft of the tibia is less compressed transeversely, its mediolateral width at midlength

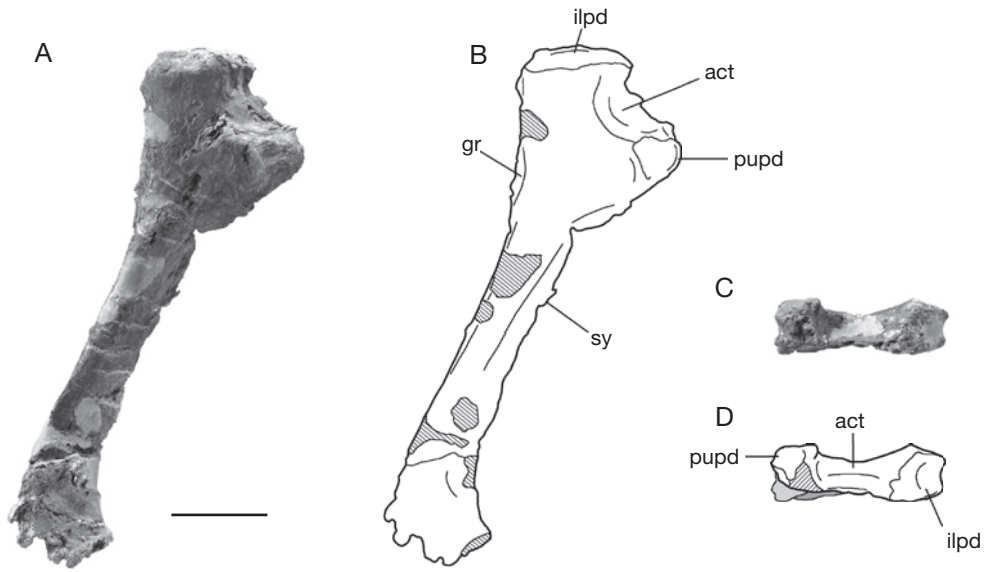

FIG. 41. — *Tazoudasaurus naimi*, right ischium (To1-379): **A**, **B**, lateral view; **C**, **D**, proximal view. Abbreviations: **act**, acetabulum; **gr**, groove; **ilpd**, iliac peduncle; **pupd**, pubic peduncle; **sy**, symphisis. Scale bar: 5 cm.

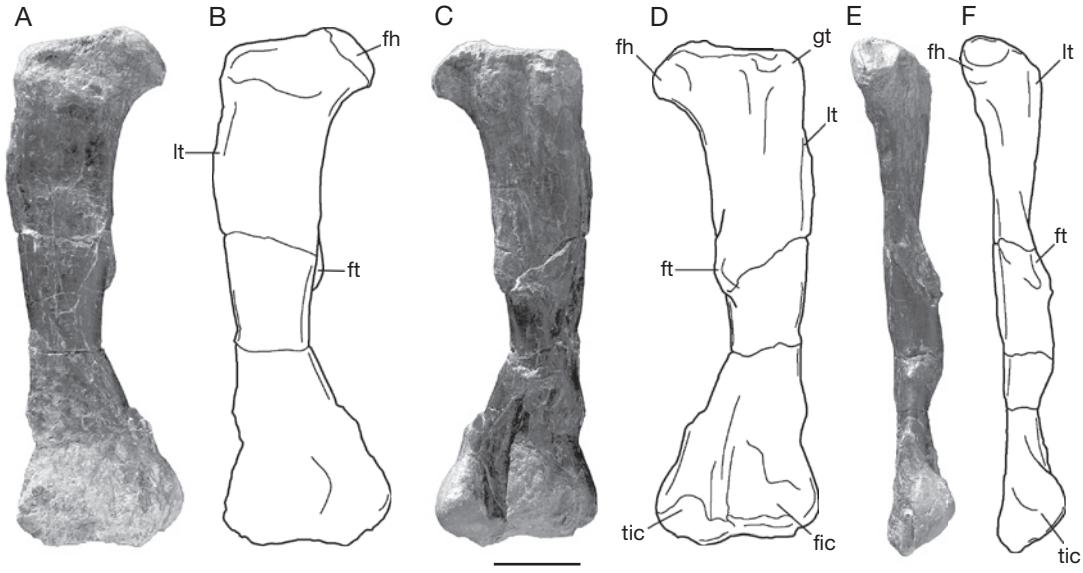

FIG. 42. — *Tazoudasaurus naimi*, right femur of a juvenile individual (To1-256): **A**, **B**, anterior view; **C**, **D**, posterior view; **E**, **F**, medial view. Abbreviations: **fic**, fibular condyle; **fh**, femoral head; **ft**, fourth trochanter; **gt**, great trochanter; **lt**, lesser trochanter; **tic**, tibial condyle. Scale bar: 5 cm.

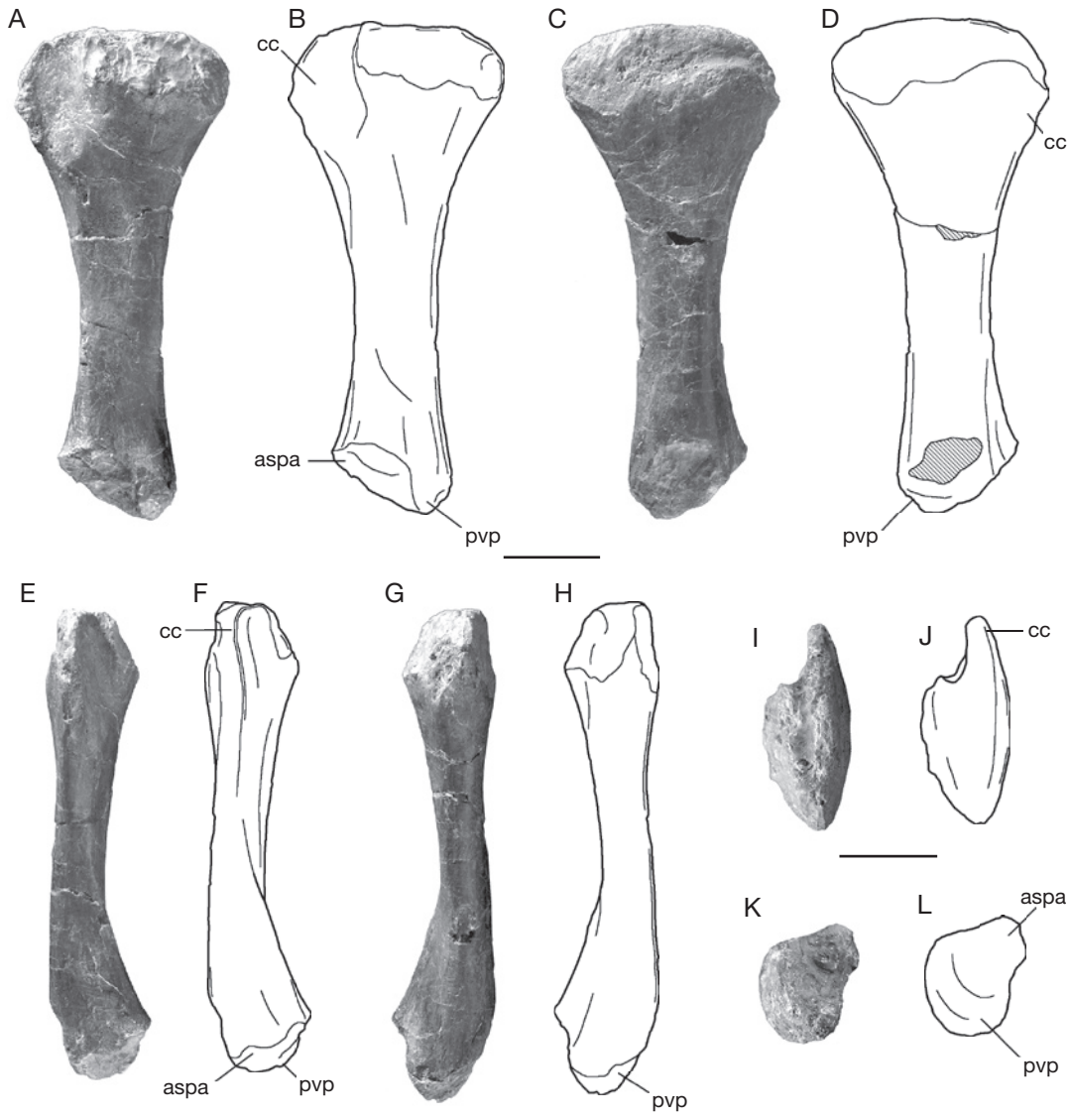

FIG. 43. — *Tazoudasaurus naimi*, left tibia of a juvenile individual (To1-76): **A**, **B**, lateral view; **C**, **D**, medial view; **E**, **F**, anterior view; **G**, **H**, posterior view; **I**, **J**, proximal view; **K**, **L**, distal view. Abbreviations: **aspa**, articular surface for the ascending process; **cc**, cnemial crest; **pvp**, posteroventral process. Scale bars: 5 cm.

being 52% its anteroposterior length, otherwise the morphology of the juvenile tibia is in all respects identical to that of the adult specimen (Fig. 43).

Astragalus

The mediolateral width of the juvenile astragalus (MHNM To1-135) is 39% that of the adult specimen described above. Most of the outer surface of the bone is shaved away, which suggests that the ossification of the astragalus was not complete (Fig. 44). The shape of the juvenile astragalus is similar to that of the adult, with a subrectangular outline in proximal view (Fig. 44C, D), and a wedge-shaped in anterior and posterior views (Fig. 44A, B). The smooth

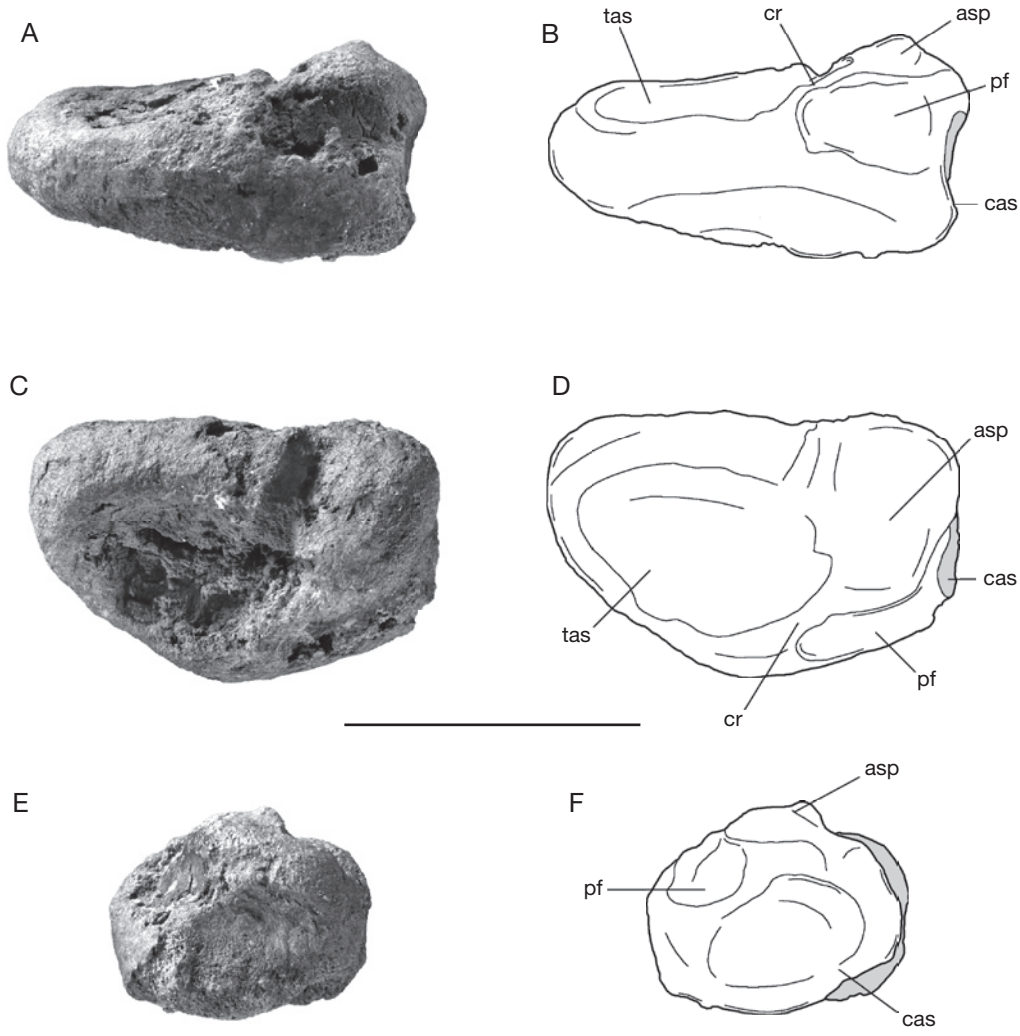

FIG. 44. — *Tazoudasaurus naimi*, right astragalus (To1-135): **A**, **B**, posterior view; **C**, **D**, proximal view; **E**, **F**, lateral view. Abbreviations: **asp**, ascending process of the astragalus; **cas**, calcaneal articular surface; **cr**, crest; **pf**, posterior fossa; **tas**, tibial articular surface. Scale bar: 5 cm.

and concave lateral fibular articular surface is more elliptical than in the adult astragalus (Fig. 44E, F). The ascending process is directed dorsoposteriorly, but its posterior extension is less than in the adult specimen and the ascending process fails to reach the posterolateral margin of astragalus (Fig. 44C, D). The main difference between the juvenile and adult specimens is in the shape of the proximal articular surface. The posterior fossa of the astragalus is undivided in the juvenile specimen and it faces more laterally. It is separated from the tibial articular surface by a sharp crest which extends from the posteromedial corner of the ascending process to the posterior tongue of the astragalus (Fig. 44C, D). The tibial articular surface is larger than in To1-31 and occupies more than a half of the transverse length of the astragalus.

TABLE 7. — Geological age, geographical range and missing data in the 21 sauropod terminal taxa used in the cladistic analysis.

Taxon / Describer	Age	Occurrence	Missing data
Antetonitrus ingenipes (Yates & Kitching 2003)	Late Triassic (Norian)	Africa, South Africa	61%
Isanosaurus attavipachi (Buffetaut *et al.* 2000)	Late Triassic (Rhaetien)	Asia, Thailand	87%
Gongxianosaurus shibeiensis (He *et al.* 1998)	Early Jurassic (Pliensbachian-Toarcian)	Asia, China	72%
Vulcanodon karibaensis (Raath 1972)	Early Jurassic (Toarcian)	Africa, Zimbabwe	68%
Tazoudasaurus naimi (Allain *et al.* 2004)	Early Jurassic (Toarcian)	Africa, Morocco	30%
Shunosaurus lii (Dong *et al.* 1983)	Middle Jurassic (Bathonian-Callovian)	Asia, China	9%
Barapasaurus tagorei (Jain *et al.* 1975)	Early Jurassic	Asia, India	52%
Patagosaurus fariasi (Bonaparte 1986)	Middle Jurassic (Callovian)	South America, Argentina	46%
Omeisaurus (Young 1939)	Late Jurassic	Asia, China	11%
Mamenchisaurus (Young 1954)	Late Jurassic	Asia, China	15%
Diplodocus (Marsh 1878)	Late Jurassic (Kimmeridgian-Tithonian)	North America, USA	4%
Dicraeosaurus (Janensch 1914)	Late Jurassic (Kimmeridgian)	Africa, Tanzania	25%
Apatosaurus (Marsh 1877)	Late Jurassic (Kimmeridgian-Tithonian)	North America, USA	8%
Nigersaurus taqueti (Sereno *et al.* 1999)	Early Cretaceous (Aptian-Albian)	Africa, Niger	77%
Jobaria (Sereno *et al.* 1999)	Early Cretaceous	Africa, Niger	17%
Camarasaurus (Cope 1877)	Late Jurassic (Kimmeridgian-Tithonian)	North America, USA	1%
Brachiosaurus (Riggs 1903)	Late Jurassic (Kimmeridgian-Tithonian)	North America, USA Africa, Tanzania	5%
Euhelopus zdanskyi (Wiman 1929)	Early Cretaceous	Asia, China	41%
Rapetosaurus krausei (Curry Rogers & Forster 2001)	Late Cretaceous (Maastrichtian)	Africa, Madagascar	42%
Opishtocoelicaudia skarzynskii (Borsuk-Bialynicka 1977)	Late Cretaceous (Maastrichtian)	Asia, Mongolia	36%
Saltasaurus (Bonaparte & Powell 1980)	Late Cretaceous (Campanian-Maastrichtian)	South America, Argentina	45%

PHYLOGENETIC ANALYSIS

Tazoudasaurus is an important taxon for understanding of the early sauropod evolution and phylogeny, mainly because many of the synapomorphies diagnosing Eusauropoda in previous cladistic analyses are ambiguously distributed due to the lack of data in more primitive sauropods (Wilson 2005a, b). In the original publication, *Tazoudasaurus* has been considered as a basal sauropod closely related to *Vulcanodon*. Both taxa was united within a monophyletic Vulcanodontidae which is the sister group of Eusauropoda (Allain *et al.* 2004).

MATRIX AND CLADISTIC ANALYSIS

The phylogenetic position of *Tazoudasaurus* within Sauropoda is evaluated here by means of a cladistic analysis based to a large extent on the recent phylogenies of Wilson (2002; 2005a). Character polarity was determined by using outgroup comparisons. The basal saurischian *Herrerasaurus* Reig, 1963 (Novas 1993; Sereno 1993; Sereno & Novas 1993; Fraser *et al.* 2002; Langer & Benton 2006), and Prosauropoda, the scoring of which was mainly based on *Plateosaurus* (Huene 1926, 1932; Galton 1984, 1985, 1986, 1998; Galton & Upchurch 2004a) and *Massospondylus* Owen, 1854 (Cooper 1981; Gow *et al.* 1990) were included as successive outgroups in this analysis. The 21 ingroup taxa were chosen on the basis of completeness, previously inferred phylogenetetic position, and geological age. Thus, all higher-level sauropod taxa are represented in the matrix (Table 7). The analysis is mainly focused on basal sauropod taxa (i.e. non-neosauropods), and ten Late Triassic to Middle Jurassic terminal taxa have been included in the matrix (Table 7). The revision of the osteology and relationships of some potentially informative

Middle Jurassic sauropods, including *Atlasaurus*, "*Cetiosaurus*" *mogrebiensis* Lapparent, 1955, *Lapparentosaurus* Bonaparte, 1986 and *Bothryospondylus* Owen, 1875 is in progress, and pending their reappraisal, these taxa have not been included in this analysis. *Kotasaurus*, a basal sauropod from the Early Jurassic of India (Yadagiri 1988, 2001) has also been omitted because the material assigned to this taxon may belong to more than one species (Wilson pers. com.).

A total of 212 parsimony-informative osteological and dental characters have been coded in the 23 taxa included in the matrix (see Appendix 1). Most of these characters have been drawn from previous cladistic analysis of sauropods (Wilson & Sereno 1998; Upchurch 1998; Wilson 2002; Upchurch *et al.* 2004). Multistate characters were left unordered. The total missing data of the matrix is 32%. The percentage of missing data in each terminal taxa is given in Table 7. With 30% missing data, *Tazoudasaurus* is confirmed to be the most complete basal sauropod (i.e. outside Eusauropoda) known to date. The data matrix (Appendix 2) was processed with NONA (Goloboff 1999) and the interface Winclada (Nixon 1999-2002). Minimum-length trees were generated using the heuristic Multiple TBR + TBR search options with a maximum of 1001 trees to keep, and 1000 replicates.

Topology and character distribution

The analysis produced two most-parsimonious trees of 370 steps (CI = 64; RI = 78), the strict consensus (L = 371; CI = 64; RI = 78) of which is presented in Figure 45. The two equally parsimonious trees record the alternate hypotheses of relationships between *Barapasaurus* and *Patagosaurus* (Fig. 45). In the first hypothesis, *Patagosaurus* is the sister taxon of *Barapasaurus* based on the presence of infradiapophyseal pneumatopores communicating with the neural cavity on the middle and posterior dorsal neural arches, while in the second hypothesis *Patagosaurus* is the sister taxon of Omeisauridae + Neosauropoda, based on the number (4) of sacral vertebrae. All other nodes are invariant. The distribution of unambiguous synapomorphies, as well as that of the ambiguous synapomorphies under the fast and slow optimizations options of Winclada, supporting the topology of the strict consensus tree is given in Table 8.

Unsurprisingly, this analysis recovered a monophyletic Neosauropoda which includes Diplodocoidea and Macronaria, in agreement with recent analyses (Wilson 2002; Upchurch *et al.* 2004). Given the limited number of neosauropod taxa included in our analysis, the phylogeny of Neosauropoda which is beyond the scope of this paper will not be discussed further. Nevertheless, we note that *Jobaria* from the Early Cretaceous of Africa is resolved in the present analysis as a basal Macronaria following Upchurch *et al.* (2004), whereas it is interpreted by Sereno *et al.* (1999) and Wilson (2002) as the outgroup to Neosauropoda. Only, the distribution of characters in basal sauropods is described below (Table 8) and compared to that published by Wilson (2002) and Upchurch *et al.* (2004).

Sauropoda

Antetonitrus Yates & Kiching, 2003, the oldest sauropod included in the matrix, is resolved as the most basal sauropod. Sauropoda monophyly is supported by seven unambiguous synapomorphies. Four of these synapomorphies have been already identified as diagnostic of the clade in previous cladisitic analyses (Norman *et al.* 2004b; Wilson 2002): a columnar obligately quadrupedal posture; a ratio of forelimb length to hindlimb length greater than 0.6; a femoral shaft elliptical in cross section; and a proximal end of the metatarsals I and V subequal to those of metatarsals II and IV. The three other unambiguous synapomorphies have been previously identified as diagnostic of Eusauropoda, they are: a tibial distal posteroventral process reduced, so that the astragalar fossa is visible in posterior view; a metatarsal I minimum shaft width greater than those of metatarsals II-IV; and a pedal digit I ungual 25% larger than that of digit II.

Given the percentage of missing data in *Antetonitrus*, *Isanosaurus* Buffetaut *et al.*, 2000 and *Gongxianosaurus* He *et al.*, 1998, no less than 43 other characters, the distribution of which is ambiguous, could support the sauropod monophyly (Table 8: fast optimization).

TABLE 8. — Character distribution at each node of the most parsimonious tree resulting from the cladistic analysis. The unambiguous changes are listed in the first column. The ambiguous character optimization attributable to missing data, based on the two optimization options in WinClada (Nixon 1999-2002), are listed in the second and third columns. The homoplastic synapomorphies are in italic. Character states if different from 1 are indicated in brackets.

Nodes	Synapomorphies		
	Unambiguous	Fast optimization	Slow optimization
Sauropoda	59, 125, 147, 174, 183, 197, 198, 206	2, 3, 5, 8, 10, 11, 19, 23, 24, 25, 26, 32, 34, 35, 42, 43, 47, 51, 52, 54, 55, 57, 58, *67(3)*, *68(0)*, 75, 76, *80(2)*, 99, 123, 139, 148, 156, 158, 160, 162, 168, 170, 186, 187, 190, 192, 207	–
Node A	142, 173	60(2), 84, 85, 87, 107, 136, 140, 144, *154(1)*, 184, 185	8, 58, 139, 192
Node B	69 81, 176	95, 120, 193, 201, 208 *71(1)*, 89, 91	87 43, 47, 55, 57, 75, 85, 95, 107, 120, 136, 140, 144, 148, 156, 158, 160, 168, 170, 184, 185, 190, 193, 201, 207, 208
Vulcanodontidae	*173(0)*, 181, *182(1)*, *191(1)*, 210	*60(0)*, *61(1)*, *73(1)*, *124(1)*	187(1)
Eusauropoda	18, 28, 29, 49, 53, 155, 166, 180, 194,199, 202, 203, 204, 209, 211	172, *187(0)*, 205	3, 7, 10, 11, 24, 25, 26, 32, 34, 35, 42, 51, 54, 60(2), 99, 162
Node D	82, 96, *126(1)*	1, 12, 16, 17, 20, 30, 33, 36, 40, 48, *67(4)*, *71(0)*, 80(3), 88, 98, 116, 149, 150, *154(0)*, 157, 200	*68(0)*, *84(1)*, *89(1)*, 205,
Node E	64, 95(2), 130	86	1, 116, *172(1)*
Node F	179, *195(1)*	70, *76(0)*, *91(0)*, 114,159, 196	17, 19, 20, *23(1)*, 30, 48, 52, 67(4), 70, 80(3), 86, *88(1)*, 98,157,200
Node G	*60(1)*, *74(1)*, *75(0)*	*71(1)*, *123(0)*	*71(1)*
Neosauropoda	4, 45, 66,104, 105, 161, 188, 189, *191(1)*	22, 106, *186(0)*, *187(1)*	12, 16, 33, 40, *123(1)*, *149(1)*, *150(1)*, 159, *187(1)*
Diplodocoidea	*1(0)*, 38, 41, 53(2), 54(2), *57(0)*, *58(2)*, 62, 117	*2(0)*, *6(1)*, 13, *21(1)*, *27(1)*, 32(2), *36(0)*, *56(1)*, 65, *79(1)*, 83, 97, 100(1), 102, 108, 115, 165	–
Node I	9, 90, 128, 171	46, 50, *67(3)*, *196(0)*	*2(1)*
Macronaria	*61(1)*, 93, *121(1)*, 151, *152(1)*, 167	119	*36(1)*, 46, 50
Titanosauriformes	39, *63(1)*, *74(1)*, 112, 118, 153, 154(1), 164, 175	52(2), *57(0)*, *120(0)*, *157(0)*	–

*Node A (*Gongxianosaurus + *[*Isanosaurus + *Gravisauria])*

This node is only supported by two unambiguous synapomorphies: a reduced or absent ulnar olecranon process previously considered to be diagnostic of Sauropoda; and the absence of a lesser trochanter on the femur which previously characterized Eusauropoda. Five additional characters with an ambiguous distribution can diagnose at least this clade (Table 8: slow optimization): the external nares retracted to the level of the orbit; the D-shaped tooth crowns; the wrinkled tooth crown enamel; the flat distal humeral condyle; and the astragalar posterior fossa divided by a vertical crest.

*Node B (*Isanosaurus + *Gravisauria)*

Although it is older than *Gongxianosaurus*, *Isanosaurus* from the Upper Triassic of Thailand (Buffetaut *et*

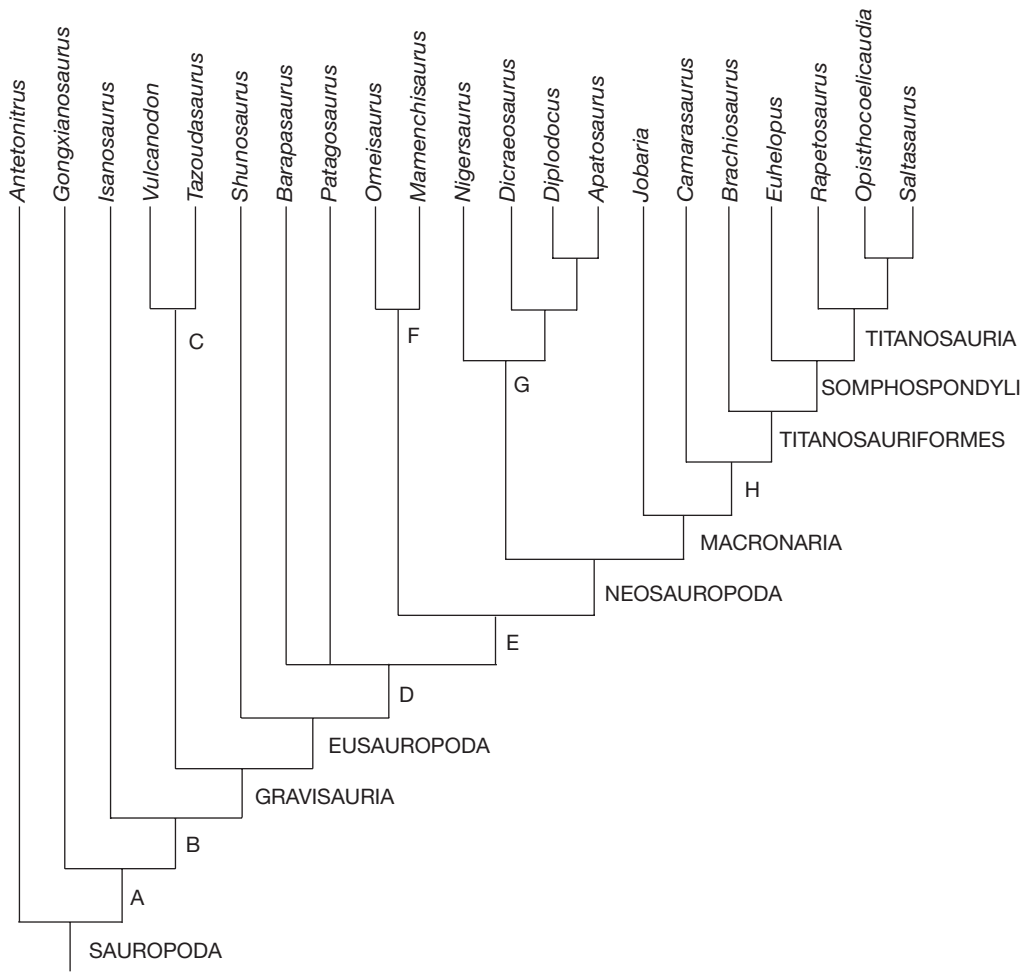

FIG. 45. — Phylogenetic relationships of *Tazoudasaurus naimi* within Sauropoda. Strict consensus tree of two most parsimonious trees. Node abbreviations: **A**, **B**, **D**, **E**, **H**, unnamed clades; **C**, Vulcanodontidae; **F**, Omeisauridae; **G**, Diplodocidea.

al. 2000) is resolved as more derived than the latter taxa. The clade B is supported by a single unambiguous synapomorphy previously recognized as characteristic of Eusauropoda: the presence of opisthocoelous cervical centra. An additional character can diagnose this clade under the slow optimization option of Winclada: the presence of spinodiapophyseal laminae on middle and posterior dorsal neural arches.

Gravisauria new taxon

The name Gravisauria is coined here to name the clade which encompasses the Vulcanodontidae and the Eusauropoda and which is common to all recent phylogenies (Salgado *et al.* 1997; Upchurch 1998; Wilson & Sereno 1998; Wilson 2002; Yates & Kitching 2003; Upchurch *et al.* 2004; Yates 2006). Gravisauria is a node-based taxon defined as the most recent common ancestor of *Tazoudasaurus* and *Saltasaurus* Bonaparte & Powell, 1980 and all its descendants. This definition encompasses the older definition of Sauropoda (McIntosh 1990). Gravisauria is diagnosed by two unambiguous and non-homoplastic synapomorphies: the dorsal neural spines which are broader transversely than

anteroposteriorly, and the asymmetry of the femoral distal condyles, with a broader tibial condyle. These two synapomorphies were previously recognized as diagnostic of Eusauropoda (Wilson, 2002). No less than 25 additional synapomorphies could diagnose the Gravisauria, but also a less inclusive clade (Table 8: slow optimization). Thirteen of them have been previously thought to be diagnostic of Sauropoda: the presence of four or more sacral vertebrae; the depth of the anterior caudal transverse processes, extending from centrum to neural arch; the reduced deltopectoral crest of the humerus; the triradiate proximal end of the ulna; the subrectangular radial distal condyle; the low and rounded ischial peduncle of the ilium; the ischial blade equal to or longer than the pubic blade; the blade-like ischial distal shaft; the absence of foramina at the base of the ascending process of the astragalus; the absent or unossified distal tarsals 3 and 4; the length of the metatarsal V being at least 70% that of the metatarsal IV; the pedal digit I ungual longer than the metatarsal I; and the sickle-shaped pedal ungual I (see Table 8 for the alternate position of these characters under fast optimization option). Nine of the remaining ambiguously distributed synapomorphies previously characterized the Eusauropoda: the deepening of the anterior end of the dentary; the crown-to-crown occlusion of the teeth; the overlapping tooth crowns; the mid-cervical neural arches which are taller than the height of the posterior centrum face; the forked chevrons; the block shaped carpals; the reduced number of phalanges of the manual digit III; the manual non-ungual phalanges broader transversely than long proximodistally; and the presence of a lateral trochanter on the fibula. Finally, the last three ambiguous synapomorphies previously diagnosed either the (*Barapasaurus* + more advanced sauropods) clade (prezygoparapophyseal laminae on the middle and posterior dorsal neural arches, and triangular proximal tibial scar on the medial surface of the fibula), or the neosauropods (presence of a surangular ridge separating adductor and articular fossae). Even if 39% of the total cranial characters have been scored in *Tazoudasaurus*, it is interesting to note that most of the characters diagnosing Gravisauria and described above are related to the postcranial skeleton (see Discussion).

Vulcanodontidae

Among the Late Triassic to Middle Jurassic taxa, only two taxa *Vulcanodon* and *Tazoudasaurus* are brought together, the remaining taxa being resolved as successive sister-taxa to (Omeisauridae + Neosauropoda) clade. Although Wilson (2005a) and Yates (2006) failed to recover this clade, the monophyly of the stem based Vulcanodontidae (Allain *et al.* 2004) is confirmed here and supported by five unambiguous derived characters (Table 8). Two of these synapomorphies are non-homoplastic: the strongly transversely flattened tibial shaft and the marked dorsoventral flattening of the unguals of pedal digits II and III. The three other synapomorphies are homoplastic, they are: the presence of a lesser trochanter on the femur (reversal), the great breadth of the distal end of the tibia (convergently acquired by Titanosauria) and the posterior extension of the ascending process of the astragalus (convergently acquired by Neosauropoda).

Eusauropoda

In spite of the inclusion of the well-known basal sauropod *Tazoudasaurus* in our analysis, Eusauropoda is still diagnosed by numerous derived characters. Thus, 16 unambiguous synapomorphies diagnose this clade: the anteroposterior length of the frontal which is less than its minimum transverse breadth; a long anterior process of the quadratojugal; the presence of a quadrate fossa; a dorsoventrally expanded prearticular; the U-shaped anterior portion of the tooth rows; the reduced number of phalanges of the manual digit II; the S-shaped pubic symphysis; the reduced femoral fourth trochanter, the laterally projected tibial cnemial crest; the spreading posture of the metatarsus; the length of the metatarsal III which is less than 25% that of the tibia; the broader transversely than long proximodistally proximal pedal phalanges; the shallow or absent collateral ligament fossae on the non-ungual pedal phalanges; the rudimentary penultimate phalanges of the pedal digits II-IV; the sickle-shaped unguals of the pedal digits II-III; and the rudimentary pedal digit IV ungual.

DISCUSSION

Taphonomy and inferred behaviour of *Tazoudasaurus*

Although fieldwork in Toundoute area is far from complete, a detailed stratigraphic sedimentological and paleoenvironmental study has already been conducted to assess the depositional setting of the site (Montenat *et al.* 2005). It indicates that both the upper (To1; To1' and Pt) and lower (To2) bone-beds are related to typical mud-flows which favoured their rapid burying and fossilization, and have protected the bones from erosion (Montenat *et al.* 2005). Such mud-flows are exceptional events compared with the channels and flood plain deposits recorded by the other continental sediments of the Toundoute series. Some taphonomic features of the Toundoute upper bone-bed are examined here.

The upper bone-bed has a thickness of 3 to 4 m and dip 45° to the northwest. Because it is usually overlain with a 4 m thick sandstone stratum, only the outcropping part of the bone-bed and its adjacent area have been exploited (Fig. 3). Nevertheless, the exploited outcrop is approximately 250 m long and nearly fossiliferous all along its length. It has yielded more than 600 bones. The latter have been concentrated probably by gravity at the base of the bone-bed, but they have no preferred orientation, and can be vertically arranged. Such a variable orientation has not been caused by animal agents or diagenetic forces, but reflects the original orientation of the bones during their deposition. A lot of these specimens including skull elements, dorsal vertebrae, caudal vertebrae series, pelvic elements and a partial hindlimb have been found articulated or associated. The vast majority of juvenile and adult remains are neither broken nor weathered and have been jumbled up together. This suggests that these skeletal elements were not transported far from the site of death as individual bones or carcasses. Some bones were affected by post-burial tectonism and are crossed by fault planes in which gypsum recrystallized, but these specimens are not deformed.

There is no sign of microvertebrates or microfossils, except woody debris, in the Toundoute upper bone-bed, and for the moment, the remains of only two dinosaur taxa have been collected. Most of them can be referred to *Tazoudasurus*. The other dinosaur remains are those of a basal abelisauroid theropod which is represented by two individuals, based on the number of right femora (Allain *et al.* 2007). Only six other bones of the skeleton of this abelisauroid have been found so far, associated with one of the two femora (Fig. 3: locality Pt). The exact number of *Tazoudasaurus* individuals is more difficult to assess. Based on the number and the size of the recovered sauropod femora, at least three adult individuals are present in the upper bone bed, and more probably four given the size and the location of the huge humerus Pt1. Although they are less represented than the adult remains, juvenile bones belong to at least two different individuals, based on the length of the humerus To1-93 (185 mm) and that of the ulna To1-374 (220 mm). Thus, at least six *Tazoudasaurus* individuals ranging from small to large size are present in the Toundoute upper bone-bed.

Given the above observations, we assume here that the low-diversity multitaxic assemblage of the Toundoute upper bone-bed has been formed in a nearly instantaneous period of time. The mud-flow in which the dinosaur remains are preserved is thought to be the cause of death of these animals. This also suggests that *Tazoudasaurus* had a gregarious behaviour, and that the herd was made up by very young to adult individuals. It is also likely that *Tazoudasaurus* may have been one of the preys of the abelisauroid found in the same unit, but this needs to be confirmed by future works.

Vertebral lamination

A considerable attention has been given to the vertebral lamination of sauropods since the work of Bonaparte (1999), and the rational nomenclature of these laminae presented by Wilson (1999). The above description of the lamination in various presacral vertebrae of *Tazoudasaurus* clarifies the distribution of vertebral laminae in basal sauropods, and underscores some aspects of vertebral lamination evolution.

The presence/absence and shape of vertebral laminae are now often used to diagnose sauropod species (Upchurch & Martin 2003; Martinez *et al.* 2004;

Salgado *et al.* 2004; Bonaparte *et al.* 2006). This practice should be regarded with caution because it does not take into account neither the ontogenetic variation nor the variation depending on the position of the vertebra in the vertebral series. For example, the development of the spinodiapophyseal laminae is highly variable in dorsal vertebrae of *Tazoudasaurus* (Table 2). It is reduced and only present at the base of the neural spine in the most anterior adult dorsal vertebra, while it is absent in the anterior juvenile dorsal vertebra, prominent on the lateral side of the neural spine of the mid-dorsal vertebrae, and merges with the spol in the posterior dorsal vertebrae.

The identification of the cpol and its homology within sauropod taxa where it has been described is another problem which should be assessed. The cpol joins the postzygapophysis to the posterior-most portion of the neurocentral junction and is thought to be present in all saurischian dinosaurs (Wilson 1999). However, we were not capable to identify it with certainty in any presacral vertebrae of *Tazoudasaurus*, and it seems this lamina is often confused with the tpol, when the vertebrae are seen in lateral view. Numerous Sauropodomorpha such as *Tazoudasaurus* (Figs 9I, J; 11C, D; 13C, D), *Lessemsaurus* (Bonaparte 1999: fig. 40a) or *Patagosaurus* (Bonaparte 1999: fig. 40b) or *Barapasaurus* (Jain *et al.* 1979: plate 101c) exhibit a single pair of laminae in the posterior region of the neural arch when the latter is seen posteriorly. These laminae clearly originate on the medial aspect of the postzygapophyses and project medially and ventrally and thus are homologous to the tpol as defined by Wilson (1999). In that case, we noticed that the tpol could extend posteroventrally as far as the neurocentral junction. When a second pair of laminae, the cpol's, is present, it is always located laterally to the tpol (Bonaparte 1999: fig. 40c, d; Wilson 1999: figs 2c, d; 3a). The fact that the tpol could merge with the cpol to form the lateral wall of the neural canal in posterior view may make sometimes difficult the identification of these laminae (Wilson 1999: fig. 3b, posterior view). If we have correctly assessed the problem of the homology of these two paired vertebral laminae, the absence of cpol could have a phylogenetic value within Sauropodomorpha, because the centropostzygapophyseal laminae are clearly present in the basal saurischian *Herrerasaurus* (Novas 1993).

Several laminae such as the acpl, prpl and spdl previously regarded as diagnostic of *Barapasaurus* and more advanced dinosaurs (Wilson 1999), have a broader distribution and characterize at least the Gravisauria.

Forefoot posture in basal sauropods

Complete articulated manus are not preserved in any known basal sauropod, even if the five metacarpals and phalanges have been reported in *Omeisaurus* (He *et al.* 1988) and *Shunosaurus* (Zhang 1988). This has led to different interpretations of the evolution of the configuration and posture of the manus in sauropods which can be tested thanks to the discovery of the complete articulated manus of *Tazoudasaurus*.

According to Wilson & Sereno (1998), *Omeisaurus* and *Shunosaurus* have a plantigrade manus with a spreading metacarpus, and with the proximal ends of the metacarpals forming a 90° arc. Thus, a semi-tubular U-shaped manus with a metacarpus arranged into a tightly bound digitigrade structure was considered to be diagnostic of the Neosauropoda (Wilson & Sereno 1998). It has to be said that in that case the inferred digitigrade posture of the manus depends on "the long intermetacarpal articular surfaces that abut one another in the metacarpus" (Wilson & Sereno 1998; Wilson 2005b). In a subsequent paper, Wilson (2005a), basing on the possible sauropod trackways from the Portozuelo Formation (Carnian) of Argentina, suggests that the semi-tubular and digitigrade manus evolved as early as the Late Triassic, even if these features are recorded later in the body fossils. In that case, *Atlasaurus* from the Bathonian of Morocco will be the oldest known sauropod to present a semi-tubular manus, even if Upchurch (1998) and Bonnan (2003) consider the possibility that the manus of *Omeisaurus* and *Shunosaurus* may be semi-tubular. On the other hand, the semi-tubular configuration and digitigrade manus posture are regarded by Upchurch (1998) as a synapomorphy of Eusauropoda linking

Omeisaurus and *Shunosaurus* to other advanced sauropods. Finally, Bonnan (2003) goes much further and considers that numerous forefoot characters form an integrated functional suite, and predicts that a semi-tubular manus was present in the most basal sauropods, in contradiction with the Upper Triassic and Early Jurassic ichnofossil record (see Wilson 2005b). In his study, Bonnan (2003) criticized Wilson & Sereno (1998) for their reconstruction of the proximal shape of the manus of *Omeisaurus*, and re-arranged the proximal ends of the metacarpals of *Omeisaurus* in a more semi-tubular configuration, "in accordance with basic orientations and articulations displayed in other known neosauropod manus" (Bonnan 2003: fig. 11). This interpretation is very doubtful for at least two reasons. The first one is that *Omeisaurus* is not a neosauropod, and thus, there is no proof that its manus shape should have more a neosauropod than a prosauropod configuration. The second is that Bonnan does not take into account the resultant orientation of the shaft and distal ends of the metacarpals when he re-arranged their proximal ends. In all Sauropodomorpha, the outer (anterior) surfaces of the metacarpals form a continuous and regular surface when they are brought together in articulation (e.g., Cooper 1981: fig. 37; Ouyang & Ye 2002: fig. 37; Bonnan 2003: fig. 2). This outer surface is never overlapped distally by adjacent metacarpal. Given the morphology of the shafts and distal ends of the metacarpals of *Omeisaurus* in anterior view (He *et al* 1988: Fig. 47B), if the *Omeisaurus* manus is reconstructed according to Bonnan interpretation, then more than half of the outer surface of metacarpal IV is overlapped by the internal surface of the metacarpal III, rendering difficult or even impossible the articulation of manual digit IV. Such a condition is unknown in Sauropodomorpha and a spreading configuration of the manus of *Omeisaurus* is assumed here (Wilson & Sereno 1998).

Whatever the *Omeisaurus* manus shape is, the one of *Tazoudasaurus* has clearly a spreading configuration more similar to prosauropod (Cooper 1981) than to neosauropod condition. This definitely contradicts the semi-tubular metacarpus predicted by Bonnan (2003) and the assertion that a digitigrade manus and a tubular metacarpus are correlated or phylogenetically linked (Upchurch 1998; Bonnan 2003). The hypothesis that the obligatory quadrupedal posture with columnar limbs, the triradiate proximal ulna, the subrectangular distal condyle, the subtriangular proximal end of the metacarpals, and the semi-tubular configuration form an integrated functional suite is less likely given these results.

The description of the complete manus of *Tazoudasaurus* underscores the mosaic evolution of the sauropod manus, and the estimated temporal origin for several sauropod manual synapomorphies based on body fossils proposed by Wilson (2005a) can be re-evaluated. A digitigrade manus appear to be present in all sauropods, the manus of which is known (Wilson 2005a); however it is probably better to describe the manus posture in *Tazoudasaurus* and *Omeisaurus* as being sub-unguligrade (Carrano 1997). With a manual phalangeal formula of 2-2-2-2-2, *Shunosaurus* can vouch for manual phalangeal reduction in Eusauropoda, but the number of manual phalanges is already reduced in the basal Gravisauria *Tazoudasaurus* which retains only three phalanges on the digit II and two on the digit III, it means less than in prosauropods. A semi-tubular configuration is probably phylogenetically linked with the presence of long intermetacarpal articular surfaces on the proximal shaft of metacarpals. In our phylogenetic analysis, the semi-tubular configuration of the manus is resolved as a synapomorphy of Neosauropoda convergently acquired in *Mamenchisaurus* (Ouyang & Ye 2002). The latter taxon received little attention in the various interpretations of manus shape in sauropods, but clearly exhibits a semi-tubular manus with long intermetacarpal articular surfaces. This casts doubt on the monophyly of Omeisauridae, which is only supported by four homoplastic synapomorphies in our phylogenetical analysis.

Early Jurassic sauropod trackways from Morocco are well documented (Monbaron *et al.* 1985; Ishigaki 1988), and preserved both manual and pedal imprints. The imprints and trackways described and figured by Ishigaki (1988: figs 11-13; 23; 24) document sauropod trackmakers with a digitigrade manus, leaving only slightly arched manus prints.

Such tracks seem to be consistent with the digitigrade manus and spreading configuration of the metacarpus seen in *Tazoudasaurus*, but their re-examination is needed to confirm this hypothesis.

Early sauropod evolution and radiation of the Gravisauria

As anticipated in previous phylogenetic works (Upchurch 1998; Wilson 2002), the inclusion of the relatively complete *Tazoudasaurus*, and in a lesser extant of *Antetonitrus*, *Isanosaurus*, and *Gongxianosaurus* in a sauropod cladistic analysis partially bridges the morphological gap that have hitherto separated basal sauropods from Eusauropoda. The gap between basal sauropods and Gravisauria remains nevertheless important due to the lack of complete sauropod skeletons from the Late Triassic and basal Jurassic as shown by the number of ambiguously distributed characters at the base of the strict consensus tree produced by our analysis (Table 8). More surprisingly, Eusauropoda is a still well-supported node in our analysis despite the inclusion of *Tazoudasaurus*. This underscores the major morphological changes that occur among Gravisauria between the Vulcanodontidae and the Eusauropoda. These changes are related to the cranial anatomy (see above characters 18, 28, 29, 49, 53) which seems to remain very primitive in *Tazoudasaurus* , and to locomotion (characters 55, 172, 180), more especially in the modification of the pes anatomy (characters 194, 199, 202, 203, 204, 209, 211). This result seems congruent with the major radiation of eusauropods (including that of neosauropods) which occurs during the end of the Early Jurassic and Middle Jurassic interval, as proposed by different authors (Wilson & Sereno 1998; Allain *et al.* 2004; Upchurch & Barrett 2005).

It is now widely recognized that sauropod history began during the Late Triassic (Buffetaut *et al.* 2000; Yates & Kitching 2003; Norman *et al.* 2004b; Wilson 2005a; Yates 2006), but the title of oldest sauropod remains controversial. *Antetonitrus* from the Norian of South Africa (Yates & Kitching 2003) and *Isanosaurus* from Rhaetian of Thailand (Buffetaut *et al.* 2000) are assumed here to be Triassic sauropods, pending a more detailed study and additional material of the numerous prosauropods referred by Yates (2006) to Sauropoda. Early Jurassic sauropods are represented by several imperfectly described taxa such as *Gongxianosaurus* (He *et al.* 1998), *Ohmdenosaurus* (Wild 1978), and *Barapasaurus* (Jain *et al.* 1975, 1979), the complete and detailed descriptions of which are crucial and needed to a better knowledge of early sauropod phylogeny and evolution; as well as better known taxa such as *Vulcanodon* (Raath 1972; Cooper 1984) and *Tazoudasaurus* (Allain *et al.* 2004; this study). The age of two of these sauropod taxa, *Barapasaurus* and *Gongxianosaurus*, is not well constrained. *Barapasaurus* comes from the Early Jurassic Kota Formation (Jain *et al.* 1975, 1979; Yadagiri 2001), but its exact stratigraphic position can not be determined although its phylogenetic position may suggest an upper Early Jurassic age. *Gongxianosaurus* comes from the Early Jurassic Dongyuemiao Member of the Ziliujing Formation, which postdates the probably basal Jurassic Lufeng fauna but predates the Middle Jurassic *Shunosaurus* fauna (He *et al.* 1998). *Ohmdenosaurus*, *Vulcanodon* and *Tazoudasaurus* are dated as Toarcian, although a Pliensbachian age can not be definitely excluded for the latter taxon. *Vulcanodon* has long been claimed to be Hettangian and this age is still recognized by some authors (Norman *et al.* 2004b; Barrett & Upchurch 2005; Upchurch & Barrett 2005). As previously stated (Allain *et al.* 2004; Yates *et al.* 2004), recent dates support a Toarcian age for the Karoo basalts (Duncan *et al.* 1997; Jones *et al.* 2001), and thus for *Vulcanodon*.

Although sauropods are known since the Late Triassic, they were not the dominant herbivorous vertebrates until the end of the Early Jurassic. This part was played by the prosauropods from the Carnian to the Pliensbachian-Toarcian (Sereno 1999; Galton & Upchurch 2004a; Barrett & Upchurch 2005). During this time interval, sauropods were rare, which can explain why their basal anatomy is still poorly understood. The prosauropods *Ammosaurus* Marsh, 1891 and *Anchisaurus* Marsh, 1885 from the Portland Formation in the United States, and *Yimenosaurus* Bai, Yang & Wang, 1990 from Fenggjiahe Formation in China are thought to be among the last representatives of their group (Galton & Upchurch 2004a). Thus, basal sauropods

evolved alongside prosauropods until the final extinction of the latter at the Pliensbachian-Toarcian boundary (Barrett & Upchurch 2005). Because prosauropods constituted only 60% and sauropod 40% of sauropodomorph taxa at that time, it has been suggested by Barrett & Upchurch (2005) that competitive replacement played an important role to explain the early stages of the sauropod radiation. We agree that interactions and competition between prosauropods and basal sauropods is very likely during the Norian-Pliensbachian time interval, but this can not explain the sudden worldwide extinction of prosauropods and the consecutive radiation of Gravisauria (Fig. 46).

Among dinosaurs, such a pattern of extinction/radiation around the Pliensbachian-Toarcian boundary is not only known in Sauropodomorpha. Within carnivorous dinosaurs, coelophysoids are widely recognized as the dominant carnivorous taxa during the Late Triassic and the lower Early Jurassic (Tykoski & Rowe 2004). At the end of this period, coelophysoids are represented by numerous taxa, the remains of which last appear around Pliensbachian-Toarcian boundary (Carrano & Sampson 2004; Tykoski & Rowe 2004; Tykoski 2005). Conversely, the first representatives of other major theropod clades which yet probably originate during the Late Triassic are neither recorded nor abundant until the end of the Early Jurassic and the beginning of the Middle Jurassic (Fig. 46). Thus, the definitely phylogenetically-identified oldest Neoceratosauria is the new abelisauroid *Berberosaurus* from Toundoute in Morocco (Allain *et al.* 2007), whereas Tetanurae remains first appear around the Aalenian-Bathonian with numerous spinosauroid taxa such as *Magnosaurus* Huene, 1932, *Poekilopleuron* Eudes-Deslongchamps, 1838, *Dubreuillosaurus* Allain, 2002 and the primitive coelurosaur *Proceratosaurus* Huene, 1926 (Allain 2002; Holtz *et al.* 2004).

Among ornithischians dinosaurs, such a pattern is more difficult to access due to the lack of data for the Late Triassic and Early Jurassic. Indeed only 11 ornisthichian genera are known during the interval from the Norian to Early Toarcian. These taxa include the three basal ornithischians *Technosaurus* Chatterjee, 1984, *Pisanosaurus* Casamiquela, 1967 and *Lesothosaurus* Galton, 1978 (Norman *et al.* 2004b), the five basal thyreophorans *Scutellosaurus* Colbert, 1981, *Emausaurus* Haubold, 1991, *Scelidosaurus* Owen, 1860, *Tatisaurus* Simmons, 1965 and *Bienosaurus* Dong, 2001 (Norman *et al.* 2004c), and the three Heterodontosauridae *Abrictosaurus* Hopson, 1975, *Heterodontosaurus* Crompton & Charig, 1962 and *Lycorhinus* Haugthon, 1924 (Norman *et al.* 2004a). Nevertheless, we note that none of these taxa is known after the early Toarcian, and that the major ornithischian clades Eurypoda and Euornithopoda are first recorded during the Middle Jurassic (Galton & Upchurch 2004b; Norman *et al.* 2004a) and seems to diversify at that time (Fig. 46). If this pattern is not really convincing given the available data, it is at least congruent with that described in saurischian dinosaurs.

Although further works on this topic are required to confirm our hypothesis, we believe that the qualitative phylogenetic pattern presented above are enough to postulate that the major dinosaur clades (i.e Gravisauria, Neoceratosauria, Tetanurae, Eurypoda, Euornithopoda) radiated after an extinction event at the Pliensbachian-Toarcian boundary, even if these clades were already present as soon as the Late Triassic (Fig. 46). Although a second-order extinction event close to the Pliensbachian-Toarcian boundary is attested in the marine communities (see below), paleontologists failed to recognize this extinction among continental tetrapods. To our knowledge, the only attempt to test quantitatively an Early Jurassic tetrapod extinction was made by Benton (1994). The graphs of diversity change obtained in this work record a high extinction rate in the Pliensbachian followed by a high origination rate in the Bathonian (Benton 1994: fig. 22.6). Nevertheless, these origination and extinction rates were interpreted as the result of gaps in the fossil record during the Toarcian-Bajocian interval suggesting poor sampling of a diverse fauna rather than a good sampling of a depauperate fauna, and not discussed further (Benton 1994). These quantitative results should be reappraised in future works in the light of recent discoveries and cladistic revisions, but if the poor sampling during the Toarcian-Bajocian interval is real, it does not necessarily imply that it does not mirror the diversity decline after the Pliensbachian-Toarcian boundary.

Our hypothesis is substantially supported by the global environmental changes, the turnovers in marine communities and the geological data recorded at the Pliensbachian-Toarcian boundary, which are examined here. The second-order Pliensbachian-Toarcian extinction event was first recognized based on data from northwestern Europe (Hallam 1961, 1986). It is now widely accepted that this mass-extinction event was global (Raup & Sepkoski 1984, 1986; Little & Benton 1995), and besides its European record, it has been documented for example in Morocco (Ettaki *et al.* 2000), in North Siberia and in the Arctic (Zakharov *et al.* 2006), in Andean Basin (Aberhan & Fürsich 2000), in Caucasus (Ruban 2004) or in Japan (Hori 1993). A lot of marine invertebrates have been affected by this mass extinction, including bivalves, brachiopods, ammonoids, crinoids, belemnites, ostracodes, and dinoflagelates (Little & Benton 1995; Hallam & Wignall 1997), and substantial changes in composition of palynological assemblages have been simultaneously established.

The cause of the Pliensbachian-Toarcian mass extinction has long been explained by the spread of anoxic bottom waters in connection with the Early Toarcian transgression (Oceanic Anoxic Event, OAE), as recorded by the deposition of the organic-rich black shales in northwestern Europe (Jenkyns 1988). Nevertheless, the role of anoxia as the sole cause of the Pliensbachian-Toarcian extinction has been challenged by various authors (Aberhan & Fürsich 1997; Morard *et al.* 2003). Recent investigations have highlighted the link between the Pliensbachian-Toarcian mass extinction, the Early Toarcian OAE and the occurrence of flood basalt volcanism in the Karoo (South Africa) and Ferrar (Antarctica) provinces (Palfy & Smith 2000; Wignall 2001; Palfy *et al.* 2002; Courtillot & Renne 2003; Morard *et al.* 2003). The synchronous (183 ± 2 Ma) Karoo and Ferrar traps together contain in excess of 2.5 Mkm^3 of lava (Encarnacion *et al.* 1996; Palfy & Smith 2000), more than the Deccan traps (2 Mkm^3) which are believed to have played an important role in the extinction of non avian dinosaurs at the end of the Cretaceous (Archibald & Fastovsky 2004).

Morard *et al.* (2003) proposed a scenario to explain what may have happened around the Pliensbachian-Toarcian boundary, based on geochemical (strontium, carbon and oxygen isotopic ratios) and biostratigraphic data. This scenario can be subdivided into three main stages. The first stage, at the end of the Pliensbachian, involves a global cooling linked to the thermal insulation caused by the large scale volcanic activity in the Karoo and Ferrar flood basal Province, which led to a major regression recorded in Late Pliensbachian European sediment. During the second stage, the vegetation colonizes the newly emerged surfaces, previously occupied by the epicontinental seas. During the subsequent Early Toarcian transgression, which is linked to a global climatic warming, the organo-humic matter which was accumulated on the colonized area, is leached and drowned by the sea and is the trigger for the paroxysmal anoxic event (Morard *et al.* 2003).

Be that as it may concerning this scenario, the numerous strong biotic, geological and geochemical evidences presented above and in the scientific literature prove the reality of a global mass extinction around the Pliensbachian-Toarcian boundary, involving both an oceanic anoxic event and flood basalt volcanism. Even if an extinction/radiation event among dinosaurs is for the moment difficult to assess using quantitative data, it is unlikely that dinosaurs were not affected by the global environmental changes recorded at the Pliensbachian-Toarcian boundary. Thus, we cannot escape the conclusion that the phylogenetic pattern presented here (Figs 45, 46) and involving the extinction of Late Triassic to Early Jurassic dominant dinosaurs such as Coelophysoidea and Prosauropoda, and the subsequent radiation of numerous dinosaur lineages such as the Gravisauria or the Tetanurae, is probably linked to Pliensbachian-Toarcian mass extinction event, although further works are needed on this topic.

Acknowledgements
This work was supported by the Committee for Research and Exploration of the National Geographic Society (Grants 7798-05 and 8186-07) and the Ministry of Energy and Mines of Morocco, the Agence universitaire de la Francophonie and the Fondation des Treilles. R. A. is indebted to N. E. Jalil and to the people of the University and of the Natural History Museum of Marrakech for their

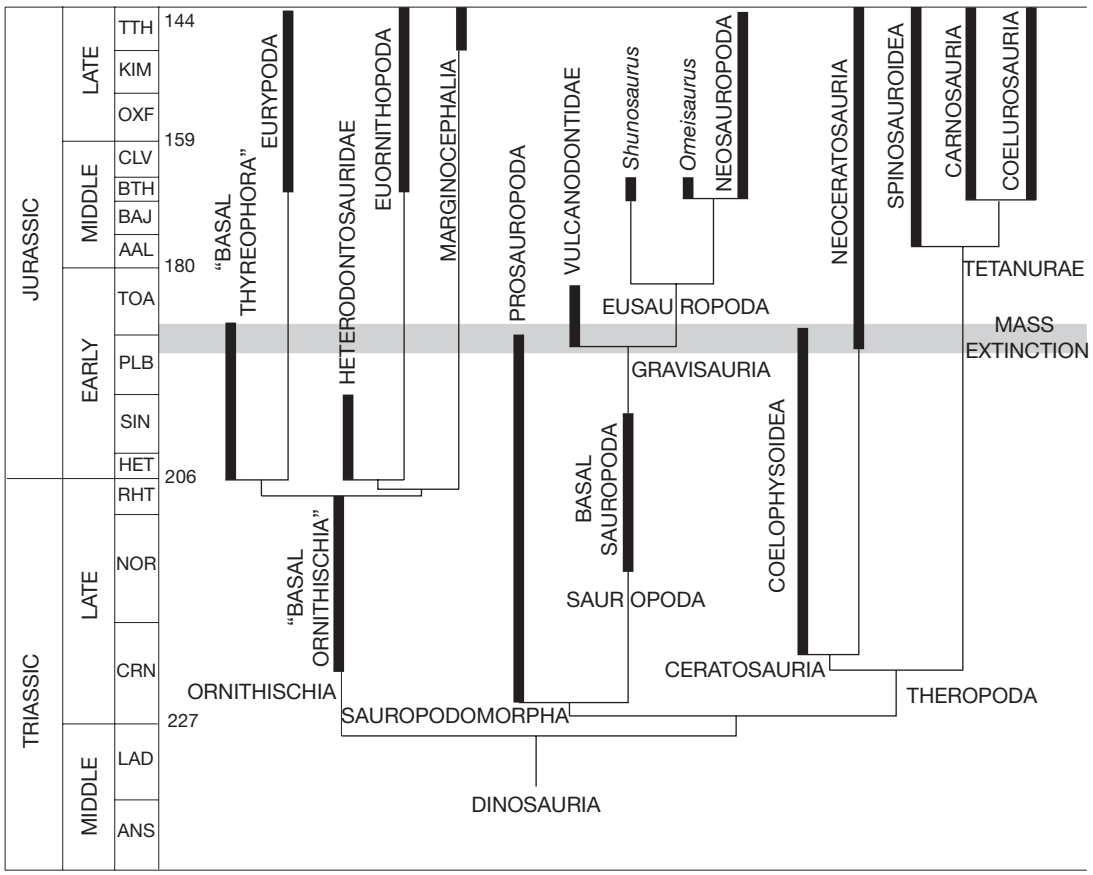

FIG. 46. — Dinosaur phylogeny superimposed on geologic time scale (Gradstein *et al.* 1999). First and last appearance datum of the major clades of dinosaur have been retrieved in the second edition of *The Dinosauria* (Weishampel *et al.* 2004) and is based on the taxa, the phylogenetical position of which has been tested by the mean of cladistic analysis and is not contested.

help and support. We thank our reviewers, A. Ohler (Muséum national d'Histoire naturelle, Paris) and K. Curry Rogers (Science Museum of Minnesota) as well as J. Wilson (Museum of Paleontology, Michigan) for their comments and suggestions which have improved this article. We thank P. Richir, R. Vacant, M. M'Ghari, M. Rochdy and A. Faskaoune for helping to the preparation of the material, P. Loubry for photographs, and all the participants in the DinoAtlas Project: P. Taquet, M. Monbaron, D. Russell, P. Richir, N. E. Jalil, M. Rouchdy, C. Montenat, M. M'Ghari, A. Faskaoune, M. Fontaine, S. Hervet, S. Ladeveze, A. Aumont, C. Sagne, and the students from Marrakech University.

REFERENCES

ABERHAN M. & FÜRSICH F. T. 1997. — Diversity analysis of Lower Jurassic bivalves of the Andean basin and the Pliensbachian-Toarcian mass extinction. *Lethaia* 29: 181-195.

ABERHAN M. & FÜRSICH F. T. 2000. — Mass origination versus mass extinction: the biological contribution to the Pliensbachian-Toarcian extinction event. *Journal of the Geological Society*, London 157: 55-60.

ALLAIN R. 2002. — *Les Megalosauridae (Dinosauria, Theropoda). Nouvelle découverte et révision systématique : implications phylogénétiques et paléobiogéographiques*. Ph. D Thesis, Muséum national d'Histoire naturelle, Paris, France, 311 p.

ALLAIN R., AQUESBI N., DEJAX J., MEYER C., MONBARON M., MONTENAT C., RICHIR P., ROCHDY M., RUSSELL D. A. & TAQUET P. 2004. — A basal sauropod dinosaur from the Early Jurassic of Morocco. *Comptes Rendus Palevol* 3: 199-208.

ALLAIN R., TYKOSKI R. S., AQUESBI N., JALIL N.-E., MONBARON M., RUSSELL D. A. & TAQUET P. 2007. — An abelisauroid (Dinosauria: Theropoda) from the Early Jurassic of High Atlas Mountains, Morocco, and the radiation of ceratosaurs. *Journal of Vertebrate Paleontology* 27: 610-624.

ARCHIBALD J. D. & FASTOVSKY D. E. 2004. — Dinosaur extinction, *in* WEISHAMPEL D. B., DODSON P. & OSMOLSKA H. (eds), *The Dinosauria.* Second edition. University of California Press, Berkeley: 672-684.

BARRETT P. M. & UPCHURCH P. 2005. — Sauropodomorph diversity through time: macroevolutionary and paleoecological implications, *in* CURRY ROGERS K. A. & WILSON J. A. (eds), *The Sauropods Evolution and Paleobiology*. University of California Press, Berkeley: 125-156.

BENTON M. J. 1994. — Late Triassic to Middle Jurassic extinctions among continental tetrapods: testing the pattern, *in* FRASER N. C. & SUES H. D. (eds), *In the Shadow of the Dinosaurs. Early Mesozoic Tetrapods*. Cambridge University Press, Cambridge: 366-397.

BONAPARTE J. F. 1986. — Les dinosaures (Carnosaures, Allosauridés, Sauropode, Cétiosauridés) du Jurassique moyen de Cerro Condor (Chubut, Argentine). *Annales de Paléontologie* 72: 325-386.

BONAPARTE J. F. 1999.— Evolucion de las vértebras presacras en Sauropodomorpha. *Ameghiniana* 36: 115-187.

BONAPARTE J. F., RIGA B. J. G. & APESTEGUIA S. 2006. — *Ligabuesaurus leanzai* gen. et sp. nov (Dinosauria, Sauropoda), a new titanosaur from the Lohan Cura Formation (Aptian, Lower Cretaceous) of Neuquen, Patagonia, Argentina. *Cretaceous Research* 27: 364-376.

BONNAN M. 2003. — The evolution of manus shape in sauropod dinosaurs: implications for functional morphology, forelimb orientation, and phylogeny. *Journal of Vertebrate Paleontology* 23 (3): 595-613.

BONNAN M. F. 2005. — Pes anatomy is sauropod dinosaurs: implications fro functional morphology, evolution, and phylogeny, *in* TIDWELL V. & CARPENTER K. (eds), *Thunder-Lizards*. Indiana University Press, Bloomington: 346-380.

BORSUK-BIALYNICKA M. 1977. — A new camarasaurid sauropod *Opisthocoelicaudia skarzynskii*, gen. n., sp. n. from the Upper Cretaceous of Mongolia. *Palaeontologia Polonica* 37: 1-64.

BUFFETAUT É. & OUAJA M. 2002. — A new specimen of *Spinosaurus* (Dinosauria, Theropoda) from the Lower Cretaceous of Tunisia, with remarks on the evolutionary history of the Spinosauridae. *Bulletin de la Société géologique de France* 173: 414-421.

BUFFETAUT É., SUTEETHORN V., CUNY G., TONG H., LE LOEUFF J., KHANSUBHA S. & JONGAUTCHARIYAKUI S. 2000. — The earliest known sauropod dinosaur. *Nature* 407: 72-74.

CARRANO M. T. 1997. — Morphological indicators of foot posture in mammals: a statistical and biomechanical analysis. *Zoological Journal of the Linnean Society* 121: 77-104.

CARRANO M. T. & SAMPSON S. D. 2004. — A review of coelophysoids (Dinosauria: Theropoda) from the early Jurassic of Europe, with comments on the late history of the Coelophysoidea. *Neues Jahrbuch für Geologie und Paläontologie*, Monatshefte 9: 537-558.

CHARRIÈRE A., HADDOUMI H. & MOJON P.-O. 2005. — Découverte de Jurassique supérieur et d'un niveau marin du Barrémien dans les « couches rouges » continentales du Haut Atlas central marocain : implications paléogéographiques et structurales. *Comptes Rendus Palevol* 4: 385-394.

CHARROUD M. & FEDAN B. 1992. — Données préliminaires sur la découverte du gisement de Boulahfa à dinosauriens (SW de Boulemane, Moyen Atlas central). *Notes et Mémoire du Service géologique du Maroc* 366: 448-449.

CHURCHER C. S. 1999. — A note on the Late Cretaceous vertebrate fauna of the Dakhleh Oasis, *in* CHURCHER C. S. & MILLS A. J. (eds), Reports from the survey of the Dakleh Oasis western desert of Egypt, 1977-1987. *Oxbow Monograph* 99: 55-67.

COOPER M. R. 1981. — The prosauropod dinosaur *Massospondylus carinatus* Owen from Zimbabwe: its biology, mode of life and phylogenetic significance. *Occasional papers of the National Museum of Rhodesia*, series B, Natural Sciences 6: 689-840.

COOPER M. R. 1984. — A reassessment of *Vulcanodon karibaensis* Raath (dinosauria: Saurischia) and the origin of the Sauropoda. *Palaeontologica Africana* 25: 203-231.

COPE E. D. 1877. — On a gigantic saurian from the Dakota epoch of Colorado. *Paleontological Bulletin* 25: 5-10.

COURTILLOT V. E. & RENNE P. R. 2003. — On the ages of flood basalt events. *Comptes Rendus Geoscience* 335: 113-140.

CURRY ROGERS K. A. & FORSTER C. A. 2001. — The last of the dinosaur titans: a new sauropod from Madagascar. *Nature* 412: 530-534.

DODSON P., KRAUSE D. W., FORSTER C. A., SAMPSON S. D. & RAVOAVY F. 1998. — Titanosaurid (Sauropoda) osteoderms from the Late Cretaceous of Madagascar. *Journal of Vertebrate Paleontology* 18: 563-568.

DUNCAN R. A., HOOPER P. R., REHACEK J., MARSH J. G. & DUNCAN A. R. 1997. — The timing and duration of the Karoo igneous event, southern Gondwana. *Journal of Geophysical Research* 102: 127-138.

DUTUIT J.-M. & OUAZZOU A. 1980. — Découverte d'une

piste de dinosaure sauropode sur le site d'empreintes de Demnat (Haut-Atlas Marocain). *Mémoire de la Société géologique de France* 139: 95-102.

ENCARNACION J., FLEMING T. H., ELLIOT D. H. & EALES H. 1996. — Synchronous emplacement of Ferrar and Karoo dolerites and the early breakup of Gondwana. *Geology* 24: 535-538.

ETTAKI M., MILHI A., CHELLAI E. A., BOUDCHICHE L. & SADKI D. 2000. — Mise en évidence de la limite Pliensbachien-Toarcien par les ammonites, les foraminifères et l'interaction tectono-eustatique dans la région de Todrha-Dadès (Haut-Atlas central, Maroc). *Revue de Paléobiologie* 19: 299-317.

FORSTER C. A., SAMPSON S. D., CHIAPPE L. M. & KRAUSE D. W. 1998. — The theropod ancestry of birds: new evidence from the Late Cretaceous of Madagascar. *Science* 279: 1915-1919.

FRASER N. C., PADIAN K., WALKDEN G. M. & DAVIS A. L. M. 2002. — Basal dinosauriform remains from Britain and the diagnosis of the Dinosauria. *Palaeontology* 45: 79-95.

GALTON P. M. 1984. — Cranial anatomy of the prosauropod dinosaur *Plateosaurus* from Knollenmergel (Middle Keuper, Upper Triassic) of Germany. I – Two complete skulls from Trossingen/Württ. with comments on the diet. *Geologica et Palaeontologica* 18: 139-171.

GALTON P. M. 1985. — Cranial anatomy of the prosauropod dinosaur *Plateosaurus* from Knollenmergel (Middle Keuper, Upper Triassic) of Germany. II – All the cranial material and details of soft-part anatomy. *Geologica et Palaeontologica* 19: 119-159.

GALTON P. M. 1986. — Prosauropod dinosaur *Plateosaurus* (= *Gresslyosaurus*) (Saurischia: Sauropodomorpha) from the Upper Triassic of Switzerland. *Geologica et Palaeontologica* 20: 167-183.

GALTON P. M. 1998. — The prosauropod dinosaur *Plateosaurus* (*Dimodosaurus*) *poligniensis* (Pidancet & Chopard, 1862) (Upper Triassic, Poligny, France). *Neues Jahrbuch für Geologie und Paläontologie*, abhandlungen 207: 255-288.

GALTON P. M. & UPCHURCH P. 2004a. — Prosauropoda, *in* WEISHAMPEL D. B., DODSON P. & OSMOLSKA H. (eds), *The Dinosauria.* Second edition. California University press, Berkeley: 232-258.

GALTON P. M. & UPCHURCH P. 2004b. — Stegosauria, *in* WEISHAMPEL D. B., DODSON P. & OSMOLSKA H. (eds), *The Dinosauria.* Second edition. California University press, Berkeley: 343-362.

GOLOBOFF P. 1999. — NONA (No Name) ver. 2, Tucumán, Argentina.

GOMANI E. 1999. — Sauropod caudal vertebrae from Malawi, Africa, *in* TOMIDA Y., RICH T. &VICHERS-RICH P. (eds), *Second Gondwanan Dinosaur Symposium*, Tokyo 15: 235-248.

GOW C. E., KITCHING J. W. & RAATH M. A. 1990. — Skulls of the prosauropod dinosaur *Massospondylus carinatus* (Owen) in the collections of the Bernard Price Institute for Palaeontological Research. *Palaeontologica Africana* 27: 45-58.

GRADSTEIN F. M., AGTERBERG F. P., OGG J. G., HARDENBOL J. & BACKSTROM S. 1999. — On the Cretaceous time scale. *Neues Jahrbuch für Geologie und Paläontologie*, abhandlungen 212: 3-14.

HADDOUMI H., ALMÉRAS Y., BODERGAT A.-M., CHARRIÈRE A., MANGOLD C. & BENSHILI K. 1998. — Âges et environnements des Couches rouges d'Anoual (Jurassique moyen et Crétacé inférieur, Haut Atlas oriental, Maroc). *Comptes Rendus de l'Académie des Sciences*, série IIa, 327: 127-133.

HALLAM A. 1961. — Cyclotherms, transgressions and faunal change in the Lias of North West Europe. *Transactions of the Edimburgh Geological Society* 18: 123-174.

HALLAM A. 1986. — The Pliensbachian and Tithonian extinction events. *Nature* 319: 765-768.

HALLAM A. & WIGNALL P. B. 1997. — *Mass Extinctions and their Aftermath*. Oxford University Press, Oxford, 320 p.

HARRIS J. D. & DODSON P. 2004. — A new diplodocoid sauropod dinosaur from the Upper Jurassic Formation of Montana, USA. *Acta Palaeontologica Polonica* 49: 197-210.

HE X., LI K. & CAI K. 1988. — *The Middle Jurassic Dinosaur Fauna from Dashanpu, Zigong, Sichuan.* vol IV. *Sauropod Dinosaurs (2).* Omeisaurus tianfuensis. Sichuan Publishing House of Science and Technology, Chengdu, China, 164 p.

HE X., WANG C., LIU S., ZHOU F., LIU T., CAI K. & DAI B. 1998. — A new species of sauropod from the Early Jurassic of Gongxian County, Sichuan. *Acta Geologica Sichuan* 18: 1-7.

HOLTZ T. R., MOLNAR R. E. & CURRIE P. J. 2004. — Basal Tetanurae, *in* WEISHAMPEL D. B., DODSON P. & OSMOLSKA H. (eds), *The Dinosauria*. Second edition. University of California Press, Berkeley: 71-110.

HORI S. R. 1993. — Toarcian oceanic event in deep-sea sediments. *Geological Survey of Japan Bulletin* 44: 555-570.

HUENE F. 1926. — Vollständige Osteologie eines Plateosauriden aus dem schwäbischen Keuper. *Geologie und Paläontologie*, abhandlungen 15: 129-179.

HUENE F. 1932. — Die fossile Reptil-Ordnung Saurischia, ihre Entwicklung und Geschichte. *Monographien zur Geologie und Paläeontologie* 4: 1-361.

ISHIGAKI S. 1988. — Les empreintes de dinosaures du Jurassique inférieur du Haut Atlas central marocain. *Notes du Service géologique du Maroc* 44: 79-86.

JACOBS L. L., WINKLER D. A., DOWNS W. R. & GOMANI E. M. 1993. — New material of an Early Cretaceous titanosaurid sauropod dinosaur from Malawi. *Palaeontology* 36: 523-534.

JACOBS L. L., WINKLER D. A. & GOMANI E. M. 1996. — Cretaceous dinosaurs of Africa : examples from Cameroon and Malawi. *Memoirs of the Queensland Museum* 39: 595-610.

JAIN S. L., KUTTY T. S., ROY-CHOWDHURY T. & CHATTERJEE S. 1975. — The sauropod dinosaur from the Lower Jurassic Kota formation of India. *Proceedings of the Royal Society of London* 188: 221-228.

JAIN S. L., KUTTY T. S., ROY-CHOWDHURY T. & CHATTERJEE S. 1979. — *Some characteristics of* Barapasaurus tagorei*, a sauropod dinosaur from the Lower Jurassic of Deccan, India*. IVth International Gondwana Symposium, Calcutta: 204-216.

JANENSCH W. 1914. — Übersicht über die Wirbeltierfauna der Tendaguru-Schichten, nebst einer kurzen Charakterisierung der neu aufgeführten Arten von Sauropoden. *Archiv für Biontologie* 3: 81-110.

JENKYNS H. C. 1988. — The early Toarcian (Jurassic) anoxic event: stratigraphic, sedimentary, and geochemical evidence. *American Journal of Science* 288: 101-151.

JENNY J. 1985. — Carte géologique du Maroc 1 : 100.000, feuille Azilal. *Notes et Mémoire du Service géologique du Maroc* 339.

JENNY J. & JOSSENS J. A. 1982. — Découverte d'empreintes de pas de dinosauriens dans le Jurassique inférieur (Pliensbachien) du Haut Atlas central (Maroc). *Comptes Rendus de l'Académie des Sciences*, Paris 294: 223-226.

JENNY J., JENNY-DESHUSSESS C., LE MARREC A. & TAQUET P. 1980. — Découvertes d'ossements de Dinosauriens dans le Jurassique inférieur (Toarcien) du Maroc. *Comptes Rendus de l'Académie des Sciences*, Paris 290: 839-842.

JENNY J., LE MARREC A. & MONBARON M. 1981a. — Les Couches Rouges du Jurassique moyen du Haut-Atlas central (Maroc): corrélations lithostratigraphiques, éléments de datations et cadre tectono-sédimentaire. *Bulletin de la Société géologique de France* 23: 627-639.

JENNY J., LE MARREC A. & MONBARON M. 1981b. — Les empreintes de pas de dinosauriens dans le Jurassique moyen du Haut Atlas central (Maroc): nouveaux gisements et précisions stratigraphiques. *Geobios* 14: 427-431.

JONES D. L., DUNCAN R. A., BRIDEN J. C., RANDALL D. E. & MACNIOCAILL C. 2001. — Age of the Bakota basalts, northern Zimbabwe, and the duration of Karoo Large igneous province magmatism. *Geochemistry, Geophysics, Geosystem* 2: 2000GC000110. doi: 10.1130/G22380C.1.

KELLNER A. W. A. & MADER B. J. 1997. — Archosaur teeth from the Cretaceous of Morocco. *Journal of Paleontology* 7: 525-527.

KNOLL F. 2002. — New skull of *Lesothosaurus* (Dinosauria: Omithischia) from the Upper Elliot Formation (Lower Jurassic) of southern Africa. *Geobios* 35: 595-603.

KNOLL F. & BATTAIL B. 2001. — New ornithischian remains from the Upper Elliot Formation Lower Jurassic) of Lesotho and stratigraphical distribution of southern African fabrosaurids. *Geobios* 34: 415-421.

KRAUSE P. M., ROGERS R. R., FORSTER C. A., HARTMAN J. H., BUCKLEY G. A. & SAMPSON S. D. 1999. — The Late Cretaceous vertebrate fauna of Madagascar: implications for gondwanan Paleobiogeography. *GSA Today* 9: 1-7.

LANGER M. C. & BENTON M. J. 2006. — Early dinosaurs: a phylogenetic study. *Journal of Systematic Palaeontology* 4: 309-358.

LAPPARENT A. F. D. 1945. — Empreintes de pas de dinosauriens du Maroc, exposées dans la Galerie de Paléontologie. *Bulletin du Muséum national d'Histoire naturelle* 17: 268-271.

LAPPARENT A. F. D. 1955. — Étude paléontologique des vertébrés du Jurassique d'El Mers (Moyen Atlas). *Notes et Mémoire du Service géologique du Maroc* 124: 1-36.

LE MARREC A. 1985. — Carte géologique du Maroc 1 :100.000, feuille Demnat. *Notes et Mémoire du Service géologique du Maroc* 338.

LITTLE C. T. S. & BENTON M. J. 1995. — Early Jurassic mass extinction: a global long-term event. *Geology* 23: 495-498.

MAHLER L. 2005. — Record of Abelisauridae (Dinosauria: Theropoda) from the Cenomanian of Morocco. *Journal of Vertebrate Paleontology* 25: 236-239.

MARTINEZ R. D., GIMENEZ O., RODRIGUEZ J., LUNA M. & LAMANNA M. C. 2004. — An articulated specimen of the basal titanosaurian (Dinosauria Sauropoda) *Epachthosaurus sciuttoi* from the Early Late Cretaceous Bajo Barreal Formation of Chubut Province, Argentina. *Journal of Vertebrate Paleontology* 24: 107-120.

MCINTOSH J. S. 1990. — Sauropoda, *in* WEISHAMPEL D. B., DODSON P. & OSMLSKA H. (eds), *The Dinosauria*. University of California Press, Berkeley: 345-401.

MONBARON M. 1985. — Carte Géologique du Maroc 1 :100.000, feuille Beni Mellal. *Notes et Mémoire du Service géologique du Maroc* 341.

MONBARON M. & TAQUET P. 1981. — Découverte du squelette complet d'un grand Cétiosaure (Dinosaure Sauropode) dans le bassin jurassique moyen de Tilougguit (Haut-Atlas central, Maroc). *Comptes Rendus de l'Académie des Sciences*, Paris 292: 243-246.

MONBARON M., DEJAX J. & DEMATHIEU G. 1985. — Longues pistes de dinosaures bipèdes à Adrar-n-Ouglagal (Maroc) et répartition des faunes de grands reptiles dans le domaine atlasique au cours du Mésozoïque. *Bulletin du Muséum national d'Histoire naturelle* 7: 229-242.

MONBARON M., KUBLER B. & ZWEIDLER D. 1990. — Detrital rubified sedimentation in the High Atlas trough in the Mesozoic: attempt at lateral correlations using

correspondence factor analysis. *Journal of African Earth Sciences* 10: 369-384.

MONBARON M., RUSSELL D. A. & TAQUET P. 1999. — *Atlasaurus imelakei*, n. g., n. sp., a brachiosaurid-like sauropod from the Middle Jurassic of Morocco. *Comptes Rendus de l'Académie des Sciences* 329: 519-526.

MONTENAT C., MONBARON M., ALLAIN R., AQUESBI N., DEJAX J., HERNANDEZ J., RUSSELL D. & TAQUET P. 2005. — Stratigraphie et paléoenvironnement des dépôts volcano-détritiques à dinosauriens du Jurassique inférieur de Toundoute (Province de Ouarzazate, Haut-Atlas – Maroc). *Eclogae Geologicae Helvetiae* 98: 261-270.

MORARD A., GUEX J., BARTOLINI A., MORETTINI E. & DE WEVER P. 2003. — A new scenario fro the Domerian-Toarcian transition. *Bulletin de la Société géologique de France* 174: 351-356.

NIXON K. C. 1999-2002. — WinClada 1.00.08. Nixon, K.C., Ithaca, N.Y.

NORMAN D. B., SUES H. D., WITMER L. M. & CORIA R. A. 2004a. — Basal Ornithopoda, *in* WEISHAMPEL D. B., DODSON P. & OSMOLSKA H. (eds), *The Dinosauria*. Second edition. University of California Press, Berkeley: 393-412.

NORMAN D. B., WITMER L. M. & WEISHAMPEL D. B. 2004b. — Basal Ornithischia, *in* WEISHAMPEL D. B., DODSON P. & OSMOLSKA H. (eds), *The Dinosauria.* Second edition. University of California Press, Berkeley: 325-334.

NORMAN D. B., WITMER L. M. & WEISHAMPEL D. B. 2004c. — Basal Thyreophora, *in* WEISHAMPEL D. B., DODSON P. & OSMOLSKA H. (eds), *The Dinosauria.* Second edition. University of California Press, Berkeley: 335-342.

NOVAS F. E. 1993. — New information on the systematics and postcranial skeleton of *Herrerasaurus ischigualastensis* (Theropoda: Herrerasauridae) from the Ischigualasto Formation (Upper Triassic) of Argentina. *Journal of Vertebrate Paleontology* 13: 400-423.

OUYANG H. & YE Y. 2002. — *The First Mamenchisaurian Skeleton with Complete Skull:* Mamenchisaurus youngi. *Sichuan Science and Technology Press*, Chengdu, 111 p.

PALFY J. & SMITH P. 2000. — Synchrony between early Jurassic extinction, oceanic anoxic event, and the Karoo-Ferrar flood basalt volcanism. *Geology* 28: 747-750.

PALFY J., SMITH P. & MORTENSEN J. K. 2002. — Dating the end-Triassic and Early Jurassic mass extinctions, correlative large igneous provinces, and isotopics events, *in* KOEBERL C. & MACLEOD K. G. (eds), Catastrophic events and mass extinctions: impact and beyond. *Geological Society of America Special Paper*, Boulder 356: 523-532.

PLATEAU H., GIBOULET G. & ROCH E. 1937. — Sur la présence d'empreintes de Dinosauriens dans la région de Demnat. *Comptes rendus sommaires de la Société géologique de France*: 241-242.

RAATH M. A. 1972. — Fossil vertebrate studies in Rhodesia: a new dinosaur (Reptilia: Saurischia) from near the Trias-Jurassic boundary. *Arnoldia* 5: 1-37.

RAUHUT O. 2005. — Post-cranial remains of "coelurosaurus" (Dinosauria, Theropoda) from the Late Jurassic of Tanzania. *Geological Magazine* 142: 97-107.

RAUHUT O. & WERNER C. 1995. — First record of the family Dromaeosauridae (Dinosauria: Theropoda) in the Cretaceous of Gondwana (Wadi Milk Formation, northern Sudan). *Paläontologische Zeitschrift* 69: 475-489.

RAUP D. M. & SEPKOSKI J. J. 1984. — Periodicity of extinctions in the geological past. *National Academy of Sciences Proceedings* 81: 801-805.

RAUP D. M. & SEPKOSKI J. J. 1986. — Periodic extinctions of families and genera. *Science* 231: 833-836.

RIGGS E. S. 1903. — *Brachiosaurus altithorax*, the largest known dinosaur. *American Journal of Science* 15: 299-306.

ROGERS R. R., KRAUSE D. W. & ROGERS K. C. 2003. — Cannibalism in the Madagascan dinosaur *Majungatholus atopus*. *Nature* 422: 515-518.

RUBAN D. A. 2004. — Diversity dynamics of Early-Middle Jurassic brachiopods of Caucasus, and the Pliensbachian-Toarcian mass extinction. *Acta Palaeontologica Polonica* 49: 275-282.

RUSSELL D. A. 1996. — Isolated dinosaur bones from the Middle Cretaceous of the Tafilalt, Morocco. *Bulletin du Muséum national d'Histoire naturelle* 19: 349-402.

SALGADO L., CORIA R. A. & CALVO J. O. 1997. — Evolution of titanosaurid sauropods I: Phylogenetic analysis based on the postcranial evidence. *Ameghiniana* 34: 3-32.

SALGADO L., GARRIDO A., COCCA S. E. & COCCA J. R. 2004. — Lower Cretaceous rebbachisaurid sauropods from Cerro Aguada del Leon (Lohan Cura Formation), Neuquen Province, northwestern Patagonia, Argentina. *Journal of Vertebrate Paleontology* 24: 903-912.

SAMPSON S. D., CARRANO M. T. & FORSTER C. A. 2001. — A bizarre predatory dinosaur from the Late Cretaceous of Madagascar. *Nature* 409: 504-506.

SAMPSON S. D., KRAUSE D. W., DODSON P. & FORSTER C. A. 1996. — The premaxilla of *Majungasaurus* (Dinosauria: Theropoda), with implications for Gondwanan paleobiogeography. *Journal of Vertebrate Paleontology* 16: 601-605.

SAMPSON S. D., WITMER L. M., FORSTER C. A., KRAUSE P. M., O'CONNOR D. W., DODSON P. & RAVOAVY F. 1998. — Predatory dinosaur remains from Madagascar: implications for the Cretaceous biogeography of Gondwana. *Science* 280: 1048-1051.

SERENO P. C. 1993. — The pectoral girdle and forelimb of the basal theropod *Herreresaurus ischigualastensis*.

Journal of Vertebrate Paleontology 13: 425-450.
SERENO P. C. 1999. — The evolution of Dinosaurs. *Science* 284: 2137-2147.
SERENO P. C. & NOVAS F. E. 1993. — The skull and neck of the basal theropod *Herrerasaurus ischigualastensis*. *Journal of Vertebrate Paleontology* 13: 451-476.
SERENO P. C., WILSON J. A., LARSSON H. C. E., DUTHEIL D. B. & SUES H. D. 1994. — Early Cretaceous dinosaurs from the Sahara. *Science* 265: 267-271.
SERENO P. C., DUTHEIL D. B., IAROCHENE M., LARSSON H. C. E., LYON G. H., MAGWENE P. M., SIDOR C. A., VARRICCHIO D. J. & WILSON J. A. 1996. — Predatory dinosaurs from the Sahara and Late Cretaceous faunal differentiation. *Science* 272: 986-991.
SERENO P. C., BECK A. L., DUTHEIL D. B., GADO B., LARSSON H. C. E., LYON G. H., MARCOT J. D., RAUHUT O. W. M., SADLEIR R. W., SIDOR C. A., VARRICCHIO D. J., WILSON G. P. & WILSON J. A. 1998. — A long-snouted predatory dinosaur from Africa and the evolution of Spinosaurids. *Science* 282: 1298-1302.
SERENO P. C., BECK A. L., DUTHEIL D. B., LARSSON H. C. E., LYON G. H., MOUSSA B., SADLEIR R. W., SIDOR C. A., VARRICCHIO D. J., WILSON G. P. & WILSON J. A. 1999. — Cretaceous sauropods from the Sahara and the uneven rate of skeletal evolution among dinosaurs. *Science* 286: 1342-1347.
SERENO P. C., WILSON J. A. & CONRAD J. L. 2004. — New dinosaurs link southern land masses in the Mid-Cretaceous. *Proceedings of the Royal Society of London* B 271: 1325-1330.
SMITH J. B., LAMANNA M. C., LACOVARA K. J., DODSON P., SMITH J. R., POOLE J. C., GIEGENGACK R. & ATTIA Y. 2001. — A giant sauropod dinosaur from an Upper Cretaceous mangrove deposit in Egypt. *Science* 292: 1704-1706.
TAQUET P. 1984. — Two new Jurassic specimens of Coelurosaurs (Dinosauria), *in* HECHTM. K., OSTROM J. H., VIOHL G. & WELLNHOFER P. (eds), *The Beginnings of Birds: Proceedings of the International Archaeopteryx Conference*. Fruende des Jura-Museums, Eichstätt: 229-232.
TAQUET P. & RUSSELL D. A. 1998. — New data on spinosaurid dinosaurs from the Early Cretaceous of the Sahara. *Comptes Rendus de l'Académie des Sciences*, série IIa, 327: 347-353.
TAQUET P. & RUSSELL D. A. 1999. — A massively-constructed iguanodont from Gadoufaoua, Lower Cretaceous of Niger. *Annales de Paléontologies* 85: 85-96.
TERMIER H. 1942. — Données nouvelles sur le Jurassique rouge à Dinosauriens du Grand et Moyen-Atlas (Maroc). *Bulletin de la Société géologique de France* 12 (5): 199-207.
TERMIER H., GUBLER J. & LAPPARENT A. F. D. 1940. — Reptiles et poissons du Bathonien d'El-Mers (Moyen Atlas marocain). *Comptes Rendus de l'Académie des Sciences*, Paris 210: 768-770.
TYKOSKI R. S. 2005. — *Anatomy, Ontogeny, and Phylogeny of Coelophysoid Theropods*. Ph. D. Thesis, University of Texas, Austin, USA, 553 p.
TYKOSKI R. S. & ROWE T. 2004. — Ceratosauria, *in* WEISHAMPEL D. B., DODSON P. & OSMOLSKA H. (eds), *The Dinosauria.* Second edition. University of California Press, Berkeley: 47-70.
UPCHURCH P. 1998. — The phylogenetic relationships of sauropod dinosaurs. *Zoological Journal of the Linnean Society* 124: 43-103.
UPCHURCH P. & BARRETT P. M. 2005. — Phylogenetic and taxic perspectives on sauropod diversity, *in* CURRY ROGERS K. A. & WILSON J. A. (eds), *The Sauropods Evolution and Paleobiology*. University of California Press, Berkeley: 104-124.
UPCHURCH P. & MARTIN J. 2002. — The Rutland *Cetiosaurus*: the anatomy and relationships of a Middle Jurassic British sauropod dinosaur. *Palaeontology* 45: 1049-1074.
UPCHURCH P. & MARTIN J. 2003. — The anatomy and taxonomy of *Cetiosaurus* (Saurischia Sauropoda) from the Middle Jurassic of England. *Journal of Vertebrate Paleontology* 23: 208-231.
UPCHURCH P., BARRETT P. M. & DODSON P. 2004. — Sauropoda, in WEISHAMPEL D. B., DODSON P. & OSMOLSKA H. (eds), *The Dinosauria*. Second edition. University of California Press, Berkeley: 259-322.
WEDEL M. J. 2003. — The evolution of vertebral pneumacity in sauropod dinosaur. *Journal of Vertebrate Paleontology* 23 (2): 344-357.
WEISHAMPEL D. B., DODSON P. & OSMOLSKA H. 2004. — *The Dinosauria*. Second edition. University of California press, Berkeley, 861 p.
WIGNALL P. B. 2001. — Large igneous provinces and mass extinctions. *Earth-Science Reviews* 53: 1-33.
WILD R. 1978. — Ein Sauropoden-Rest (Reptilia, Saurichia) aus dem Posidonienschiefer (Lias, Toarcium) von Holzmaden. *Stuttgarter Beiträge zur Naturkunde* B 41: 1-15.
WILSON J. A. 1999. — A nomenclature for vertebral laminae in sauropods and other saurischian dinosaurs. *Journal of Vertebrate Paleontology* 19: 639-653.
WILSON J. A. 2002. — Sauropod dinosaur phylogeny: critique and cladistic analysis. *Zoological Journal of the Linnean Society* 136: 217-276.
WILSON J. A. 2005a. — Integrating ichnofossil and body fossil records to estimate locomotor posture and spatiotemporal distribution of early sauropod dinosaurs: a stratocladistic approach. *Paleobiology* 31: 400-423.
WILSON J. A. 2005b. — Overview of sauropod phylogeny and evolution, *in* CURRY ROGERS K. A. & WILSON J. A. (eds), *The Sauropods Evolution and Paleobiology*. University of California Press, Berkeley: 15-49.
WILSON J. A. 2005c. — Redescription of the Mongolian Sauropod *Nemegtosaurus mongoliensis* Nowinski

(Dinosauria: Saurischia) and comments on Late Cretaceous Sauropod diversity. *Journal of Systematic Palaeontology* 3: 283-318.

WILSON J. A. & MOHABEY D. M. 2006. — A titanosauriform (Dinosauria: Sauropoda) axis from the Lameta Formation (Upper Cretaceous: Maastrichtian) of Nand, Central India. *Journal of Vertebrate Paleontology* 26: 471-479.

WILSON J. A. & SERENO P. C. 1998. — Early evolution and higher-level phylogeny of sauropod dinosaurs. *Memoirs of the Society of Vertebrate Paleontology* 18: 1-68.

WIMAN C. 1929. — Die Kreide-Dinosaurier aus Shantung. *Palaeontologia Sinica* 6: 1-67.

YADAGIRI P. 1988. — A new sauropod *Kotasaurus yamanpalliensis* from Lower Jurassic Kota Formation of India. *Records of the Geological Survey of India* 11: 102-127.

YADAGIRI P. 2001. — The osteology of *Kotasaurus yamanpalliensis*, a sauropod dinosaur from the Early Jurassic Kota Formation of India. *Journal of Vertebrate Paleontology* 21: 242-252.

YATES A. M. 2006. — Solving a dinosaurian puzzle: the identity of *Aliwalia rex* Galton. *Historical Biology* 2006: 1-31.

YATES A. M. & KITCHING J. W. 2003. — The earliest known sauropod dinosaur and the first steps towards sauropod locomotion. *Proceedings of the Royal Society of London* B 270: 1753-1758.

YATES A. M., HANCOX P. J. & RUBIDGE B. S. 2004. — First record of a sauropod dinosaur from the upper Elliot Formation (Early Jurassic) of South Africa. *South African Journal of Science* 100: 504-506.

YOUNG C.-C. 1939. — On a new sauropoda, with notes on other fragmentary reptiles from Szechuan. *Bulletin of the Geological Society of China* 19: 279-315.

ZAKHAROV V. A., SHURYGIN B. N., IL'INA V. I. & NIKITENKO B. L. 2006. — Pliensbachian-Toarcian biotic turnover in North Siberia and the Arctic region. *Stratigraphy and Geological Correlation* 14: 399-417.

ZHANG Y. 1988. — The Middle Jurassic dinosaur fauna from Dashanpu, Zigong, Sichuan. Sauropod dinosaurs. *Shunosaurus*. Sichuan Publishing House of Science and Technology, Chengdu, China, 3: 1-106.

Submitted on 25 January 2007;
accepted on 12 October 2007.

APPENDIX 1

List of characters used in the phylogenetic analysis (mainly based on Wilson 2002). Characters are ordered by anatomical region.

1. **Posterolateral processes of premaxilla and lateral processes of maxilla, shape**: (**0**) without midline contact; (**1**) with midline contact forming marked narial depression, subnarial foramen not visible laterally.
2. **Premaxillary anterior margin, shape**: (**0**) without step; (**1**) with marked step, anterior portion of skull sharply demarcated.
3. **Maxillary border of external naris, length**: (**0**) short, making up much less than one-fourth narial perimeter; (**1**) long, making up more than one-third narial perimeter.
4. **Preantorbital fenestra**: (**0**) absent; (**1**) present.
5. **Subnarial foramen and anterior maxillary foramen, position**: (**0**) well distanced from one another; (**1**) separated by narrow bony isthmus.
6. **Antorbital fenestra, maximum diameter**: (**0**) much shorter; (**1**) subequal to orbital maximum diameter.
7. **Antorbital fossa**: (**0**) present; (**1**) absent.
8. **External nares, position**: (**0**) terminal; (**1**) retracted to level of orbit; (**2**) retracted to a position between orbits.
9. **External nares, maximum diameter**: (**0**) shorter; (**1**) longer than orbital maximum diameter.
10. **Orbital ventral margin, anteroposterior length**: (**0**) broad, with subcircular orbital margin; (**1**) reduced, with acute orbital margin.
11. **Lacrimal, anterior process**: (**0**) present; (**1**) absent.
12. **Jugal-ectopterygoid contact**: (**0**) present; (**1**) absent.
13. **Jugal, contribution to antorbital fenestra**: (**0**) very reduced or absent; (**1**) large, bordering approximately one-third its perimeter.
14. **Prefrontal, posterior process size**: (**0**) small, not projecting far posterior of frontal-nasal suture; (**1**) elongate, approaching parietal.
15. **Prefrontal, posterior process shape**: (**0**) flat; (**1**) hooked.
16. **Postorbital, ventral process shape**: (**0**) transversely narrow; (**1**) broader transversely than anteroposteriorly.
17. **Frontal contribution to supratemporal fossa**: (**0**) present; (**1**) absent.
18. **Frontal, anteroposterior length**: (**0**) approximately twice; (**1**) less than minimum transverse breadth.
19. **Parietal occipital process, dorsoventral height**: (**0**) short, less than the diameter of the foramen magnum; (**1**) deep, nearly twice the diameter of the foramen magnum.
20. **Parietal, anterolateral process**: (**0**) absent; (**1**) present.
21. **Parietal, contribution to post-temporal fenestra**: (**0**) present; (**1**) absent.
22. **Parietal, distance separating supratemporal fenestrae**: (**0**) less than; (**1**) twice the long axis of supratemporal fenestra.
23. **Supratemporal fenestra, long axis orientation**: (**0**) anteroposterior; (**1**) transverse.
24. **Supratemporal region, anteroposterior length**: (**0**) temporal bar longer; (**1**) shorter anteroposteriorly than transversely.
25. **Supratemporal fossa, lateral exposure**: (**0**) not visible laterally, obscured by temporal bar; (**1**) visible laterally, temporal bar shifted ventrally.
26. **Laterotemporal fenestra, anterior extension**: (**0**) posterior to orbit; (**1**) ventral to orbit.
27. **Squamosal-quadratojugal contact**: (**0**) present; (**1**) absent.
28. **Quadratojugal, anterior process length**: (**0**) short, anterior process shorter than dorsal process; (**1**) long, anterior process more than twice as long as dorsal process.
29. **Quadrate fossa**: (**0**) absent; (**1**) present.
30. **Quadrate fossa, depth**: (**0**) shallow; (**1**) deeply invaginated.
31. **Palatobasal contact, shape**: (**0**) pterygoid with small facet; (**1**) dorsomedially orientated hook; (**2**) or rocker-like surface for basipterygoid articulation.
32. **Pterygoid, transverse flange (i.e. ectopterygoid process) position**: (**0**) posterior of orbit; (**1**) between orbit and antorbital fenestra; (**2**) anterior to antorbital fenestra.
33. **Pterygoid, palatine ramus shape**: (**0**) straight, at level of dorsal margin of quadrate ramus; (**1**) stepped, raised above level of quadrate ramus.
34. **Palatine, lateral ramus shape**: (**0**) plate-shaped (long maxillary contact); (**1**) rod-shaped (narrow maxillary contact).
35. **Epipterygoid**: (**0**) present; (**1**) absent.
36. **Vomer, anterior articulation**: (**0**) maxilla; (**1**) premaxilla.
37. **Paroccipital process, ventral nonarticular process**: (**0**) absent; (**1**) present.
38. **Basipterygoid processes, length**: (**0**) short, approximately twice; (**1**) elongate, at least four times basal diameter.
39. **Basioccipital depression between foramen magnum and basal tubera**: (**0**) absent; (**1**) present.

40. **Basisphenoid/basipterygoid recess**: (**0**) present; (**1**) absent.
41. **Basipterygoid processes, orientation**: (**0**) perpendicular to; (**1**) angled approximately 45° to skull roof.
42. **Occipital region of skull, shape**: (**0**) anteroposteriorly deep, paroccipital processes oriented posterolaterally; (**1**) flat, paroccipital processes oriented transversely.
43. **Dentary, depth of anterior end of ramus**: (**0**) slightly less than that of dentary at midlength; (**1**) increases anteriorly towards the symphysis.
44. **Dentary, anteroventral margin shape**: (**0**) gently rounded; (**1**) sharply projecting triangular process or "chin".
45. **External mandibular fenestra**: (**0**) present; (**1**) absent.
46. **Surangular depth**: (**0**) less than twice; (**1**) more than two and one-half times maximum depth of the angular.
47. **Surangular ridge separating adductor and articular fossae**: (**0**) absent; (**1**) present.
48. **Coronoid process of the surangular**: (**0**) reduced; (**1**) prominent.
49. **Adductor fossa, medial wall depth**: (**0**) shallow; (**1**) deep, prearticular expanded dorsoventrally.
50. **Splenial posterior process, position**: (**0**) overlapping angular; (**1**) separating anterior portions of prearticular and angular.
51. **Splenial posterodorsal process**: (**0**) present, approaching margin of adductor chamber; (**1**) absent.
52. **Coronoid, size**: (**0**) extending to dorsal margin of jaw; (**1**) reduced, not extending dorsal to splenial; (**2**) absent.
53. **Tooth rows, shape of anterior portions**: (**0**) narrowly arched, anterior portion of tooth rows V-shaped; (**1**) broadly arched, anterior portion of tooth rows U-shaped; (**2**) rectangular, tooth-bearing portion of jaw perpendicular to jaw rami.
54. **Tooth rows, length**: (**0**) extending to orbit; (**1**) restricted anterior to orbit; (**2**) restricted anterior to subnarial foramen.
55. **Crown-to-crown occlusion**: (**0**) absent; (**1**) present.
56. **Occlusal pattern**: (**0**) interlocking, V-shaped facets; (**1**) high-angled planar facets; (**2**) low-angled planar facets.
57. **Tooth crowns, orientation**: (**0**) aligned along jaw axis, crowns do not overlap; (**1**) aligned slightly anterolingually, tooth crowns overlap.
58. **Tooth crowns, cross-sectional shape at midcrown**: (**0**) elliptical; (**1**) D-shaped; (**2**) cylindrical.
59. **Enamel surface texture**: (**0**) smooth; (**1**) wrinkled.
60. **Marginal tooth denticles**: (**0**) present; (**1**) absent on posterior edge; (**2**) absent on both anterior and posterior edges.
61. **Dentary teeth, number**: (**0**) greater than 20; (**1**) 18 or fewer.
62. **Replacement teeth per alveolus, number**: (**0**) two or fewer; (**1**) more than four.
63. **Presacral bone texture**: (**0**) solid; (**1**) spongy, with large, open internal cells, "camellate".
64. **Presacral centra, pneumatopores (pleurocoels)**: (**0**) absent or shallow depressions; (**1**) present and bordered by a sharp lip.
65. **Atlantal intercentrum, occipital facet shape**: (**0**) rectangular in lateral view, length of dorsal aspect subequal to that of ventral aspect; (**1**) expanded anteroventrally in lateral view, anteroposterior length of dorsal aspect shorter than that of ventral aspect.
66. **Axial neural spine, orientation**: (**0**) more horizontally than vertically; (**1**) more vertically than horizontally.
67. **Cervical vertebrae, number**: (**0**) nine or fewer; (**1**) 10; (**2**) 12; (**3**) 13; (**4**) 15 or greater.
68. **Cervical neural arch lamination**: (**0**) well developed, with well-defined laminae and coels; (**1**) rudimentary; diapophyseal laminae only feebly developed if present.
69. **Cervical centra, articular face morphology**: (**0**) amphicoelous; (**1**) opisthocoelous.
70. **Cervical pneumatopores (pleurocoels), shape**: (**0**) simple, undivided; (**1**) complex, divided by bony septa.
71. **Anterior cervical centra, height: width ratio**: (**0**) less than 1; (**1**) approximately 1.25.
72. **Anterior cervical neural spines, shape**: (**0**) single; (**1**) bifid.
73. **Middle and posterior cervical vertebrae, infraprezygapophyseal fossa**: (**0**) shallow; (**1**) deep, extends posteriorly above the neural canal.
74. **Mid-cervical centra, anteroposterior length/height of posterior face**: (**0**) 2.5-3.0; (**1**) > 4.
75. **Mid-cervical neural arches, height**: (**0**) less than that of posterior centrum face; (**1**) greater than that of posterior centrum face.
76. **Middle cervical vertebrae, intrapostzygapophyseal lamina**: (**0**) contact each other above the neural canal; (**1**) do not contact each other above the neural canal and define a median furrow.
77. **Middle and posterior cervical neural arches, centroprezygapophyseal lamina (cprl), shape**: (**0**) single; (**1**) divided.
78. **Posterior cervical and anterior dorsal neural spines, shape**: (**0**) single; (**1**) bifid.
79. **Posterior cervical and anterior dorsal bifid neural spines, median tubercle**: (**0**) absent; (**1**) present.
80. **Dorsal vertebrae, number**: (**0**) 15; (**1**) 14; (**2**) 13; (**3**) 12; (**4**) 11; (**5**) 10 or fewer.
81. **Dorsal neural spines, breadth**: (**0**) narrower; (**1**) much broader transversely than anteroposteriorly.

82. **Anterior dorsal centra, articular face shape**: (**0**) amphicoelous; (**1**) opisthocoelous.
83. **Middle and posterior dorsal neural arches, centropostzygapophyseal lamina (cpol), shape**: (**0**) absent or single; (**1**) divided.
84. **Middle and posterior dorsal neural arches, anterior centroparapophyseal lamina (acpl)**: (**0**) absent; (**1**) present.
85. **Middle and posterior dorsal neural arches, prezygoparapophyseal lamina (prpl)**: (**0**) absent; (**1**) present.
86. **Middle and posterior dorsal neural arches, posterior centroparapophyseal lamina (pcpl)**: (**0**) absent; (**1**) present.
87. **Middle and posterior dorsal neural arches, spinodiapophyseal lamina (spdl)**: (**0**) absent; (**1**) present.
88. **Middle and posterior dorsal neural arches spinopostzygapophyseal lamina (spol) shape**: (**0**) single; (**1**) divided.
89. **Middle and posterior dorsal neural arches, spinodiapophyseal lamina (spdl) and spinopostzygapophyseal lamina (spol) contact**: (**0**) absent; (**1**) present.
90. **Middle and posterior dorsal neural spines, shape**: (**0**) tapering or not flaring distally; (**1**) flared distally, with pendant, triangular lateral processes.
91. **Middle and posterior dorsal neural arches, "infradiapophyseal" pneumatopore between acdl and pcdl**: (**0**) absent; (**1**) present; (**2**) present and communicates with the neural cavity.
92. **Middle and posterior dorsal neural spines, orientation**: (**0**) vertical; (**1**) posterior, neural spine summit approaches level of diapophyses.
93. **Posterior dorsal centra, articular face shape**: (**0**) amphicoelous; (**1**) opisthocoelous.
94. **Posterior dorsal neural arches, hyposphene- hypantrum articulations**: (**0**) present; (**1**) absent.
95. **Sacral vertebrae, number**: (**0**) 3 or fewer; (**1**) 4; (**2**) 5; (**3**) 6.
96. **Sacrum, sacricostal yoke**: (**0**) absent; (**1**) present.
97. **Sacral neural spines, length**: (**0**) approximately twice; (**1**) four times length of centrum.
98. **Sacral ribs, dorsoventral length**: (**0**) low, not projecting beyond dorsal margin of ilium; (**1**) high extending beyond dorsal margin of ilium.
99. **Caudal transverse processes**: (**0**) persist through caudal 20 or more posteriorly; (**1**) disappear by caudal 15; (**2**) disappear by caudal 10.
100. **First caudal centrum, articular face shape**: (**0**) flat; (**1**) procoelous; (**2**) opisthocoelous; (**3**) biconvex.
101. **Anterior caudal centra (excluding the first), articular face shape**: (**0**) amphiplatyan or platycoelous; (**1**) procoelous; (**2**) opisthocoelous.
102. **Anterior caudal neural arches, spinoprezygapophyseal lamina (sprl)**: (**0**) absent; (**1**) present and extending onto lateral aspect of neural spine.
103. **Anterior caudal neural arches, spinoprezygapophyseal lamina (sprl) –spinopostzygapophyseal lamina (spol) contact**: (**0**) absent; (**1**) present, forming a prominent lamina on lateral aspect of neural spine.
104. **Anterior caudal neural arches, prespinal lamina (prsl)**: (**0**) absent; (**1**) present.
105. **Anterior caudal neural arches, postspinal lamina (posl)**: (**0**) absent; (**1**) present.
106. **Anterior caudal neural spines, transverse breadth**: (**0**) approximately 50% of; (**1**) greater than anteroposterior length.
107. **Anterior caudal transverse processes, proximal depth**: (**0**) shallow, on centrum only; (**1**) deep, extending from centrum to neural arch.
108. **Anterior caudal transverse processes, shape**: (**0**) triangular, tapering distally; (**1**) "wing-like", not tapering distally.
109. **Anterior caudal transverse processes, diapophyseal laminae (acdl, pcdl, prdl, podl)**: (**0**) absent; (**1**) present.
110. **Anterior caudal transverse processes, anterior centrodiapophyseal lamina (acdl), shape**: (**0**) single; (**1**) divided.
111. **Anterior and middle caudal centra, ventral longitudinal hollow**: (**0**) absent; (**1**) present.
112. **Middle caudal vertebrae, location of neural arches**: (**0**) over the midpoint of the centrum with approximately subequal amounts of the centrum exposed at either end; (**1**) on the cranial half of the centrum.
113. **Middle and posterior caudal centra, anterior articular face shape**: (**0**) flat; (**1**) procoelous (cone-shaped); (**2**) opisthocoelous.
114. **Distalmost caudal centra, articular face shape**: (**0**) platycoelous; (**1**) biconvex.
115. **Distalmost biconvex caudal centra, length-height ratio**: (**0**) less than 4; (**1**) greater than 5.
116. **Cervical rib, tuberculum-capitulum angle**: (**0**) greater than 90°; (**1**) less than 90°, rib ventrolateral to centrum.
117. **Cervical ribs, length**: (**0**) much longer than centrum, overlapping as many as three subsequent vertebrae; (**1**) shorter than centrum, little or no overlap.
118. **Dorsal ribs, proximal pneumatocoels**: (**0**) absent; (**1**) present.
119. **Anterior dorsal ribs, cross-sectional shape**: (**0**) subcircular; (**1**) plank-like, anteroposterior breadth more than three times mediolateral breadth.
120. **"Forked" chevrons with anterior and posterior projections**: (**0**) absent; (**1**) present.
121. **Chevrons, "crus" bridging dorsal margin of haemal canal**: (**0**) present; (**1**) absent.
122. **Chevron haemal canal, depth**: (**0**) short, approx-

imately 25%; (**1**) long, approximately 50% chevron length.

123. **Chevrons**: (**0**) persisting throughout at least 80% of tail; (**1**) disappearing by caudal 30.
124. **Posterior chevrons, distal contact**: (**0**) fused; (**1**) unfused (open).
125. **Posture**: (**0**) bipedal; (**1**) columnar, obligately quadrupedal posture.
126. **Scapular acromion process, size**: (**0**) narrow; (**1**) broad, width more than 150% minimum width of blade.
127. **Scapular blade, orientation**: (**0**) perpendicular to; (**1**) forming a 45° angle with coracoid articulation.
128. **Scapular blade, shape**: (**0**) acromial edge not expanded; (**1**) rounded expansion on acromial side; (**2**) racquet-shaped.
129. **Scapular glenoid, orientation**: (**0**) relatively flat or laterally facing; (**1**) strongly bevelled medially.
130. **Scapular blade, cross-sectional shape at base**: (**0**) flat or rectangular; (**1**) D-shaped.
131. **Coracoid, proximodistal length**: (**0**) less than; (**1**) approximately twice length of scapular articulation.
132. **Coracoid, anteroventral margin shape**: (**0**) rounded; (**1**) rectangular.
133. **Coracoid, infraglenoid lip**: (**0**) absent; (**1**) present.
134. **Sternal plate, shape**: (**0**) oval; (**1**) crescentic.
135. **Humeral proximolateral corner, shape**: (**0**) rounded; (**1**) square.
136. **Humeral deltopectoral attachment, development**: (**0**) prominent; (**1**) reduced to a low crest or ridge.
137. **Humeral deltopectoral crest, shape**: (**0**) relatively narrow throughout length; (**1**) markedly expanded distally.
138. **Humeral distal condyles, articular surface shape**: (**0**) restricted to distal portion of humerus; (**1**) exposed on anterior portion of humeral shaft.
139. **Humeral distal condyle, shape**: (**0**) divided; (**1**) flat.
140. **Ulnar proximal condyle, shape**: (**0**) subtriangular; (**1**) triradiate, with deep radial fossa.
141. **Ulnar proximal condylar processes, relative lengths**: (**0**) subequal; (**1**) unequal, anterior arm longer.
142. **Ulnar olecranon process, development**: (**0**) prominent, projecting above proximal articulation; (**1**) rudimentary, level with proximal articulation.
143. **Ulna, length-proximal breadth ratio**: (**0**) gracile; (**1**) stout.
144. **Radial distal condyle, shape**: (**0**) round; (**1**) subrectangular, flattened posteriorly and articulating in front of ulna.
145. **Radius, distal breadth**: (**0**) slightly larger than; (**1**) approximately twice midshaft breadth.
146. **Radius, distal condyle orientation**: (**0**) perpendicular to; (**1**) bevelled approximately 20° proximolaterally relative to long axis of shaft.
147. **Humerus-femur ratio**: (**0**) less than 0.60; (**1**) 0.60 or more.
148. **Carpal bones, shape**: (**0**) round; (**1**) block-shaped, with flattened proximal and distal surfaces.
149. **Metacarpus, shape**: (**0**) spreading; (**1**) bound, with subparallel shafts and articular surfaces that extend half their length.
150. **Metacarpals, shape of proximal surface in articulation**: (**0**) gently curving, forming a 90° arc; (**1**) U-shaped, subtending a 270° arc.
151. **Longest metacarpal-to-radius ratio**: (**0**) close to 0.3; (**1**) 0.45 or more.
152. **Metacarpal I, length**: (**0**) shorter than; (**1**) longer than metacarpal IV.
153. **Metacarpal I, distal condyle shape**: (**0**) divided; (**1**) undivided.
154. **Metacarpal I distal condyle, transverse axis orientation**: (**0**) bevelled approximately 20° proximodistally; (**1**) perpendicular with respect to axis of shaft.
155. **Manual digit II phalangeal number**: (**0**) 3 or more; (**1**) reduced, 2; (**2**) absent or unossified.
156. **Manual digit III phalangeal number**: (**0**) 3 or more; (**1**) reduced, 2 or less; (**2**) absent or unossified.
157. **Manual phalanx I.1, shape**: (**0**) rectangular; (**1**) wedge-shaped.
158. **Manual nonungual phalanges, shape**: (**0**) longer proximodistally than broad transversely; (**1**) broader transversely than long proximodistally.
159. **Pelvis, anterior breadth**: (**0**) narrow, ilia longer anteroposteriorly than distance separating preacetabular processes; (**1**) broad, distance between preacetabular processes exceeds anteroposterior length of ilia.
160. **Ilium, ischial peduncle size**: (**0**) large, prominent; (**1**) low, rounded.
161. **Ilium, ischial peduncle position**: (**0**) large or only moderately reduced, so that a chord through the articular surfaces of the ischial and pubic peduncles passes ventral to the caudal lobe of the ilium; (**1**) highly reduced, so that the chord through the articular surfaces of the ischial and pubic peduncles passes through or above the ventral margin of the caudal lobe of the ilium.
162. **Iliac blade dorsal margin, shape**: (**0**) flat; (**1**) semicircular.
163. **Iliac preacetabular process, orientation**: (**0**) anterolateral to; (**1**) perpendicular to body axis.
164. **Iliac preacetabular process, shape**: (**0**) pointed, arching ventrally; (**1**) semicircular, with posteroventral excursion of cartilage cap.

165. **Pubis, ambiens process development**: (**0**) small, confluent with; (**1**) prominent, projecting anteriorly from anterior margin of pubis.
166. **Pubic apron, shape**: (**0**) flat (straight symphysis); (**1**) canted anteromedially (gentle S-shaped symphysis).
167. **Puboischial contact, length**: (**0**) approximately one-third; (**1**) one-half total length of pubis.
168. **Ischial blade, length**: (**0**) much shorter than; (**1**) equal to or longer than pubic blade.
169. **Ischial blade, shape**: (**0**) emarginate distal to pubic peduncle; (**1**) no emargination distal to pubic peduncle.
170. **Ischial distal shaft, shape**: (**0**) triangular, depth of ischial shaft increases medially; (**1**) blade-like, medial and lateral depths subequal.
171. **Ischial distal shafts, cross-sectional shape**: (**0**) V-shaped, forming an angle of nearly 50° with each other; (**1**) flat, nearly coplanar.
172. **Femoral fourth trochanter, development**: (**0**) prominent; (**1**) reduced to crest or ridge.
173. **Femoral lesser trochanter**: (**0**) present; (**1**) absent.
174. **Femoral midshaft, transverse diameter**: (**0**) subequal to; (**1**) 125-150%; (**2**) at least 185% anteroposterior diameter.
175. **Femoral shaft, lateral margin shape**: (**0**) straight; (**1**) proximal one-third deflected medially.
176. **Femoral distal condyles, relative transverse breadth**: (**0**) subequal; (**1**) tibial much broader than fibular.
177. **Femoral distal condyles, orientation**: (**0**) perpendicular or slightly bevelled dorsolaterally; (**1**) bevelled dorsomedially approximately 10° relative to femoral shaft.
178. **Femoral distal condyles, articular surface shape**: (**0**) restricted to distal portion of femur; (**1**) expanded onto anterior portion of femoral shaft.
179. **Tibial proximal condyle, shape**: (**0**) narrow, long axis anteroposterior; (**1**) expanded transversely; (**2**) subcircular.
180. **Tibial cnemial crest, orientation**: (**0**) projecting anteriorly; (**1**) laterally.
181. **Tibia, shaft**: (**0**) cylindrical or slightly wider transversely than long anteroposteriorly; (**1**) strongly flattened transversely, with a mediolateral width less than 40% the anteroposterior length at midshaft.
182. **Tibia, distal breadth**: (**0**) approximately 125%; (**1**) more than twice midshaft breadth.
183. **Tibial distal posteroventral process, size**: (**0**) broad transversely, covering posterior fossa of astragalus; (**1**) shortened transversely, posterior fossa of astragalus visible posteriorly.
184. **Fibula, proximal tibial scar, development**: (**0**) not well-marked; (**1**) well-marked and deepening anteriorly.
185. **Fibula, lateral trochanter**: (**0**) absent; (**1**) present.
186. **Fibular distal condyle, size**: (**0**) subequal to shaft; (**1**) expanded transversely, more than twice midshaft breadth.
187. **Astragalus, shape in anterior view**: (**0**) rectangular; (**1**) wedge-shaped, with reduced anteromedial corner.
188. **Astragalus, shape in dorsal view**: (**0**) wide; (**1**) narrow anteroposteriorly toward its medial end.
189. **Ventral surface of the astragalus**: (**0**) flat or slightly concave transversely; (**1**) convex transversely.
190. **Astragalus, foramina at base of ascending process**: (**0**) present; (**1**) absent.
191. **Astragalus, ascending process length**: (**0**) limited to anterior two-thirds of astragalus; (**1**) extending to posterior margin of astragalus.
192. **Astragalus, posterior fossa shape**: (**0**) undivided; (**1**) divided by vertical crest.
193. **Distal tarsals 3 and 4**: (**0**) present; (**1**) absent or unossified.
194. **Metatarsus, posture**: (**0**) bound; (**1**) spreading.
195. **Metatarsal I proximal condyle, transverse axis orientation**: (**0**) perpendicular to; (**1**) angled ventromedially approximately 15° to axis of shaft.
196. **Metatarsal I distal condyle, posterolateral projection**: (**0**) absent; (**1**) present.
197. **Metatarsal I, minimum shaft width**: (**0**) less than; (**1**) greater than that of metatarsals II-IV.
198. **Metatarsal I and V proximal condyle, size**: (**0**) smaller than; (**1**) subequal to those of metatarsals II and IV.
199. **Metatarsal III length**: (**0**) more than 30%; (**1**) less than 25% that of tibia.
200. **Metatarsals III and IV, minimum transverse shaft diameters**: (**0**) subequal to; (**1**) less than 65% that of metatarsals I or II.
201. **Metatarsal V, length**: (**0**) shorter than; (**1**) at least 70% length of metatarsal IV.
202. **Proximal pedal phalanges, shape**: (**0**) longer proximodistally than broad transversely; (**1**) broader transversely than long proximodistally.
203. **Collateral ligament pits on non-ungual pedal phalanges**: (**0**) deep; (**1**) shallow or absent.
204. **Pedal digits II-IV, penultimate phalanges, development**: (**0**) subequal in size to more proximal phalanges; (**1**) rudimentary or absent.
205. **Pedal unguals, orientation**: (**0**) aligned with; (**1**) deflected lateral to digit axis.
206. **Pedal digit I ungual, length relative to pedal digit II ungual**: (**0**) subequal; (**1**) 25% larger than that of digit II.
207. **Pedal digit I ungual, length**: (**0**) shorter; (**1**) longer than metatarsal I.
208. **Pedal ungual I, shape**: (**0**) broader transversely than dorsoventrally; (**1**) sickle-shaped, much deeper

dorsoventrally than broad transversely.

209. **Pedal ungual II-III, shape**: (**0**) broader transversely than dorsoventrally; (**1**) sickle-shaped, much deeper dorsoventrally than broad transversely.

210. **Marked dorsoventral flattening of the unguals of pedal digits II and III**: (**0**) absent; (**1**) present.

211. **Pedal digit IV ungual, development**: (**0**) subequal in size to unguals of pedal digits II and III; (**1**) rudimentary or absent.

212. **Osteoderms**: (**0**) absent; (**1**) present.

APPENDIX 2

Character-taxon matrix used in the phylogenetical analysis. **?**, incomplete data; **9**, inapplicable.

Characters 1 to 71

Prosauropoda	00000000000000000000000000000900000000000000000000000009000000000011090
Herrerasaurus	00000000000000000000000000000900000000000000000000000009000000000001090
Isanosaurus	??0????190
Gongxianosaurus	????????1??112???0????0?0
Antetonitrus	??0??00????09?
Vulcanodon	??0????19?
Tazoudasaurus	????????????????000?0??1???0009?????????????1000100???0?10111010000?0?0101
Shunosaurus	01100011011000000?0?0011101100101100?0011000?0101?11101112O?000031101
Barapasaurus	??1?1111??00???010?
Patagosaurus	10100?11?????????????????????????????????????10????????1?100112??00?0?0100
Omeisaurus	11100011011?000?1111001111?111?1?111000?011000?11???11101111?010040111
Mamenchisaurus	111??011011?000?1111001111011?1?111000?011000111011111?1111001?0401?1
Jobaria	11110011111100011111001110111?1?11?0?0?0100?????????11101110000?1??30110
Diplodocus	00111112011111111111111111111002111001011111101010122120212110111401l0
Apatosaurus	0011111201l?111?111111111111002?1?0010011?????????2212020121?011140110
Dicraeosaurus	00?11?????0??00?111111111????1???100101111?????????2212021?1?011120110
Nigersaurus	00110?1100???001901??99991?111??????01??11101001????2211021201101???0110
Camarasaurus	11110011111100011111011110011111111000101101111111111101112100101201l0
Brachiosaurus	111100111111000111110011111111011110011011011111112111001120110130110
Euhelopus	11100?11??1????1???????????110???111??????1011??????1?101112101l??41111
Opisthocoelicaudia	??1???????
Rapetosaurus	0011?111?10?000?0100111010?11211???10?1010011?1????111102121011???110?
Saltasaurus	????????????00?11??011?????????????101??1?????????????????????11?1?0110

Characters 72 to 142

Prosauropoda	00000009100000000000000000000000000000000900000000000000000000000090
Herrerasaurus	00000009000000000000000000000000000000000900000000001000000000010090
Isanosaurus	??0??????0?????10000?????????????????????????????????????0??????????????
Gongxianosaurus	0?0????09?00???????0?00?0?????0????0??????0??????00???1000?000?00???1??1
Antetonitrus	??0???09?000000009000??????00900?0?00100??????????1000?????2100??090
Vulcanodon	?????????????????????????1????00?????10001?????????00??10?????????100?111
Tazoudasaurus	01011009?10011?10101000??????0??000100000009??00100?11000??000?01001l?1
Shunosaurus	0001?00921000?00000000?1000100090001000?00090?0011010100000000001001101
Barapasaurus	??01?009?11011010102000110??00?????10000?009???0100?011000000?01001111
Patagosaurus	01011009?11011010?020002?0??000900010O?000091?00100??11000?000?01001111
Omeisaurus	00100009311?111111000002101100090001000?00??100?100001100?000001001101
Mamenchisaurus	0?100110311O?1?1?10?0002???111090001000?00??1000100?011000?000000001111
Jobaria	0?01?009311011111110000210110009110100O0?0??100010010110101000001001111
Diplodocus	10110111511111111100000211111111111111110011110010010110011000001001111
Apatosaurus	10010111511111111100000211111011111111000111100100101100110000001001101
Dicraeosaurus	10010011311110011100000211?110101111100000111100100??11000100?01001111
Nigersaurus	0?01??09?????????????????????????????????????1100??????1020?0???????????
Camarasaurus	10010010311011011110010210110009111100000009100?110101101010000001001111
Brachiosaurus	00110009311011111110010210110009110100001O??1011?10??110101000000001111
Euhelopus	0?11?0112110111?11011?3?01?????????????????1011?????1100100001100l???
Opisthocoelicaudia	?0??00104110111101101113l0?222091111000112l0??110111111001111111111O110
Rapetosaurus	0?11??09?1101?0101101113?????10???????00??1??1????????1110??100111010l?0
Saltasaurus	00010109?1101?110110111310l??109111100011110l????11?011101011111111O110

Characters 143 to 212

Prosauropoda	00000000010000000000000000000000000000000000000000000000000000000000000000000000
Herrerasaurus	00000000000000000000000000000000000000000000000000000000000000000900000000000000
Isanosaurus	??????????????????????????????0110000??????????????????????????????????????
Gongxianosaurus	???01?????????????????????????????110?????001???1?0??100?0110000000?0000?
Antetonitrus	00001?0???00??0????????00????001000000?100????????0001100?0??01?0000?
Vulcanodon	01001???0?????????1????000101000?0???0011?11?10011110?0010010000?1110100
Tazoudasaurus	01001100?0010101010?00000?0100010100001111111001117?00011?0100001?10100
Shunosaurus	0100110000011101010100010?0?1101001100?1?000010?1110111011117?1111010
Barapasaurus	0100?????????????01010001010100110100210011111???1?1??00?????????1??110?0
Patagosaurus	01001?????????????0101000101010111010021001?????????100?????????????????0
Omeisaurus	0100110000001111?10100010101017?1000?110011??000101111111111111111111010
Mamenchisaurus	0100111100001?1?10100010101011101001100?1?1000101117??111111111??11??0
Jobaria	0100111100001111111100010101111101002100111017??1111110111117?????????0
Diplodocus	0100111?000??1?111100110100011101012100?1?0111111111111111111111?111010
Apatosaurus	0100111100001111111100110100011101002100111011111111111111?11111?11010
Dicraeosaurus	0???1?????????????111100110100011101002100111011111?11111?11?????11???0
Nigersaurus	??
Camarasaurus	0100111111001111111100011101111101002100111011111111101111111111111010
Brachiosaurus	0100111111111101111101011101111111002100111111111111110111?111?1??110?0
Euhelopus	????????????????11?10101010111111100210017?1011111??1101111?1???1110?0
Opisthocoelicaudia	1111191111112299111117?0110111112111021011110111110111011111111110111010
Rapetosaurus	0110?????1?1?????111101011011111?1101?????????????????????????????????1
Saltasaurus	1111?????????????111111011011111211112101111?????????????????????????1